Desalination 581 (2024) 117584

Contents lists available at ScienceDirect

Desalination

journal homepage: www.elsevier.com/locate/desal

Progress in module design for membrane distillation

Aamer Ali [a,*], Mohammad Mahdi Agha Shirazi [b], Lebea Nthunya [c], Roberto Castro-Muñoz [d], Norafiqah Ismail [e], Naser Tavajohi [e,**], Guillermo Zaragoza [f,g,**], Cejna Anna Quist-Jensen [b]

[a] Department of Energy, Pontoppidanstræde 111, 9220 Aalborg Øst, Denmark
[b] Center for Membrane Technology, Department of Chemistry and Bioscience, Fredrik Bajers Vej 7H, 9220 Aalborg Øst, Denmark
[c] Molecular Sciences Institute, School of Chemistry, University of Witwatersrand, Private Bag X3, Johannesburg 2050, South Africa
[d] Gdansk University of Technology, Faculty of Civil and Environmental Engineering, Department of Sanitary Engineering, G. Narutowicza St. 11/12, 80-233 Gdansk, Poland
[e] Department of Chemistry, Umeå University, Umeå, Sweden
[f] CIEMAT-Plataforma Solar de Almería, Ctra. de Senés s/n, Tabernas 04120, Almería, Spain
[g] Centro Mixto CIESOL, ceia3, Universidad de Almería, Ctra. Sacramento s/n, Almería 04120, Spain

HIGHLIGHTS

- Significant interest in developing new module designs for MD is emerging.
- Progress in hollow fiber and flat sheet membrane modules for MD is reviewed.
- Key areas for future research in MD modules are highlighted.

GRAPHICAL ABSTRACT

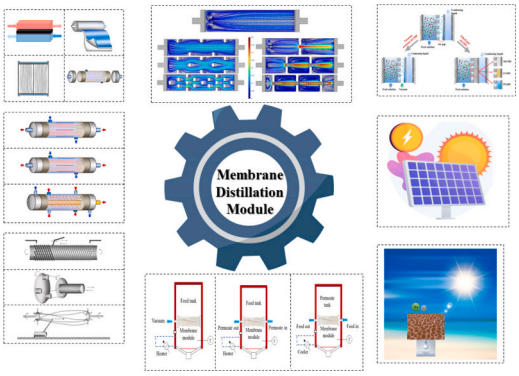

ARTICLE INFO

Keywords:
Membrane distillation
Module design
Hollow fiber membranes
Flat sheet membranes
Energy efficiency

ABSTRACT

There have been tremendous advances in membrane distillation (MD) since the concept was introduced in 1961: new membrane designs and process configurations have emerged, and its commercial viability has been evaluated in several pilot-scale studies. However, its high energy consumption has hindered its commercialization. One of the most promising ways to overcome this obstacle is to develop more energy-efficient membrane modules. The MD research community has therefore developed diverse new module configurations for hollow fiber and flat sheet membranes that increase the thermal energy efficiency of MD by minimizing thermal polarization, increasing mass transfer across the membrane, and improving heat recovery from the condensed vapor. This review summarizes the progress made in the design of hollow fiber and flat sheet membrane modules

* Corresponding author.
** Co-corresponding authors.
E-mail addresses: aal@energy.aau.dk (A. Ali), naser.tavajohi@umu.se (N. Tavajohi), guillermo.zaragoza@psa.es (G. Zaragoza).

https://doi.org/10.1016/j.desal.2024.117584
Received 17 October 2023; Received in revised form 15 March 2024; Accepted 25 March 2024
Available online 2 April 2024

for MD applications. It begins with a brief introduction to MD and its configurations before describing developments in module fabrication and highlighting key areas where further research is needed.

Abbreviations

AGMD	air gap membrane distillation
CFD	computational fluid dynamic
CNT	carbon nanotube
CPC	compound parabolic concentrator
CPV-MD	concentrating photovoltaic membrane distillation
FO	forward osmosis
GOR	gained output ratio
gpm	gallon per minute
HF	hollow fiber
IA	image analysis
LCOW	levelized cost of water
LGMD	liquid gap membrane distillation
LPM	liter per minute
MBR	membrane bioreactor
MCr	membrane crystallization
MD	membrane distillation
MDBR	membrane distillation bioreactor
MDCr	membrane distillation crystallization
ME-AGMD	multi-effect air gap membrane distillation
MGMD	material gap membrane distillation
MS-AGMD	multi-stage air gap membrane distillation
PGMD	permeate gap membrane distillation
PP	polypropylene
PTFE	polytetrafluoroethylene
PVDF	polyvinylidene fluoride
PVs	photovoltaics
RO	reverse osmosis
RSM	response surface methodology
SGMD	sweeping gas membrane distillation
TLCs	Thermochromic Liquid Crystals
TPMS	triply periodic minimal surfaces
TSGMD	thermostatic sweeping gas membrane distillation
UF	ultrafiltration
VMD	vacuum membrane distillation
VMEMD	vacuum multi-effect membrane distillation
WGMD	water gap membrane distillation

1. Introduction

Membrane distillation (MD) is a versatile emerging separation technology that was introduced in the 1960s but has recently attracted renewed interest [1–6]. MD harnesses the principles of thermal and membrane separation by using a vapor pressure gradient across a porous membrane with at least one hydrophobic layer to separate volatiles from a solution. The vapor pressure gradient is established by a temperature difference across the membrane [7]. Because the membrane has at least one hydrophobic layer, only the gas/vapor phase from the heated feed

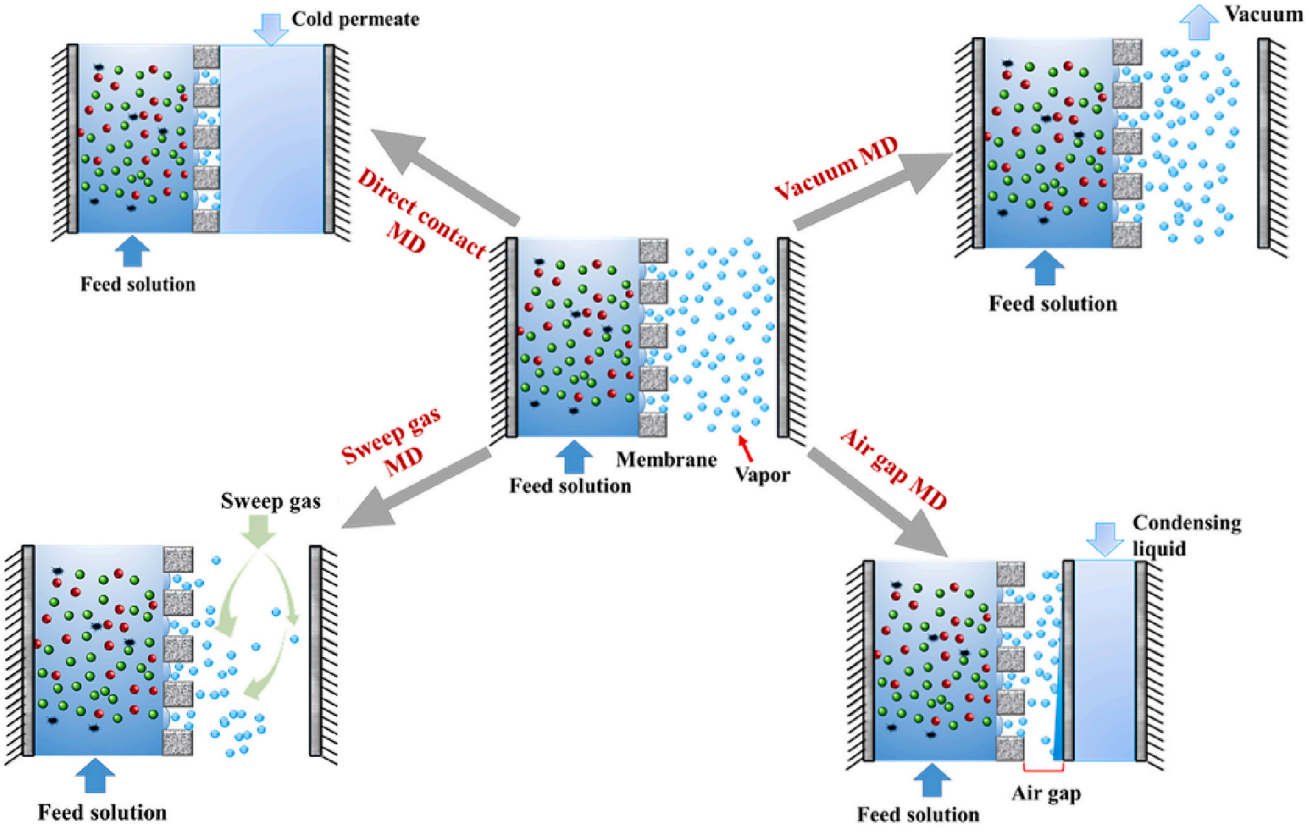

Fig. 1. General scheme of the four main MD configurations.

can pass through its pores; liquids and non-volatile solutes are retained [8]. MD was initially proposed for use in desalination and has been studied extensively in that context, but it has also recently found diverse new applications in wastewater treatment as well as nutrient and resource recovery due to its several advantages over other separation techniques [9–14]. For example, despite being a non-isothermal separation process, it can use low-grade heat from various renewable or waste sources (e.g., solar, geothermal, and industrial waste thermal energy), which can considerably increase its primary energy efficiency [15]. Moreover, because the theoretical rate of rejection of non-volatiles is 100 %, MD can produce ultra-pure permeate. Finally, increasing the solute concentration in the feed solution has lesser effects on the MD permeate flux and its quality compared to the other membrane systems [1,16–18].

1.1. Conventional MD configurations

MD systems can be operated in four main configurations, as shown in Fig. 1 [19]. In direct contact MD (DCMD), the heated feed and the condensing cold liquid are in direct contact with the membrane faces. This allows internal condensation of vapor molecules in the permeate channel to occur, which is one of the advantages of DCMD. The vapor pressure difference across the membrane in DCMD is established by maintaining the feed stream at a higher temperature than the condensing (permeate) stream. Despite its simplicity in terms of required equipment and module design, its efficiency is limited by the fact that the membrane is in direct contact with both the hot and cold streams, leading to high energy losses due to thermal conduction across the membrane [4,20]. This also means that the membrane's surface temperatures may significantly differ from those in the bulk of the channels, causing a phenomenon known as temperature polarization that adversely affects the DCMD performance [21–25]. It is also worth noting that efficient utilization of heat in DCMD requires effective heat recovery from the permeate stream, which is traditionally achieved by using an external heat exchanger [26].

Air gap MD (AGMD) has recently drawn attention because it can minimize energy losses caused by thermal conduction across the membrane and allows heat recovery systems to be integrated into the membrane module [27]. A typical AGMD module features an air gap between the membrane and a condensing surface in the distillate channel. This allows the use of the feed as a coolant and thus directly recovering the latent heat of condensation as sensible heat for preheating inside the module. In addition, the air gap minimizes conductive energy losses via the membrane matrix because the thermal conductivity of air is orders of magnitude lower than that of water [28,29]. Reducing heat transfer across the membrane also reduces thermal polarization within the feed channels. However, the air gap increases the distance that vapor molecules must travel before condensing and thus increases resistance to vapor transport, which may reduce the system's overall mass flux [30]. There is a lower limit on the acceptable width of the air gap because narrower gaps lead to reduced thermal efficiency and water bridging, which acts as an additional source of resistance to water condensation. Various designs and operational modifications have been introduced to improve heat and mass transport in AGMD [28,29].

The problem of resistance to vapor transport through the air gap in AGMD systems can be avoided by performing so-called vacuum MD (VMD), in which the permeate side is maintained at reduced pressure to remove vapor, creating a strong driving force for vapor transport [31,32]. As there is no cold stream on the permeate side, heat loss via thermal conduction is minimal. VMD systems have higher overall fluxes than comparable DCMD and AGMD systems and some innovative VMD module designs also offer the possibility of internal heat recovery [19,33]. However, they also have two notable drawbacks: (*i*) they require additional equipment, namely a vacuum pump and external condenser and (*ii*) due to their high transmembrane pressures, the risk of membrane wetting and fouling is higher than in DCMD or AGMD [34,35].

The final major MD configuration is known as sweeping gas MD (SGMD), which uses a flow of gas such as dried air to remove vapor molecules from the permeate channels. Like other MD configurations, SGMD can be used to treat highly concentrated solutions [36–38]. However, it has a relatively low permeate production rate and may collect large volumes of the sweeping gas. Like VMD, SGMD requires an external condenser, but its cooling requirements are higher due to the large volume (vapor and sweeping gas) needing to be cooled. It is therefore, the least studied MD configuration, and its proposed applications mainly relate to the removal of volatile organic substances and dissolved gases from liquid streams [39,40].

1.2. Current trends in MD development

MD has been studied considerably using theoretical and experimental methods since its introduction [41]. However, many barriers remain to be overcome to enable its widespread commercialization. Current research on MD technology is focused on several problems, such as energy consumption, fouling and scaling, and pore wetting, that are briefly reviewed in this section [42].

Most well-developed membrane technologies such as pressure-driven membrane processes can be used to perform isothermal separation, which is seen as an important advantage over other separation techniques [43]. The non-isothermal nature of MD can make it less attractive than isothermal methods because it may lead to unacceptably high energy consumption in large-scale systems during long-term operation [44]. This drawback can be managed by using alternative energy sources such as renewable energy (e.g., solar, wind, or geothermal energy sources) or industrial waste thermal energy to reduce the net heating cost for the feed streams [45,46]. Moreover, multi-effect MD (MEMD) and heat pump-linked MD have improved MD's efficiency. MEMD uses latent heat from one effect (or stage) to drive distillation in another, greatly enhancing energy efficiency. Heat pumps efficiently recycle energy within the system, lowering net energy need when used with MD [47,48]. These novel methods reduce energy usage and make MD more energy-efficient and environmentally beneficial.

MD membranes can be less prone to traditional fouling than membranes used in pressure-driven processes because MD operating conditions are comparatively mild and require relatively low input pressures in the feed channel. Nevertheless, hydrophobic membranes for MD can still suffer from fouling and biofouling, especially when used to process highly polluted wastewater samples. Due to the high salinity of the solution traditionally treated with MD, scaling issues are often reported in MD literature [49–53]. Additionally, pore wetting has been identified as an important failure mode of MD membranes and substantial efforts have been made to identify and develop new materials and techniques for fabricating highly efficient and durable membranes with favorable anti-wetting properties [54,55]. These efforts have led to the emergence of hollow fiber, nanofiber, and photothermal membranes, advanced membrane surface modifications, and mixed matrix and (nano)composite membranes [56–58]. The development of new materials and methods, including suitable module designs, for mitigating fouling and scaling is thus a major area of interest in current MD research [59,60].

A third major area of intense research in MD is modeling and process optimization to improve efficiency and facilitate the development of new applications that integrate MD with other separation processes for nutrient and mineral recovery [8,61]. Some notable systems that combine MD with other processes include membrane distillation bioreactors (MDBR) and membrane distillation crystallization systems for the recovery of nutrients and minerals [62–64].

The design of new membrane modules will be crucial for the advancement of MD technology and for addressing the issues mentioned above. MD involves multiple transport phenomena, including momentum and heat transfer in the feed and permeate channels as well as heat and mass transfer across a microporous hydrophobic membrane.

Modules must therefore be designed in a way that ensures proper separation of the feed solution and permeate streams while maintaining high heat transfer rates, minimizing polarization effects, and sustaining a high and pure permeate flux. The design must also ensure that the membrane is properly supported and protected from mechanical stress and damage to maximize its lifetime. Finally, an ideal module design should be scalable, offer high ease of operation, and be straightforward to clean, maintain, and replace when necessary to make processes efficient and cost-effective with long-term reliability and high performance.

1.3. Scope of this work

Several reviews on MD technology have been published, focusing on MD membranes [55,58], energy sources for MD [45,46], specific MD configurations [65–69], fouling and pore wetting in MD [59,70], simulation and modeling of MD processes [8,71], and new applications of MD [63]. However, there have been no comprehensive reviews of key issues in MD module design or recent advances in MD modules for emerging applications. This work therefore aims to provide a thorough and critical overview of these topics for academic and industrial researchers. It covers various MD module designs including modules for hollow fiber and flat sheet membranes, multi-effect modules, simulation efforts for module and spacer design, and solar-assisted modules, analyzing the characteristics of each design in detail. In addition, it explores strategies to improve the performance of MD modules.

2. Fundamentals of module design

2.1. Module design concepts

Conventional membrane modules are units comprising a membrane fixed in a housing containing feed inlet, retentate outlet, and permeate inlet/outlet channels [72–74]. However, the emergence of new membrane applications and new module designs have changed perceptions about what defines a module. For example, in submerged membrane modules, as the name suggests, the module is directly soaked in the feed solution with no external housing and the module's only connection is a channel for removal of the permeate [75–77]. Conversely, air gap and permeate-gap MD (AGMD and PGMD, respectively) modules require additional inlet and outlet channels for a cooling stream [65].

A module's primary purpose is to hold a membrane in place so that it can be used effectively in the specified application. However, a well-designed module should also satisfy several other requirements; in particular, it should enable high membrane packing density. The packing density is defined in terms of the functional membrane surface area in a given volume [73,78], and should ideally be high enough to avoid inefficient use of the module housing. However, it is important to note that in the case of hollow fiber membranes, increasing the packing density above a critical value can create stagnant or “dead” regions within the module where heat and mass transfer are poor [79,80]. Typical packing densities for flat sheet membrane modules are in the range of 100–400 m^2/m^3, while hollow fiber membrane modules can achieve and perform well at much higher packing densities of up to 3000 m^2/m^3 [81].

Another important requirement is that a well-designed module should facilitate scale-up and integration into existing processes. To enable reliable techno-economic evaluation of a module's commercial potential, its performance should be predictable using an appropriate mathematical model over a wide range of operating conditions (defined by parameters such as the crossflow velocity and temperature) and feed characteristics (defined by parameters such as concentration and viscosity). To be practically useful, the module must maintain its integrity during long-term operation (typically for up to 5 years) and should be designed in a way that minimizes the deposition of foulants in the system (i.e., on the membrane surface, the solution transfer tubing, and inside the module). Finally, the module should be resistant to thermal and chemical degradation under the intended process conditions and should ensure easy cleaning.

2.2. Requirements for MD modules

MD implies a series of mass transport processes involving the feed, membrane, and permeate, each of which is characterized by a specific transfer coefficient. These coefficients can be determined using established theories and are affected by changes in the design of membrane modules [82]. The performance of MD systems is sensitive to mass transfer resistance at the boundary layer, so modules should be designed systematically to minimize this resistance [83]. Moreover, an MD module should have favorable hydrodynamic properties to minimize temperature and concentration polarization to maintain low energy consumption. This can be achieved by disturbing the normal flow patterns within the module. One way of achieving this is to increase the fluid's flow rate, but this approach increases pressure losses and thus leads to higher mechanical energy consumption as well as an increased probability of undesirable pore wetting [84]. A better alternative is to adopt a module design with superior hydrodynamic properties on the shell and lumen side. An MD module should also maximize the potential for heat recovery, be easy and economical to fabricate, and minimize leakage issues [72].

3. Module design for MD

The two most used membrane types in MD are hollow fiber and flat sheet membranes. A range of different module designs for such membranes have been proposed, as shown in Fig. 2. Flat sheet membranes are generally housed in plate-and-frame (Fig. 2(a)) or spiral wound (Fig. 2 (b)) membrane modules, whereas modules for hollow fiber membranes can be broadly classified into shell and fiber (Fig. 2(c)) and submerged (Fig. 2(d)) configurations. As discussed in Section 3.2, several new flat sheet membrane designs for MD applications using plate-and-frame and spiral wound membrane modules have been introduced recently. Similarly, diverse surface topographies and structural designs have been proposed for hollow fiber membrane modules [85]. Further details and different variations of these module configurations are discussed later in this article whereas an overview of commercially developed MD modules is provided in Table 1. The fundamental objective of these new designs is to improve process performance by increasing the rate of heat and mass transport within the module, boosting heat recovery, and/or increasing the membrane area that can be packed within a single module.

3.1. Hollow fiber membrane modules

As shown in Fig. 2(c), the key components of a hollow fiber membrane module include the hollow fiber membrane bundle, the tube-sheets, the end caps and feed and permeate ports. The module's functional element is a bundle of hollow fiber membranes that are packed together [102,103]. A liquid potting substance is pumped into a mold to form the tube-sheet, which then solidifies to create the seal and serves as a fluid-tight barrier between the fibers. The tube-sheet separates the streams flowing through the module's lumen and shell sides. The potting materials must be compatible with the other components of the module and possess adequate mechanical strength, chemical resistance, thermal resistance, and compatibility. The number of fibers inside the shell determines the module's packing density which is an important determinant of module performance [102].

The simplest hollow fiber modules for DCMD have a shell and tube heat exchanger configuration in which the feed flows on one side of the module and the permeate on the other side. The design of the feed compartment will generally depend on the properties of the feed solution. Modules used for the feed solutions containing foulant and suspended particles or precipitating crystals generally have a so-called

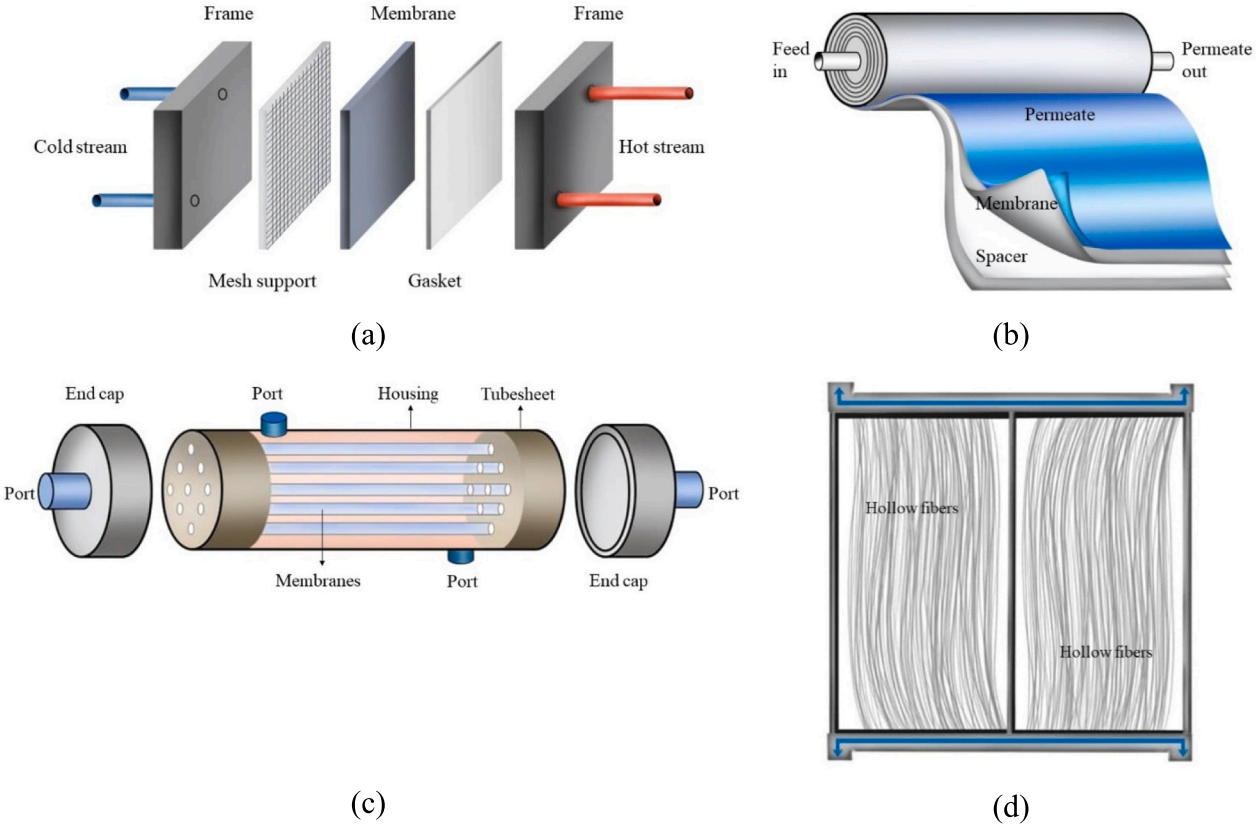

Fig. 2. Basic configurations of flat sheet and hollow fiber membrane modules. (a) Plate-and-frame, (b) spiral wound, (c) shell and fiber (d) submerged hollow fiber membrane modules.

outside-in configuration where the feed is introduced on the shell side to avoid blockage of the fiber lumen. This strategy is also adopted when DCMD is used in membrane crystallization processes where the solution is concentrated to induce precipitation of some dissolved components [106,107]. An alternative operational mode is inside-out, in which the feed is introduced on the lumen side of the fibers while the permeate is introduced on the shell side. In this mode the hot feed is not in direct contact with the module wall, reducing heat transfer to the environment [108].

In both the inside-out and outside-in configurations, the feed and permeate streams can be introduced in either axial or crossflow modes, as shown in Fig. 3. Moreover, axial flow systems may use either co-current (Fig. 3(a)) or counter-current flows (Fig. 3(b)) (meaning that the feed and permeate streams flow in parallel or opposite directions, respectively). The counter-current flow arrangement provides a more uniform temperature distribution along the module's length and is therefore used more frequently in MD applications.

Cross flow is used in axial flow designs to reduce the emergence of stagnant regions and concentration polarization effects (Fig. 3(c)). A radial flow pattern can be established on the shell side by using a perforated central tube such that both the feed and the retentate can enter through the perforations, and both can leave through the port of the cartridge [109–112]. This configuration makes the flow distribution on the shell side more uniform. The first rectangular crossflow DCMD device was developed in 2004 and had membrane surface areas of 113 to 257 cm^2 [113]. The device was subsequently scaled up to 2864 cm^2, allowing it to accommodate up to 10 modules simultaneously in parallel or in series [114]. In pilot plant desalination tests, this DCMD system was used in a range of configurations using different brine feed splits, multiple modules, and co-current or counter-current distillate feeds. The distillate production rate for the pilot plant was 0.62 gal/min (gpm), equal to 2.35 L/min (LPM), with average flows ranging from 15 to 33 kg/m^2h. A setup with single-pair units arranged in parallel with a high brine temperature (92 °C) achieved a production capacity of 0.95 gpm (equal to 3.6 LPM) and generated highly pure distilled water with a salt content below 1 ppm from a 10 % NaCl solution.

Furthermore, some interesting innovations have been proposed for designing fiber and module configurations for MD. Many of these modifications are applicable for multiple configurations of MD; however, in the current review, the modifications are discussed as they were originally proposed for a particular configuration in the reference literature.

3.1.1. *Hollow fiber modules for DCMD*

3.1.1.1. Undulating fiber geometries. The simple flow patterns in traditional parallel hollow fiber modules make them prone to high temperature and concentration polarization, particularly at low fluid flows. Another frequent problem is non-uniform fiber packing resulting from difficulties in producing parallel fiber bundles. This creates regions within the shell where fluid movement is reduced because neighboring fibers are in proximity or even in contact with one another, creating sluggish or “dead” zones. Moreover, fibers are employed inefficiently in these stationary zones, leading to reduced separation efficiency. In other regions, fibers may be less well-packed than they should be, resulting in channeling or bypassing that reduces separation efficiency [115,116].

One way to increase the uniformity of hollow fiber packing is to weave the fibers into different structural geometries such as helical, wavy, or twisted shapes [115]. This generates more uniform shell flows with fewer dead zones and reduces concentration polarization by enhancing fluid mixing [117–120]. The latter effect occurs because flows within helical geometries generate Dean vortices or secondary flows perpendicular to the axial direction, which improves solution mixing from the bulk towards the membrane surface [121]. A few

Table 1
Overview of some of the commercially developed MD modules.

Module type	Configuration	Developer	Area (m^2)	Ref.
Plate-and-frame	AGMD	Scacab AB	2.4	[86]
Plate-and-frame	PGMD	Keppel Seghers	3–9	[86]
Spiral wound	AGMD/V-AGMD	Aquastill BV, The Netherlands	7.2–25.9	[87]
HF shell and tube	VMD	Zhejiang University, China	12.3	[88]
HF shell and tube	VMD	Econity	5.3	[89]
Capillary	VMD	KMX Technologies	N.A.	[90]
HF shell and tube	SGMD	Tanal Water	18	[91]
HF shell and tube	N.A.	Memsift	N.A	[92]
Crossflow HF	DCMD	NJIT, USA	0.6	[93]
Spiral wound	PGMD	ISE, Germany	5–14	[94]
Spiral wound	DCMD	ISE, Germany	0.6–27.5	[95]
Spiral wound	PGMD	ISE, Germany	8.96	[95]
Spiral wound	PGMD	SolarSpring, Germany	10	[96]
Spiral wound	AGMD/PGMD	SolarSpring, Germany	14	[97]
Spiral wound	PGMD/DCMD	Aquastill BV, The Netherlands	7.2–14.4	[98]
Spiral wound	AGMD	Aquastill BV, The Netherlands	7.2	[99]
Plate-and-frame	V-MEMD/AGMD	Scarab development AB, TNO Keppel Seghers, Aquastill BV, Memsys	6.4/4.6	[100,101]

N.A.: not available.

studies have reported the use of such geometries for MD applications. For example, Teoh et al. found that the use of different hollow fiber configurations including wavy, braided, and twisted geometries could increase fluxes during MD by up to 36 % when compared to simple linear configurations [122].

Yang et al. compared five designs for hollow fiber modules: a traditional straight fiber design, a curly fiber design, a feeding by central tubing design, a spacer-wrapped fiber design, and a spacer-knitted fiber design, are shown in Fig. 4 [123]. The curly fibers (Fig. 4(b) and (c)) were fabricated by initially following the conventional method for hollow fiber production and then collecting the fibers with a stainless-steel rod at a winding angle of 60°. The collected fibers were then heated at 60 °C for 1 h so that their curled shape was retained (Fig. 4(b) and (c)). The flux, hydrodynamic properties, flow distribution, and heat-transfer properties of the resulting membrane modules were then evaluated in a DCMD system. The new module designs all yielded higher permeate fluxes than the traditional linear design, with the space-knitted fiber design (Fig. 4(e)) providing a 90 % improvement. This configuration also provided improved fluid dynamics, created a more even flow distribution, increased vapor permeability, and reduced thermal polarization and energy losses. The authors attributed these improvements primarily to the more favorable shell-side hydrodynamics generated by the modified fiber geometry and the generally uniform shell-side flow distribution.

Ali et al. also studied the effect of helical and wavy fiber geometries on DCMD performance, revealing that helical and wavy configurations yielded flux improvements of 47 % and 52 %, respectively, when compared to straight fibers [121]. These improvements were accompanied by substantial gains in energy efficiency. However, the new geometries had up to 37 % lower packing densities than straight fibers.

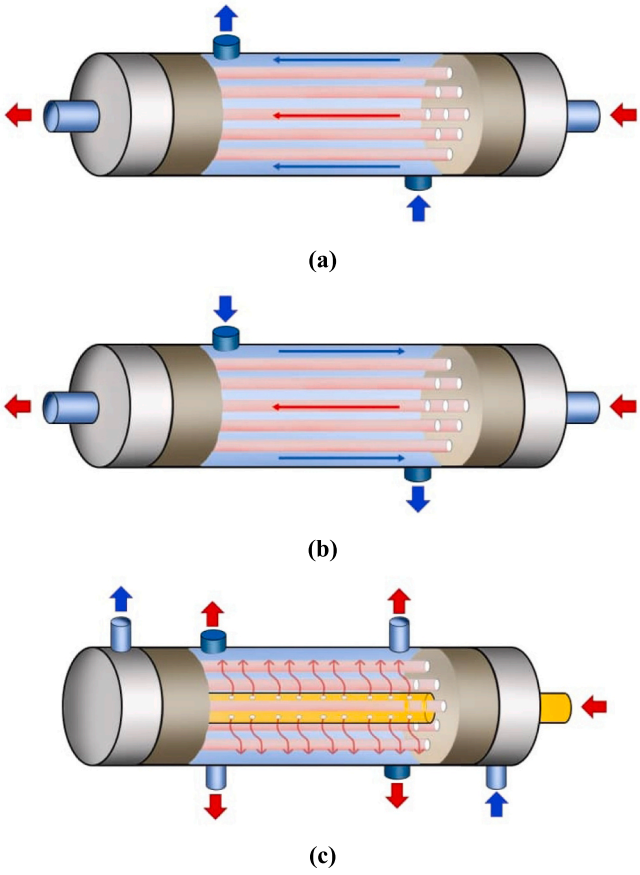

Fig. 3. Various flow patterns for a hollow fiber module: (a) co-current, (b) counter-current [104], and (c) cross-flow [105], configurations. Blue and red arrows are to differentiate feed and permeate streams from each other.

Some techniques and methods for fabricating undulating hollow fibers on commercial scales have been patented. For example, McLain invented a method for spirally winding hollow fibers onto a spinning central support tube using a guide that oscillates along the tube's axial direction, as shown in Fig. 5(a) [124]. This approach is expected to yield a higher membrane area-to-volume ratio than is possible with parallel bundles. Mahon and Oldershaw patented another way of preparing a structured bundle that is depicted in Fig. 5(b) [125]. Their strategy involves collecting multiple hollow fiber threads in a receiving ring that is rotated onto a reciprocating center tube. The winding angle and the pitch between hollow fibers can be adjusted by varying the ring's rate of rotation and the movement of the traveling tube. Finally, Albany International Corporation developed a method using a movable/adjustable central tube to produce a coreless bundle. After removing the central tube, the bundle is stretched several times to achieve the desired fiber orientation.

While methods based on winding hollow fibers around a central tube increase the uniformity of fiber packing, they also have disadvantages. First, the use of a central tube may reduce the module's effective membrane surface area. Moreover, the winding angle is constrained by fiber slippage. Therefore, Albany International Corporation introduced coreless helically wound hollow fiber bundles that are formed by guiding fibers onto two alternately reciprocating spider-shaped spokes (Fig. 5(c)) [126]. This eliminates the need for a central tube and could allow multiple hollow fiber membrane types to be wound into a bundle [74].

Variations in fiber length can also have important effects on the lumen pressure drops and the uniformity of flow rates. This factor can be minimized by increasing the winding angle with the bundle diameter to

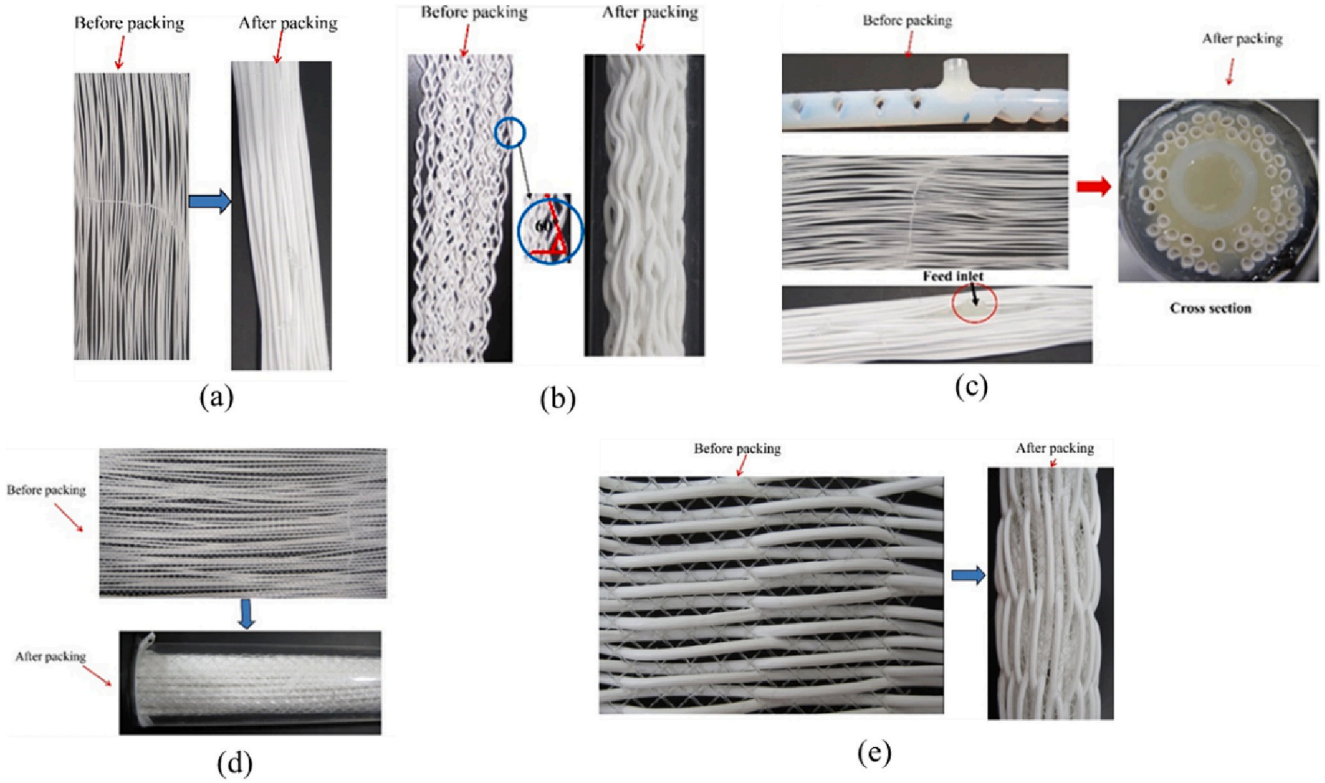

Fig. 4. Five fiber arrangements for hollow fiber membrane modules: (a) traditional straight design, (b) curly-fiber design, (c) central-tubing design, (d) spacer-wrapped design, and (e) spacer-knitted design.
(Adapted from [123]).

reduce the number of helical routes. It should however be noted that this approach causes the fiber length to increase if the winder's rotational and reciprocal speed remain constant [126,127].

An alternative to modifying the shape of the hollow fibers to improve MD performance that has drawn interest in recent years is to use membranes with corrugated surfaces to promote micro-turbulence and thereby reduce concentration and temperature polarization, leading to increased transmembrane fluxes [129]. Corrugated membranes can be prepared using a range of techniques; some approaches rely on micro-engineered spinnerets, while others use spacers that serve as templates to imprint corrugation during the casting step. Several studies have focused on optimizing the shape and size of the corrugations to maximize permeate flux. For example, Nawi et al. produced a novel corrugated PVDF membrane using the imprinting method (Fig. 6) [128]. In preliminary studies, this membrane exhibited reduced temperature polarization effects and higher permeate fluxes than conventional flat membranes in both short-term and long-term MD experiments [128,130]. Similarly, García-Fernández et al. used a micro-engineered spinneret to fabricate novel hollow fiber modules with various corrugated surface patterns that showed improved DCMD performance due to the microturbulence-inducing effect of the patterned surfaces [130]. Other studies have demonstrated the beneficial effect of using corrugation to expand the external condensing surface of membrane modules [128,130]. Separately, a corrugation-like effect was induced on the surfaces of tubular ceramic membranes by wrapping a wire around the ceramic membrane to produce spiral flow channels that increase turbulence at the membrane surface and thereby reduce temperature polarization [131].

3.1.1.2. Submerged hollow fiber modules. Submerged hollow fiber MD modules are drawing interest because they are straightforwardly fabricated and eliminate the need to circulate the feed stream within the module, which reduces electric energy consumption during MD processes. These designs have been proposed for both VMD and DCMD applications [132–135] (see Fig. 7). When operating in DCMD configuration, either the feed or permeate stream can be recirculated while the module is submerged in the other stream, as is shown in Fig. 7(b) and (c).

Submerged MD modules were first proposed in 2009 for use in integrated membrane bioreactors (MBRs) [136]. Conventional membrane filtration systems used in MBRs are unable to reject low-molecular weight compounds and due to the passage of the solute through the membrane pores, the residence time of organic substances in the solution is equal to the hydraulic retention time, which can lead to inefficient treatment of slowly degrading substances. To overcome this drawback, a new system was developed that combines MD with a thermophilic MBR. This so-called MDBR uses the heat from the thermophilic bioreactor to drive the MD process [136]. Tests using flat sheet and tubular membrane modules showed that the MDBR system could produce a high-quality permeate with a flux two orders of magnitude higher than that of a conventional submerged nanofiltration process.

A later study investigated the use of submerged hollow fiber MD modules for the desalination of Red Sea water [137]. PTFE-based hollow fibers were immersed into the clean water and the hot feed was introduced inside the fibers. The temperature of the clean water was controlled using an external cooling system to maintain a constant driving force across the membrane. The flux achieved with this system was comparable to that for a conventional DCMD module, but the new module's design and construction were much simpler than those of the DCMD system.

Despite the growing interest in submerged MD modules, they present some inherent challenges. Submerging the module inside a stagnant fluid gives rise to high temperature and concentration polarizations, which can reduce flux and increase fouling and scaling at the membrane surface [138]. A few strategies have been proposed to overcome these issues. First, it was found that mixing the feed solution with a magnetic

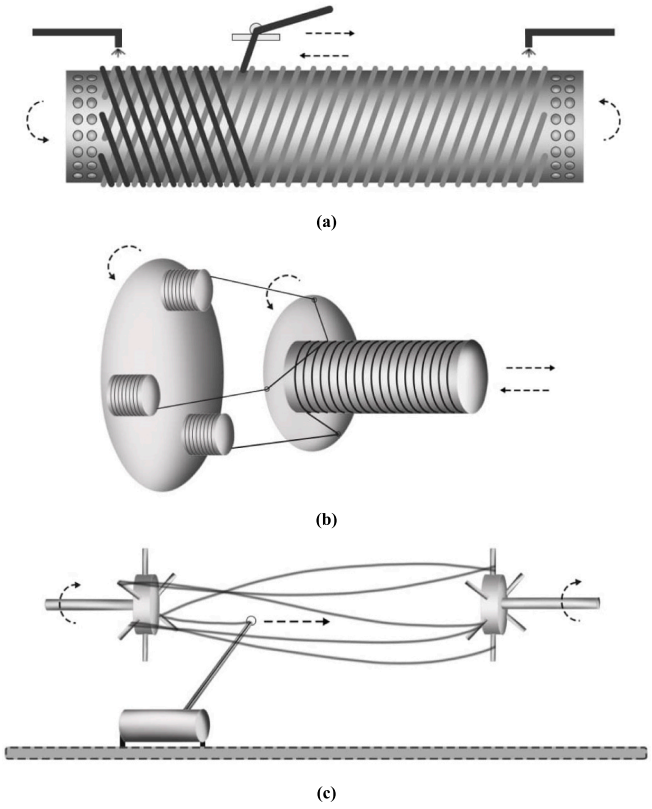

Fig. 5. Novel strategies for hollow fiber module production: (a) A spinning central tube gathers a continuous hollow fiber from a guide that moves back and forth along the tube's axial direction to generate a helically coiled hollow fiber bundle (redrawn from [124]); (b) a revolving ring creates a helically coiled bundle by winding continuous hollow fibers onto a central tube that moves back and forth along its axial direction (redrawn from [125]); (c) a hollow fiber is pulled from a drum by a guide that moves back and forth and then alternately looped onto two spider-shaped spokes to make a helically wound coreless bundle (redrawn from [126]).

stirrer increased the permeate flux [133]. Transmembrane vibrations were also found to increase permeate flux but did not reduce scale formation [138]. Moreover, scale formation increased when transmembrane vibration was combined with periodic air backwashes and aeration. In another study, low-power ultrasonication was found to increase transmembrane flux by up to 24 % and it was shown that a new ultrasound-assisted submerged VMD module design could provide a stable flux and maintain high-quality water on the permeate side in a long-term experiment [135].

3.1.2. Hollow fiber modules for AGMD

Most AGMD modules use traditional flat sheet membranes, but efforts have also been made to use hollow fiber membranes in such systems. Three main strategies, which differ in relative positions between the porous hollow fiber membrane and the condensing surface, have been applied in designing the hollow fiber AGMD modules. The first strategy uses the inside surface of the module to condense the vapor passing through the membrane. This approach was exemplified in the first published study on hollow fiber membranes for AGMD, which used a single fiber surrounded by a concentric annulus in which the cooling water flowed [139]; the vapor permeating through the hollow fiber was condensed on the inner surface of the annulus as shown in Fig. 8(a). Cho et al. proposed an extension of this design in which hollow fibers were enclosed between cooling channels that formed two flat condensing surfaces as illustrated in Fig. 8(b) [140]. The second design strategy uses a condensing surface that is located inside the shell and may consist of a dense hollow fiber or a metallic tube. In one study, porous and dense hollow fibers were packed inside a module, with the surfaces of the dense fibers acting as the condensing medium (Fig. 8(c)) [141–143]. To increase the efficiency of heat transfer from the condensing vapor to the cooling media, the cooling channels were replaced with stainless steel tubes [144]. The modules could be operated in either AGMD or water gap MD (WGMD) configurations. In the third strategy, clusters of dense hollow fibers or metallic tubes are submerged into a cooling medium (e.g., cold feed solution), while the porous hollow fibers containing feed solution are nested inside the dense fibers or metallic tubes as shown in Fig. 8(d) [145]. Conversely, porous hollow fibers are immersed in a warm feed solution, and dense condensing fibers are inserted inside the porous fibers to condense the vapor passing through them [146]. Finally, multiple units following this configuration are arranged within the shell of the ultimate hollow fiber membrane module. All these designs offer the potential for improved energy efficiency and permeate flux due to enhanced heat transfer in the permeate channel. Additionally, the air gap width is an important parameter in all these new AGMD module designs because of its effects on the mass transfer resistance in the permeate channel.

3.1.3. Hollow fiber module for VMD

Hollow fiber modules have been used in VMD since the 1990s for applications including the removal of organic compounds from aqueous media [147–149]. Most studies in this area have used conventional shell and tube hollow fiber modules [66], but some have investigated new module designs to enhance VMD performance. For example, Li and Sirkar [150] introduced a novel VMD module design for desalination using polypropylene (PP) hollow fibers (Fig. S1). This design features

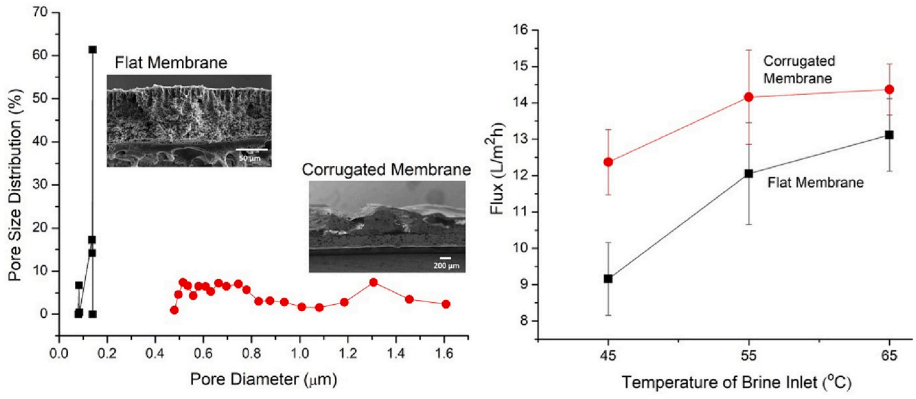

Fig. 6. Comparison between flat membrane and corrugated membrane designs. (Adopted from [128], Open Access).

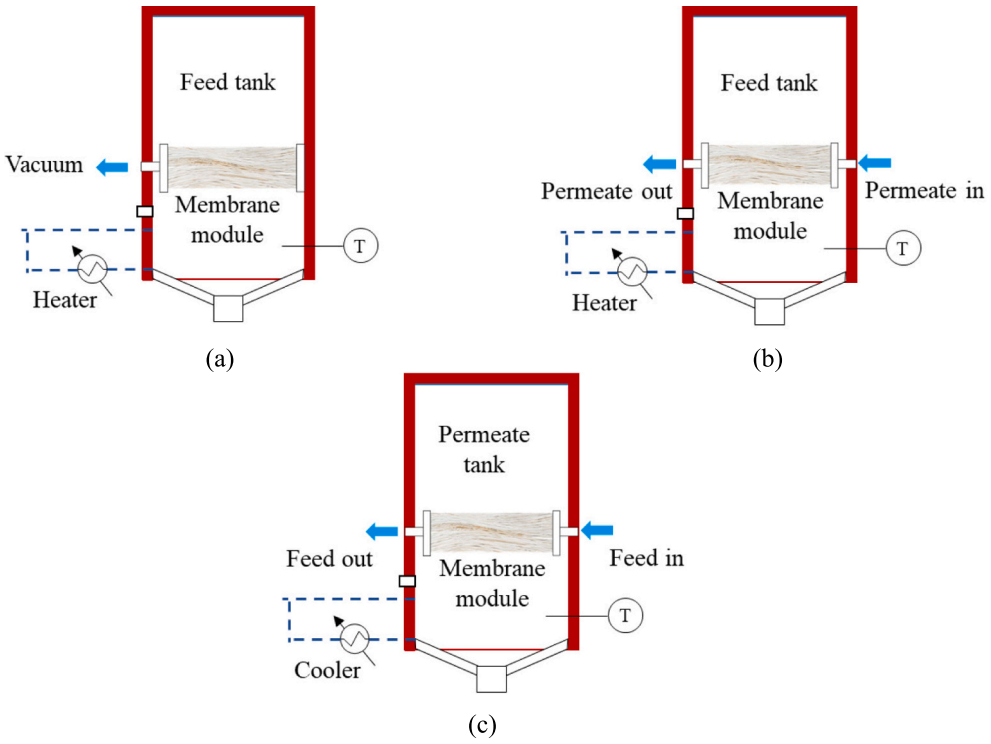

Fig. 7. Submerged hollow fiber MD module configurations for (a) VMD, (b) DCMD with the hollow fiber module submerged in the feed tank and (c) DCMD with the hollow fiber module submerged in the permeate tank.

diverging and converging sections at the entrance and exit of the module that was made from two curved boxes perforated with holes having a wide range of diameters (Fig. S1a). The heated feed solution is introduced into one face chamber, dispersing evenly as it exits through the face plate openings and enters the flow pathway. On the other side, the liquid feed exits the channel via the perforations in the face plate, collecting in the face chamber, and then continuing beyond the chamber and the module (Fig. S1c). This design ensures that the liquid traverses the fiber layer uniformly and perpendicularly, reducing the degree of temperature polarization and promoting efficient heat and mass transfer.

As noted previously, MD module designs can be classified in terms of their flow arrangement, which is typically, either inside/out or outside/in. Wirth and Cabassud investigated VMD module designs of both types using two different hollow fiber membranes with differing permeabilities (Fig. S2) [151]. For the inside/out design, the feed stream was introduced into the fibers and a vacuum was imposed on the shell side, while the opposite was true for the outside/in design. Both configurations achieved similar performance when using a sufficiently permeable membrane such as polyvinylidene fluoride (PVDF) hollow fiber membrane. However, the inside/out configuration provided better results with a less permeable membrane such as polyethylene hollow fiber membrane. It should also be noted that an inside/out configuration may pose a significant problem with a feed solution containing inorganic salts and perceptible compounds which could block the fiber mouth. This configuration may thus be best used with feed solutions containing organic compounds such as benzene or toluene [152].

Liu et al. investigated the effects of varying the fiber arrangement (i.e., the row spacing and angle of intersection) on VMD performance with hollow fiber modules by using simulations to study the module's flow field and permeate fluxes [153]. The simulations' results were experimentally validated and showed that the fiber arrangement strongly affected module performance. The permeate flux was high for modules with row spacing of 2.5 times the fibers' outer diameter and intersection angles of 60° or 90°. Increasing the row spacing or intersection angle caused the temperature and concentration polarization to increase initially and then fall. Increasing the feed inlet velocity increased both polarization and the simulated flux in all simulated modules.

In a study, Omar et al. investigated the multi-effect concept for VMD using hollow fiber membranes and developed a multi-effect hollow fiber VMD module [154]. The proposed module design features hollow helical baffles that promote internal recovery of the permeate vapor's latent heat via multiple effects, yielding a gained output ratio (GOR) of 1.5–3.5 under various operating conditions (see Fig. S3). An optimal four-effect module design with a length of 0.5 m and a packing density of 500 m^2/m^3 was found to reduce specific energy consumption by over 60 % when compared to a single-effect design.

3.1.4. Hollow fiber modules for SGMD

In SGMD, vapor in the permeate channel is swept out by a dry gas stream that is cooler than the feed solution. This can reduce heat losses via thermal conduction while maintaining a relatively high permeate flux. However, the need for an external condenser to collect the permeate in liquid form can increase production and operating costs [65–69], which may be why SGMD has received comparatively little attention [1–6]. Nevertheless, some new designs for hollow fiber SGMD modules have been proposed.

Although the thermal conductivity of air is very low (0.02 W/m·K), the temperature of the sweeping gas rises due to the capture of hot vapor molecules as it flows through the module [155]. To address this issue and increase the productivity of SGMD in terms of mass transfer, García-Payo et al. designed a new tubular SGMD module concept with temperature control that they called thermostatic SGMD (TSGMD) [156]. The TSGMD module consists of TF200 hollow fibers and a glass tube. A mixture of air and permeating vapors was circulated outside the tubular membranes in a closed loop and the sweeping gas flowed through the space between the membrane and the glass tube (cold wall). The cold wall was maintained at the same temperature as the inlet sweeping gas to enhance the driving force for separation within the module and a spiral turbulence promoter was wrapped around the tubular membranes

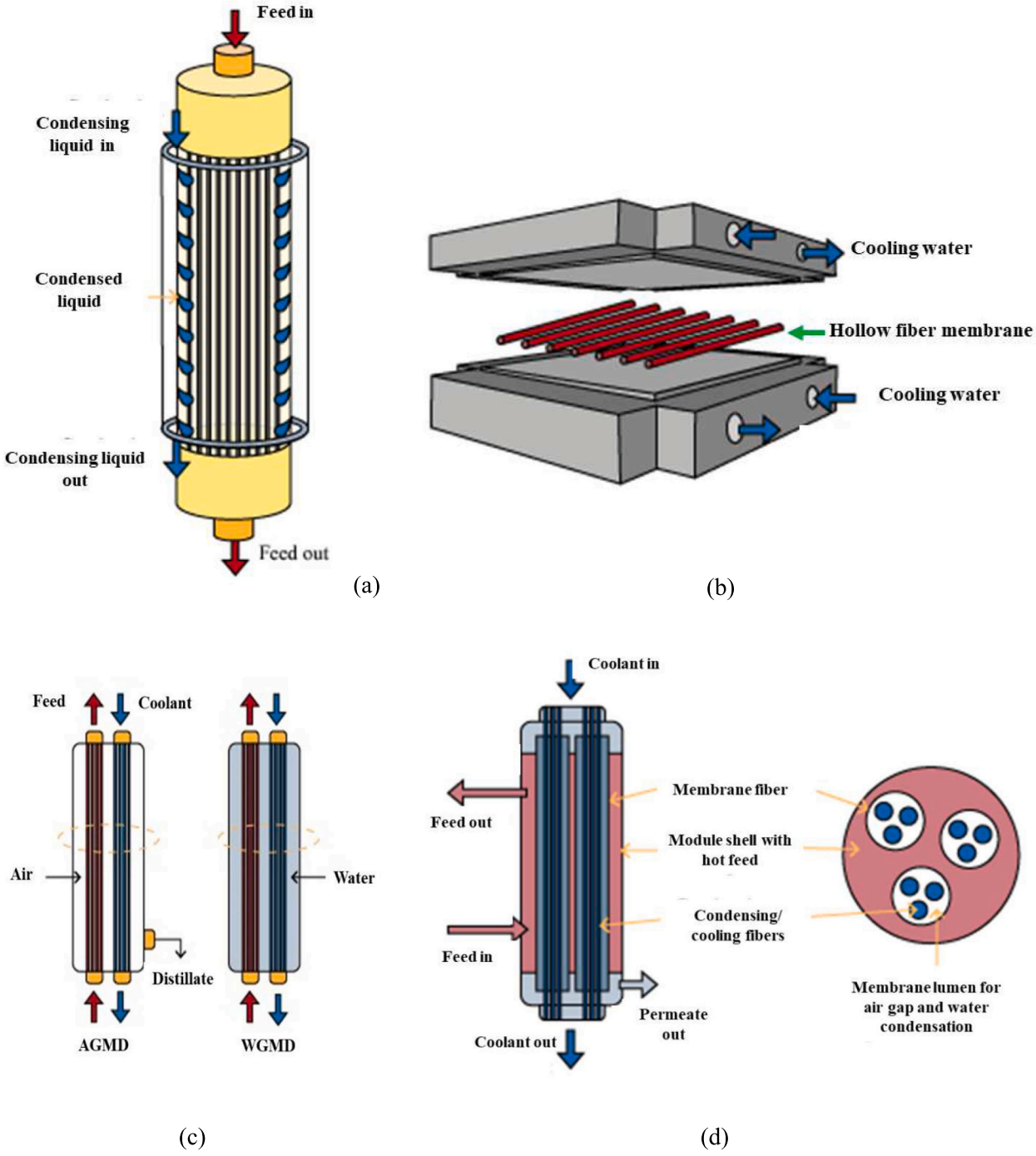

Fig. 8. Hollow fiber AGMD module designs (a) inner wall of the annulus as the condensing surface, (b) hollow fibers enclosed between two cooling plates, (c) use of hollow fibers/metallic plates present inside the shell as the condensing surface and (d) condensing fiber bundles present in the hollow fiber membrane enclosed inside the shell.

to minimize temperature polarization in the permeate channel (see Fig. S4). This caused partial condensation of the permeate within the module, reducing the load on the external condenser when separating binary mixtures.

3.2. Flat sheet membrane modules

3.2.1. Plate-and-frame modules

The plate-and-frame module configuration is one of the most widely used and studied designs for various membrane processes [81]. In this module configuration, a flat sheet membrane and spacers are clamped inside a frame. In addition to creating turbulence, the spacers provide mechanical support to the thin membrane. The flow channels, which may be supported by similar frames and placed on top of each other, can have widths of 0.5 to 5 mm. In these module designs, the membrane should be connected to the frame. However, maintaining an adequate seal between the two can be challenging. Sealing can be performed by welding or the use of gaskets. The module's outer plate provides mechanical support and hosts the fluid inlet and outlet connections. The overall membrane area can be adjusted simply by varying the number of

frames connected in parallel or series, and the design is compatible with multiple flow arrangements including co-current, counter-current, and crossflow [157]. One advantage of plate-and-frame modules is the simplicity of their design and their minimal external plumbing, which allows easy scale-up, facilitates the use of customized designs and automation, and gives easy access to membranes for cleaning, replacement, and/or analysis.

Despite these benefits, the usefulness of plate-and-frame modules is limited by certain factors. The primary obstacle hindering the adoption of P&F designs is achieving leak-proof integrity. Further to this, the larger drawback regarding fouling is dead zones in the feed channel, which can aggravate the membrane fouling. Although the cleaning process is relatively simple, back-wash cleaning presents certain challenges. Plate-and-frame modules for MD applications have been developed to be used in AGMD and vacuum multi-effect membrane distillation (VMEMD) systems by various companies including Scarab, MEMSYS, Solarspring and Keppel Seghers (discussed later) [158].

The spiral-wound module configuration (Fig. 2(b)) can be regarded as a variant of the basic plate-and-frame configuration in which a membrane envelope consisting of a spacer placed between two membrane sheets is wound around a tube, which is traditionally porous [159]. In conventional spiral-wound modules for pressure-driven processes (e.g., RO and UF), a feed solution is introduced into the feed channel in an axial direction across the membrane and the permeate spirals towards the center where it is collected in the porous tube. The spacer between the wound membrane layers forms the permeate channel [160].

The use of spiral-wound modules for MD dates to 1985, when a PGMD module called the Gore-Tex Membrane Distillation system was developed and patented by W.L. Gore & Associates [161]. This module has since been analyzed in several experimental and theoretical studies [162]. During the last decade, the Fraunhofer Institute for Solar Energy Systems has reported the production of single-channel and multi-channel spiral-wound MD membrane modules that are fabricated by rolling a membrane, condenser foil, and various spacer materials around a motorized main spindle (see Fig. S5) [163]. The channels are then sealed by covering the spiral coil's facing sides with a resin, and O-rings are used to force the potted coil into a glass fiber tube and seal it [94]. Further development of this process enabled the production of multi-channel spiral-wound MD modules with multiple pairs of evaporator/condenser flow channels [164]. Depictions of these modules and the winding machine used in their production are presented in Fig. S1, and their fabrication has been described in the literature [94]. The main advantage of spiral wound modules is a better counter-current circulation of the hot and cold streams for more efficient heat recovery. The latent heat of condensation of the vapor passing the membrane from the evaporator channel and condensing on the surface of the condenser channel is recovered to preheat the feed circulating as coolant in the condenser channel.

3.2.1.1. Plate-and-frame modules for AGMD. The air gap width is the most important parameter in the AGMD module design because of its impact on the distillate production rate. The main purpose of the air gap is to prevent direct contact between the condensing media and the membrane surface to minimize conductive heat losses. However, the air gap also increases the distance vapor must travel before condensing and thus provides additional resistance to vapor transport and reduces the mass flux through the system. Ideally, therefore, the air gap should be as narrow as possible. Its minimum width is determined by the reduction in thermal efficiency as it is shortened and by water bridging, which increases resistance to water condensation [165,166]. The typical range for air gap width of 0.5–13 mm is reported in the literature [167–170]. Published studies on AGMD have examined a wide range of membrane configurations including flat sheet, tubular, hollow fiber, and spiral wound, but most studies on this topic have used flat sheet membranes in traditional configurations or newer designs [65]. Fig. 9 illustrates some notable AGMD module configurations using flat sheet membranes whereas a timeline of significant advances in the development of membrane modules for the "gap MD" is presented in Fig. 10.

Many modifications to the fundamental module design for AGMD have been introduced. For instance, the space between the membrane and the condensing plate can be filled with various substances, such as sand or a polymeric sponge composed of polyurethane, commonly referred to as material gap MD (MGMD) [171]. Alternatively, the void can be occupied by a liquid substance, such as the permeate liquid, referred to as the permeate gap MD (PGMD) [172]. Experimental tests have shown that the PGMD module has a greater GOR (gained output ratio) compared to the typical AGMD module. This can be attributed to the internal heat recovery potential of the PGMD arrangement [94]. Inserting a conductive material, such as a metal mesh, can boost the total conductance of the gap in the PGMD design. The altered AGMD structure is referred to as the conductive gap MD (CGMD) [173]. Unlike earlier modified AGMD module designs, such as MGMD, which involved the addition of low-conductivity materials like sand to the gap space,

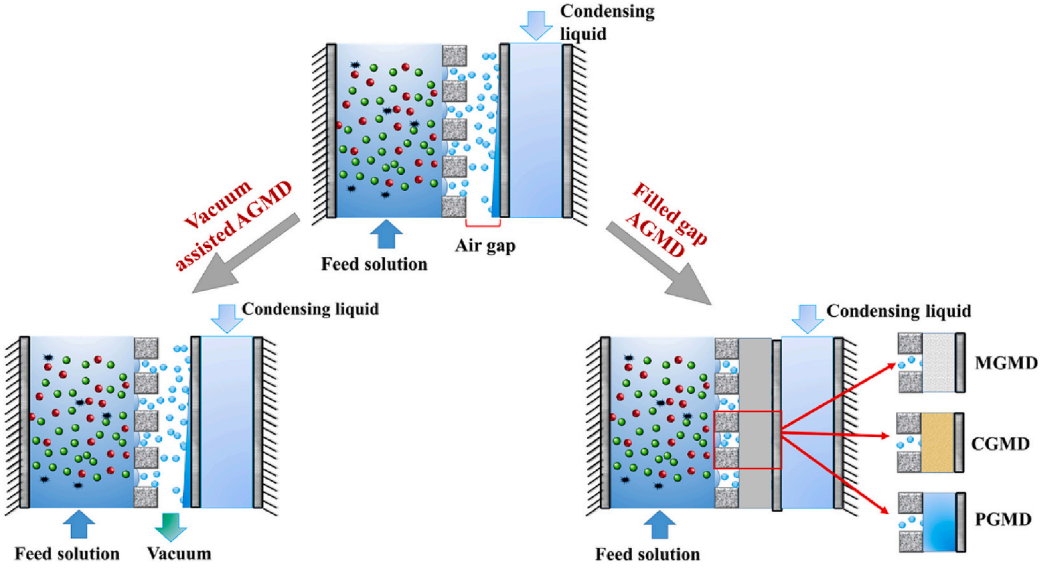

Fig. 9. A figure summarizing some published variants of AGMD configuration.

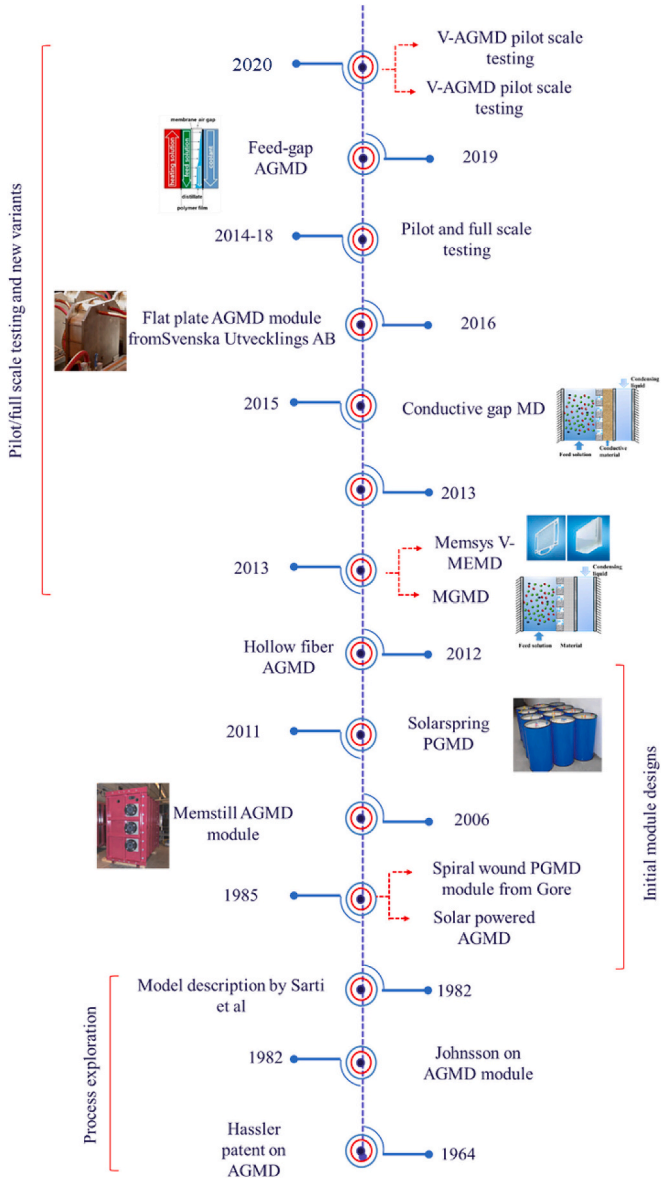

Fig. 10. A timeline of important milestones in the development of membrane modules for gap MD.

this design does not use such materials. This statement challenges both the commonly accepted beliefs and the historical progress in the field of designing configurations for MD that have reduced heat loss compared to DCMD [174]. Possible implementations include substituting a metal spacer for a plastic spacer or adding fins to the conductive surface that reach up to the membrane [173]. These modifications aimed to improve the permeate flux and internal heat recovery by increasing the overall conductivity of the gap.

Another study investigated the effect of placing spacers with varying orientations and shapes in the feed channel [22]. As in DCMD, the spacers reduced temperature polarization in AGMD and thus increased the vapor flux. Another study examined the potential for increasing the efficiency of heat removal from the coolant by placing a cooling plate on the coolant channel [175]. The performance achieved with flat and channeled plates was compared, revealing that both designs increased the system's flux by up to 50 %. This improvement was attributed to better heat transfer from the vapor, leading to more extensive vapor condensation on the condensing plate and a greater difference in vapor pressure between the feed and air gap compartments. The cooling plate with the channels also provided a significantly higher flux than the flat plate.

Multi-effect AGMD (ME-AGMD) is another concept that could facilitate the industrialization of MD by improving module performance. As the name suggests, ME-AGMD involves multiple stages (effects) to enhance the overall efficiency of membrane distillation. The ME-AGMD system consists of several membrane modules arranged in a series, with each module having its own air gap. Each module typically contains a flat-sheet or hollow-fiber hydrophobic membrane. Pangarkar and Deshmukh [176] developed a novel ME-AGMD module for water treatment and evaluated its performance over a wide range of operating conditions characterized by different air gap thicknesses and varying temperatures and flow rates of both the feed and the coolant. An ME-AGMD design was also investigated experimentally by Khalifa et al., who analyzed the performance and energy consumption of single-stage AGMD systems and multi-stage (MS-AGMD) systems with both series and parallel feed and coolant connections [177]. The study revealed that the system with parallel stage connections performed better than the one with series connections in terms of both permeate flow and energy utilization. Moreover, the permeate volumes obtained with the MS-AGMD system in its series and parallel configurations were 2.6 and 3 times that achieved with the single-stage AGMD module, respectively. However, the multistage system's energy usage was only 1.5 times that of the single-stage system. Finally, GOR of the MS-AGMD system at 90 °C was 0.6 in the parallel configuration and 0.45 in the series.

In separate experimental studies, the pressure inside the air gap of a conventional AGMD module was reduced below atmospheric pressure to remove non-condensable gaseous molecules [178,179]. This increased the distillate flux up to three-fold when compared to the standard case with the air gap at atmospheric pressure. However, reducing the pressure in the gap requires the use of an additional vacuum pump and thus increases the energy consumption of the system, unless the Venturi effect exploiting existing circulation flows is used to suck out the air from the gap, as in the case of Aquastill vacuum-enhanced spiral wound AGMD modules [180]. The effectiveness of air cooling in AGMD has also been investigated, yielding a design with the potential to significantly reduce the energy consumption and cost of desalination by minimizing or eliminating plant components needed by liquid coolant flow systems [181].

Some AGMD modules have been deployed and tested on an industrial scale. For example, a plate-and-frame AGMD module was designed and developed by Scarab Development AB (see Fig. S6). The Scarab flat-sheet AGMD module consists of a hydrophobic PTFE membrane (pore size: 0.2 μm, porosity: 80 %, thickness: 0.2 mm) that is supported by a permeate spacer and a backing layer. The module also includes a feed channel for saline water and an air gap channel for hot air [182]. Each module consists of 10 plastic cassettes housing two membranes each, giving a total membrane area of 2.8 m^2. As shown in Fig. S2, these cassettes are plastic frames containing channels for the feed stream and permeate, two condensing walls, and two parallel flat sheet membranes. The feed channels are formed by appropriately placed spacers and the cooling water stream can flow between the condensing walls of adjacent cassettes. This module design has the potential to increase energy efficiency while reducing the risk of pore wetting, leading to overall performance gains.

Keppel Seghers, a Singapore-based company, has created flat-sheet MD modules for PGMD (see Fig. S7). Modules with different membrane areas are available, and the small area modules can be connected in series in a counter-current configuration where the coolant stream circulates from one module to the next one to increase heat recovery. After exiting the final module, external heat can be applied to the coolant to raise its temperature to the specified inlet value before it is reintroduced to the module as a feed solution [183].

Guillén-Burrieza et al. performed a techno-economic analysis of a 100 m^3/day desalination plant fitted with plate-and-frame MD modules using heat supplied by a static solar collector field [86]. The analysis

examined AGMD and PGMD modules from Scarab AB and Keppel Seghers, respectively, and three affordable solar technologies: compound parabolic collectors, flat-plate collectors, and evacuated tube collectors. The water production cost (WPC) achieved in each case was then compared to that for a fossil fuel-powered system. When the solar collector was coupled with the most efficient MD module, the calculated WPC was in the range of 10–11.30 €/m^3, whereas that for the fossil fuel-powered system was around 7.19 €/m^3. The authors concluded that solar-driven MD can be seen as a competitor for photo-voltaic RO systems based on published data for systems with similar capacities (~100 m^3/day) but that further work to reduce their WPC would be needed to compete with fossil fuels.

Several other design modifications have been proposed to improve AGMD module performance. Most of these modifications seek to increase heat transfer within the module's feed channel or improve cooling in the condensation channel. For example, Tian et al. introduced a new modification that improves the hydrodynamic properties of the feed flow and ensures partial contact between the membrane and condensing plate [184]. These modifications increased the distillate flux up to 2.5 folds relative to a conventional module. In another study, a specially designed portable channeled coolant plate was integrated into an AGMD module to create a fin effect and reportedly increased permeate production by up to 50 % [185]. Vandita introduced a new helical condensation channel design that increased the condensation area by 45 % and improved heat transfer within the module [186], while Pan et al. introduced the concept of using two-phase flow (with the feed solution mixing with nitrogen gas) in AGMD modules, leading to improved momentum, heat, and mass transfer [187]. The authors claimed that the proposed two-phase flow system could increase trans-membrane flux up to 4.5-fold when compared to conventional single-phase flow.

Another effort to improve the permeate flux of AGMD was reported by Warsinger et al., who investigated the possibility of improving distillate production rates and thermal efficiency by using superhydrophobic surfaces on the permeate side [188]. Their experiments examined a wide range of condensation surfaces including traditional, hydrophobic, and superhydrophobic variants, revealing that permeate production in systems with superhydrophobic surfaces was up to 60 % higher than in conventional AGMD systems. In another work, the authors investigated the effects of condensate flow patterns and air gap design on permeate flux and thermal efficiency in AGMD modules by varying parameters including module slope angles, inlet temperatures, gap spacer design, and condensing surface hydrophobicity [189]. This work also introduced a novel visualization technique in which a transparent sapphire plate with high thermal conductivity is used as the condenser surface to observe flow patterns in the air gap. The slope of the AGMD flat-plate module had little effect on the permeate flow except at extreme positive angles (>80°) and intermediate negative angles (−30°), where the condensate touched the membrane surface. Surfaces with hydrophobic coatings showed improved droplet shedding and reduced droplet bridging. Similar features were seen on superhydrophobic surfaces, but with smaller droplet sizes, suggesting that superhydrophobic surfaces could increase the efficiency of AGMD without creating a risk of flooding, allowing the use of lower gap widths (0.2 mm) than would be possible in systems exhibiting film-wise condensation, which would require gaps >1 mm. In contrast, pinned water patches were frequently observed close to hydrophilic condensing surfaces. These findings imply that for all tilt degrees and most module designs, the commonly accepted model based on the formation of a laminar condensate film does not correctly reflect flow patterns in actual systems. The performance of the studied system is probably intermediate between those of pure AGMD modules and permeate gap membrane distillation (PGMD) modules. Other module modifications that have been proposed are listed in Table 2 below.

Table 2
Proposed modifications of flat sheet membrane modules.

Modification	Objective	Effect	Ref.
Spacer and corrugated feed channels	Heat transfer improvement in the feed channel	• 20–50 % improvement in permeate flux • 10–40 % improvement in GOR	[190]
Combining two consecutive AGMD modules	Heat recovery improvement	• Thermal efficiency increased up to 261 % • Productivity increased up to 193 % • Specific heat input reduced up to 6.7 %	[191]
A common cooling chamber for two feed channels	Improvement and simplification of module design	• A compact double-stage module design • Reduction in energy consumption and total costs	[192]
Tubular shaped condenser	To improve the condensation process	• 66 % increase in water flux by using a simple tubular condenser • 215 % increase in water flux by adding zigzag-shaped copper ribbons to a tubular condenser	[193]
Variable module length	To improve thermal energy utilization	• Water output increased by 64.5 % • GOR increased by 50 % • Energy consumption reduced by 57.7 % • Heat input reduced by 34 %	[194]
Application of different hollow fiber module designs	To study the effect of packing density and thermal conductivity of the cooling plate on the process performance	• Higher HF packing density and gap channel density provided higher flux • Higher conductivity of cooling plate provided higher flux and lower energy consumption	[195]
Fabrication of rough surface channels	To improve heat transfer within the channel using real RO brine	• 11 % higher flux was achieved compared with smooth wall channels	[196]
Coupling of AGMD module with evaporative crystallizer	To achieve zero liquid discharge in desalination	• Maximizing flux, GOR, and water recovery	[197]
Separating feed from heating and coolant by adding a gap	Maximize once through recovery ratio, and designed for industrial purpose	• High recovery ratio of up to >90 % • Similar performance to AGMD module at high salinities • Minimizing of components in contact with highly corrosive solutions, for cost reduction and reduced maintenance	[198]

3.2.1.2. Plate-and-frame modules for DCMD. While plate-and-frame modules have gotten significant attention for AGMD applications, their use in DCMD has been limited to lab-scale systems only where a membrane is mounted in a single frame. This is mainly due to the lower energy efficiency of DCMD compared to some other configurations such as AGMD and VMEMD. The inferior energy efficiency of DCMD arises from high heat losses associated with the conductive heat transfer from the hot feed to the cold permeate side. Another issue is that it is hard to guarantee proper hydraulic circulation (counter-current and balanced) inside the large modules in DCMD which results in poor performance. Furthermore, the lab-scale systems are used to test the preliminary performance of the membranes synthesized in the laboratory or purchased commercially. Both sides of the frame have inlet and outlet ports

and the membrane is generally supported using spacers on both sides that could create greater pressure drops in full-scale modules.

Another innovation in plate-and-frame DCMD modules was created by integrating forward osmosis (FO) and DCMD into a single module [194]. In this module design, the FO part is used to extract freshwater from impaired water while the MD component concentrates the FO draw solution. Integrating the two processes yields a system that is more compact and less costly than having separate MD and FO systems.

3.2.1.3. Vacuum multi-effect MD modules. VMEMD systems operate under reduced pressure and can achieve higher water recovery rates than AGMD. A VMEMD system features multiple MD stages connected in series, allowing each stage to operate at successively lower operating temperatures and pressures. Plate-and-frame modules are typically arranged in a stacked configuration to create compact high-efficiency systems. Solar thermal collectors can be used to supply heat for the steam raiser [200,201]. Moreover, the VMEMD design enables internal heating and condensation. This can consequently reduce the overall energy consumption. The construction and working principles of these modules are described in detail elsewhere [202]. The MEMSYS VMEMD design uses PTFE-based hydrophobic microporous membranes that separate vapor from the warm feed solution, an evaporator or steam raiser, and foils over which vapor condenses (see Fig. S8). The membrane has an average pore size of 0.2 μm and the dimensions of each piece are around 335 mm × 475 mm. The steam raiser consists of alternating empty and membrane frames, starting with an empty one, and the polymeric condensation foil is around 20 μm thick. The membrane and condensation foil are separated by polypropylene mesh spacers and each membrane frame has an effective membrane surface area of about 0.31 m^2.

The evaporation point can be reduced by lowering the pressure in the steam raiser, allowing the use of lower operating temperatures (50–80 °C). This generates water vapor that can transfer the heat of condensation to the first effect. The vapor produced in the first stage in turn transfers heat to the second stage, so each stage recovers heat from the preceding one while also generating fresh water in each stage. The steam from the last effect is condensed by the condenser, whose performance is enhanced using a cooling water stream.

Studies have shown that the performance of the MEMSYS VMEMD modules (see Fig. S8) depends mainly on the temperature of the heating and cooling streams [202]. GOR values up to 2.79 and distillate flux of 3.0 L/h·m^2 were reported for a four-effect module using seawater as feed. Enhanced heat recovery was achieved by using the feed water as a cooling stream in the condenser [203]. Najib et al. showed that the use of VMEMD reduced the electrical energy required for desalination from 74.9 kWh/m^3 for a conventional system to 6.3 kWh/m^3, achieving water production rates of up to 31.8 L/h and recoveries of 36.8 % [204]. The VMEMD pilot module designs were developed by MEMSYS, which was acquired by New Concepts Holdings Limited in 2016.

3.2.2. Spiral wound MD modules

Due to their advantages over traditional plate-and-frame modules, spiral-wound modules have also been investigated for MD applications. Most of these studies have focused on AGMD and its variants [205]. Fraunhofer Institute for Solar Energy Systems introduced the technology and module fabrication principles of a full-scale (5–14 m^2) spiral wound MD module [94]. Various tests were performed to evaluate the performance of spiral wound modules in terms of water vapor flux, salt rejection, and energy consumption. The authors also explored the interaction between feed inlet temperature, feed flow rate, feed salinity, and geometrical module design parameters. The authors found that higher feed water temperatures and flow rates resulted in increased water vapor flux and improved salt rejection. Additionally, increasing the brine concentration had a negative impact on water vapor flux. The study also focused on analyzing the energy consumption of the MD process and found that the energy requirements varied based on the feed water temperature, flow rate, and brine concentration. By optimizing these parameters, it is possible to enhance the energy efficiency of the desalination process. Overall, the experimental studies provided valuable insights into the performance of full-scale spiral wound modules for desalination using membrane distillation.

In a later study, Ruiz-Aguirre et al. compared the performance of two commercial spiral wound MD modules operating in LGMD and AGMD with a membrane area of 10 and 24 m^2, respectively [206]. It was noted that the LGMD module exhibited higher flux than the AGMD module; however, the AGMD module outperformed the LGMD module in terms of GOR (7 and 3, respectively). It was also observed that distillate quality in the AGMD module was inferior to the LGMD module. In a follow-up study, Ruiz-Aguirre et al. compared the performance of the same two modules in AGMD [207]. The authors found that the larger module yields poorer productivity but better energy efficiency due to better energy recovery within the module.

In another study, a pilot-scale spiral-wound AGMD system was utilized, with a total effective membrane area of 155.52 m^2 and a design capacity of 10 m^3/day, over a 50-day operation period [208]. During the experimentation, it was observed that the flux increased from 1.16 to 1.33 L/m^2·h as the flow velocity was raised from 1.5 cm/s to 2.0 cm/s. However, as the flow velocity was further increased, the flux decreased to 1.25 L/m^2 h. This decrease was attributed to an inefficient energy source, resulting in a general temperature decrease. The evaluation of energy efficiency was done using GOR, which showed values exceeding 2. Regarding the distillate quality, it was found to be acceptable, with most conductivity values of the distillate below 200 μS/cm for a feed salinity of 35 g/L. Additionally, a minimum rejection rate of 99.0 % was achieved for concentrated water used as the feed solution. To improve the system's performance, it was recommended to introduce proper temperature control in the feed and cooling tanks, as the temperature of natural seawater varies and significantly affects the plant's operation. In another study, Andrés-Mañas et al. explored the use of vacuum enhancement in AGMD for improving permeate production and thermal efficiency using three different multichannel spiral wound modules with different internal designs, varying operating conditions including feed temperatures and flow rates [209]. Vacuum enhancement was found to have a significant impact on performance, especially at low hot temperatures and longer residence times. Vacuum enhancement was found to improve the permeate production and thermal efficiency, especially in the module with long residence time operated at low feed temperature. Vacuum enhancement showed the potential to increase the permeate flux by as much as 88 %, while simultaneously reducing specific thermal energy consumption by up to 70 % as compared to the conventional AGMD operation. Vacuum enhancement also reduced hydraulic pressure drop, resulting in a 26 % decrease in specific electrical consumption.

A few studies on spiral-wound modules have examined the potential of this module construction mode in DCMD. In conventional DCMD, the cold feed is heated at the evaporator channel inlet and flows in the opposite direction to the permeate. The concentrate then exits the module at the evaporator outlet while vaporized water passes through the hydrophobic membrane, condenses in a distillate channel, and exits through the distillate outlet [210,211]. Compared to others, the spiral wound module displays minor heat losses due to its compactness and the fact that hot streams in the inner part of the module are naturally insulated by the cold streams circulating in the outer part of the module [211–213]. Winter et al. tested multi-channel spiral wound modules in DCMD applications and found that their use reduced the spatial footprint of MD systems while also providing an optimized flow distribution and requiring less complex and costly external hydraulic connections than alternative systems [164]. The new modules generated distillate flow rates as high as 126 kg/h at a thermal efficiency of 66 % and had a specific thermal energy demand of just 215 kWh/t with an optimal heat recovery arrangement.

The effect of varying the channel length and width on the performance of spiral-wound membrane modules in DCMD and PGMD has also been analyzed; DCMD was found to yield higher fluxes than PGMD and was therefore declared more suitable for large-scale applications [214]. In another study, the performance of spiral-wound MD modules supplied by Aquastill BV was tested in DCMD and AGMD configurations [215]. Although the AGMD configuration had substantially (four-fold) lower fluxes than DCMD in lab-scale trials, it had a slightly higher flux and GOR in pilot-scale trials. This was attributed to the filling of the gap compartment, membrane compression, and restrictions on inflow velocity and energy in the pilot-scale trials.

Najib et al. performed a comprehensive investigation using experimental data to assess the performance of a DCMD system under various operating conditions, both with and without a heat recovery device operated on spiral wound membrane modules [216]. Through energy and exergy analysis, multiple performance parameters of the spiral wound MD module were estimated. The study showcased the advantages of employing a heat recovery system, particularly in terms of enhancing energy-related performance parameters such as performance ratio, gain output ratio, specific energy consumption, and specific exergy consumption for the evaporator and condenser streams. It was observed that the maximum production of distillate water occurred at the highest operating conditions ($Q = 300$ L/h and $T = 80$ °C), yielding around 17.4 kg/h, with a recovery ratio of 6.5 %. However, an inherent tradeoff was identified between high operating conditions (i.e., feed temperature and flow rate) and improving system productivity, as higher operating conditions lead to increased energy demands for the membrane module's separation process. Despite the significant positive impact of the heat recovery system on energy-related performance parameters, its influence on the productivity of distillate water in the membrane module was found to be negligible. Evaluation of the specific energy consumption for the evaporator, condenser, and the entire MD system demonstrated a considerable decrease to <300 kWh/m^3 when heat recovery was enabled. The study's main performance criteria, including recovery ratio, performance ratio, gain output ratio, and specific energy consumption, aligned with findings from existing literature.

To the best of our knowledge, there is no study reported on using spiral wound membrane modules for traditional VMD configuration.

3.3. Optimizing the contact length of MD modules

An important issue in MD module design relates to the module's dimensions and the overall contact length. The contact length can be defined as the overall distance over which the hot feed stream is in contact with the membrane without being reheated. In principle, high contact lengths can be achieved by increasing the membrane length (i.e., the fiber length in hollow fiber systems, or the channel length in flat-sheet ones). However, technical, handling, and installation problems make the preparation and deployment of very long modules impractical. Alternatively, high contact length can be achieved by connecting multiple modules in series or increasing the number of channels in the same module. As thermal energy demand of MD can be simply and effectively mitigated by recovering the latent heat of condensation from the permeate for feed preheating, therefore, a long contact length is needed for effective recovery of heat within the feed. Some recent publications on the design of MD modules for large-scale applications have highlighted this issue. For example, in a study on spiral-wound flat sheet membranes, Winter et al. found that the gain-to-output ratio could be improved up to three-fold by increasing the flow channel length from 1 to 7 m [217]. Similar observations were reported by Ruiz-Aguirre et al., who reduced the specific thermal energy of MD consumption from 296 to 107 kWh/m^3 by increasing the channel length from 1.5 to 5 m [218]. Ali et al. also demonstrated that increasing the channel length (whose effect is similar to increasing the module length) from 1 to 10 m reduced the specific energy consumption of DCMD by over 20 % [219]. Another study showed that increasing the channel length from 3.5 to 10 m reduced the specific energy consumption of AGMD by up to 46 % [94].

To incorporate large hollow fiber lengths and membrane areas within a single module, Tsai et al. introduced multipass hollow fiber membrane modules, as illustrated in Fig. 11 [220]. By varying the operational mode of the modules (i.e., the order in which the feed and permeate flow in counter-current and co-current directions on different passes) as well as the number and length of passes and the operating temperature (see Fig. S9a–d), it was discovered that a traditional single-pass configuration provided the highest permeate flux. However, the energy consumption when using the multipass module in pure counter-current mode was up to 35 % lower than when using conventional single-pass modules. Additionally, reversing the flow direction at the end of each pass did not cause a significant pressure drop within the module. These findings may provide a basis for the design of more energy-efficient next-generation MD modules for desalination and brine management.

It is worth quoting that an increased channel length in MD modules can lead to increased capital expenditure. Put simply, the relationship between channel length and permeate flux is always a matter of weighing the capital expenditure (CAPEX) against the operational expenditure (OPEX).

3.4. Spacer design for MD modules

Spacers are key elements in the design of membrane modules whose purpose is to provide mechanical support to the membrane [160]. Fig. 12 provides general spacer configurations which have been used in various membrane modules whereas a timeline of important milestones in spacer development is provided in Fig. 13. The use of spacers improves MD performance by increasing turbulence while minimizing temperature and concentration polarizations in the feed channel [8]. Spacers also create channels for the feed and distillate streams by separating the membrane from the condensing surface in AGMD modules [221]. It is therefore unsurprising that the properties of the spacer material strongly affect process performance. For instance, the temperature distribution along the interfacial region of the membrane depends on the design and makeup of the spacer material. Spacers can be made from insulating (plastic) or photothermally and electrically conductive (steel) materials. Other insulative and conductive materials may also be used, depending on their costs [222]. According to Cai et al., the use of thermally conductive materials reduces the spacers' thermal resistance and thus improves heat transfer [223]. Moreover, photothermal and electrically conductive materials enable localized heating induced by light irradiation and Joule heating, which increases the membrane surface temperature and thus the vapor pressure and permeate flux [224].

Spacers can also differ in opening size and thickness, which may affect performance in specific applications. According to simulation results, relatively thick spacers providing a spacing gap of 3–4 mm are preferable for use in MD channels [226,227]. However, spacing gaps in the range of 1.5–3.5 mm also produce acceptable rates of water recovery. In addition, conductive spacers were found to increase the temperature polarization coefficient, heat distribution, thermal efficiency, top and bottom membrane surface heat transfer coefficients, and permeate flux when compared to non-conductive alternatives [228].

Membrane modules may use either net or tricot spacers. Net spacers are characterized by large openings and thus require moderate operating pressures. Conversely, tricot spacers have dense structures and small openings and thus provide acceptable mechanical support with high deformation resistance at high pressures. However, these spacers tend to reduce productivity due to increased mass transfer resistance. Spacers should also provide optimal pore opening sizes to give the membrane adequate support while ensuring minimal resistance to mass flow and maximizing the effective membrane surface area [229,230].

A range of new spacer designs have been investigated to improve MD

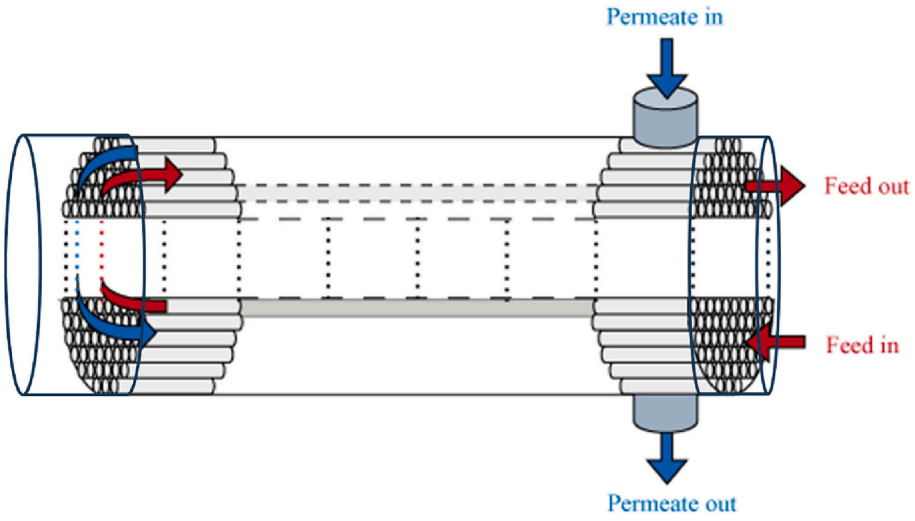

Fig. 11. A schematic illustration of multipass hollow fiber membrane modules introduced by Tsai et al [193].

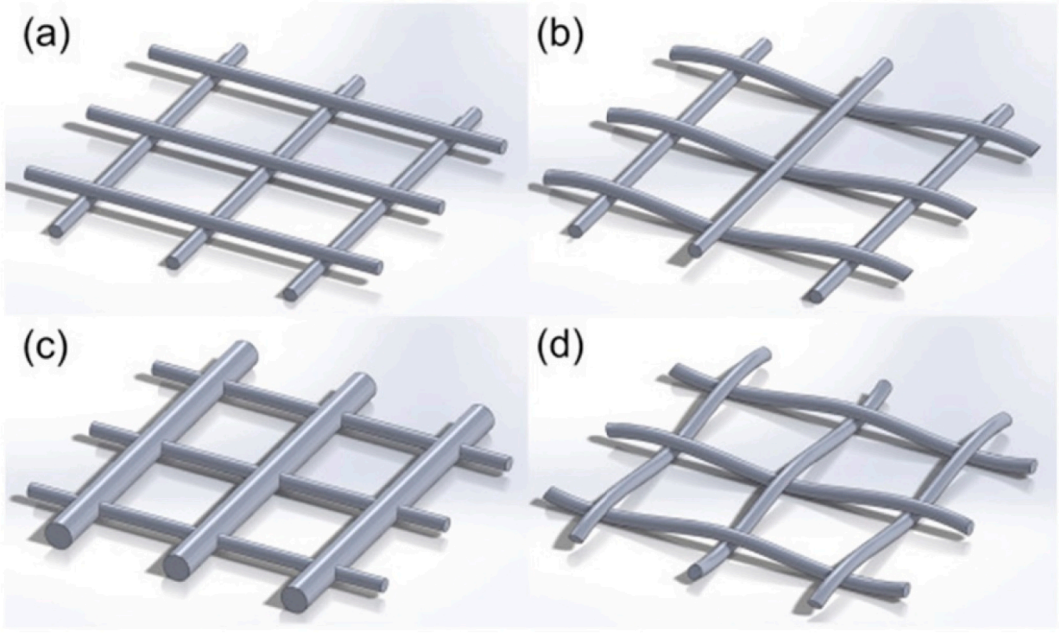

Fig. 12. General spacer configurations. (a) Nonwoven spacers, (b) partly woven spacers, (c) intermediate layers, and (d) completely woven spacers [225].

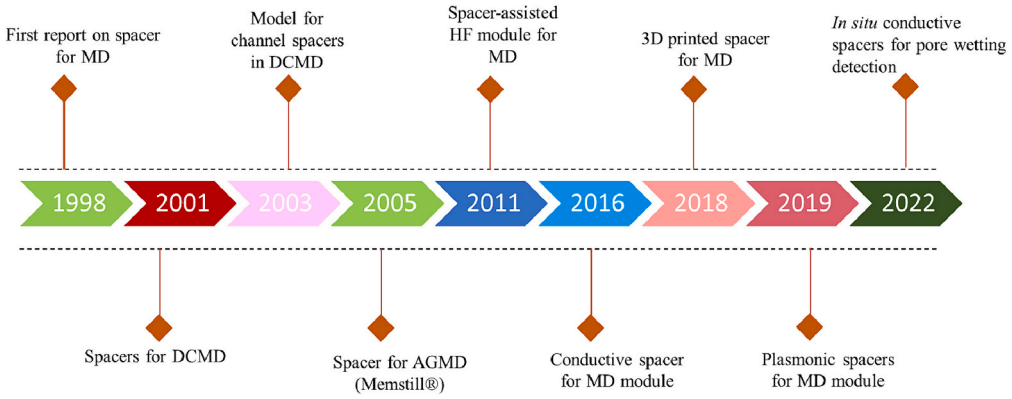

Fig. 13. A timeline of important milestones in spacer development for MD.

processes by increasing permeate flux while reducing energy consumption. For example, conductive spacers can be used in electrochemical sensing systems to detect membrane wetting in MD modules. In such systems, when an electrical potential is applied to a conductive spacer, a detectable current will be generated upon interaction with the dissolved salts of the distillate. This current serves as a signal warning of membrane wetting that could be used to trigger the implementation of corrective measures to maintain optimal operating conditions that provide high separation efficiency and mass transfer [231,232].

Specific applications may call for the use of spacers with diverse shapes and structures including helical or cross-diagonal designs, mesh-like structures, or cylindrical filaments [224,233,234]. Experiments and numerical simulations have shown that spacer design can significantly affect permeate fluxes and separation factors, prompting Ho et al. to propose a new design for DCMD modules using cross-diagonal carbon-fiber spacers with various hydrodynamic angles in flow channels to increase turbulence intensity and thus improve the rate of water production and rejection efficiency [233]. The enhanced turbulence produced by these spacers generated wakes and eddies that reduced temperature polarization and increased heat and mass transfer, leading to improved permeate fluxes [199]. In addition, heat transfer coefficient calculations using simplified mathematical models indicated that the permeate flux was higher when using the counter-current flows for which the spacers' hydrodynamic designs were optimized than when using co-current flows, validating the experimental findings [233]. A separate study confirmed that varying the properties of spacer-filling channels can strongly affect heat transfer and permeate flux; coarse spacers with larger openings increased permeate fluxes by approximately 30 % and roughly doubled the associated heat transfer coefficients [235].

New spacers for MD have recently been designed and produced using 3D printing technology. For instance, Castillo et al. investigated the efficacy of innovative 3D-printed spacers in controlling scale formation during DCMD experiments [236]. These spacers, which were designed to have triply periodic minimal surfaces (TPMS), were assessed under $CaSO_4$ scaling conditions. The most effective TPMS spacer (the tCLP model) delivered a 50 % increase in flux compared to a conventional spacer, although it also caused the pressure drop to increase. In addition, modules using commercial spacers showed more scaling than those with TPMS spacers. On the other hand, the TPMS spacers' micro-rough surfaces caused more scaling to form on the spacers themselves (Fig. 14). In another study, Li et al. systematically examined the effect of a 3D-printed helical baffle on VMD performance with a high salinity feed solution [237]. The new baffle increased permeate flux by 6–46 % (depending on flow rate) and boosted average membrane shear by approximately 60 % without significant additional pumping power. In another study, Thomas et al. investigated the use of 3D-printed TPMS spacers in AGMD and DCMD. Their effects on MD were evaluated based on the flux, the feed channel pressure drop, and the levelized cost of water (LCOW) [238]. When compared to a commercial spacer, the TPMS design increased the DCMD flux by 57 % but delivered only a 17 % flux improvement in AGMD. The authors also noted that in an MD process using thermal energy from waste combustion or waste thermal energy in industry, the reduction in channel pressure caused by the new spacer design was the most important factor affecting LCOW. These results suggested that DCMD processes powered by waste thermal energy are more sensitive to spacer-induced reductions in channel pressure than AGMD processes.

In a recent study, Jeong et al. investigated a novel carbon nanofiller-embedded 3D printed spacer with multi-scale roughness that was designed to enhance MD efficiency by mitigating polarization effects [239]. Their results showed that the use of these spacers increased permeate flux substantially — a design with 2 % incorporated CNT yielded flux increases of up to 75 %. This improvement was attributed to local turbulence enhancement due to the spacer's multi-scale roughness, which also increased the rate of vapor transport through the membrane.

Modifying the feed spacers' surface rather than the membranes could be an effective anti-scaling strategy in MD because it does not interfere with the MD membrane's functionality. To test this hypothesis, Thomas et al. developed a 3D-printed polyamide spacer coated with fluorinated silica nanoparticles for DCMD applications and compared its performance to that of spacers coated with other materials having different chemical properties [240]. It was found that the fluorinated coating reduced sealant attachment by 74 % compared to the uncoated 3D spacer and also reduced foulant deposition on the membrane surface by 60 %. These beneficial effects were attributed to the spacer's enhanced hydrophobicity, which resulted from its microscale roughness, and its low surface free energy, which weakened the interaction between the scalant and the spacer surface. Furthermore, the authors contended that the scalants are rapidly displaced from the fluorinated spacer as a result of the combination of feeble adhesion and intense shear forces during dynamic flow circumstances. As a result, the use of the fluorinated spacer is anticipated to interrupt the consistent growth of crystals on the membrane surface, causing the observed reduction in scaling [240].

Another novel strategy for module design in membrane technologies (including MD) involves the use of membranes with engineered surface patterns [241]. Ray et al. used this approach to develop a novel anti-wetting membrane surface with hierarchical microstructures for MD [242]. This unique surface-engineered design with micropatterned

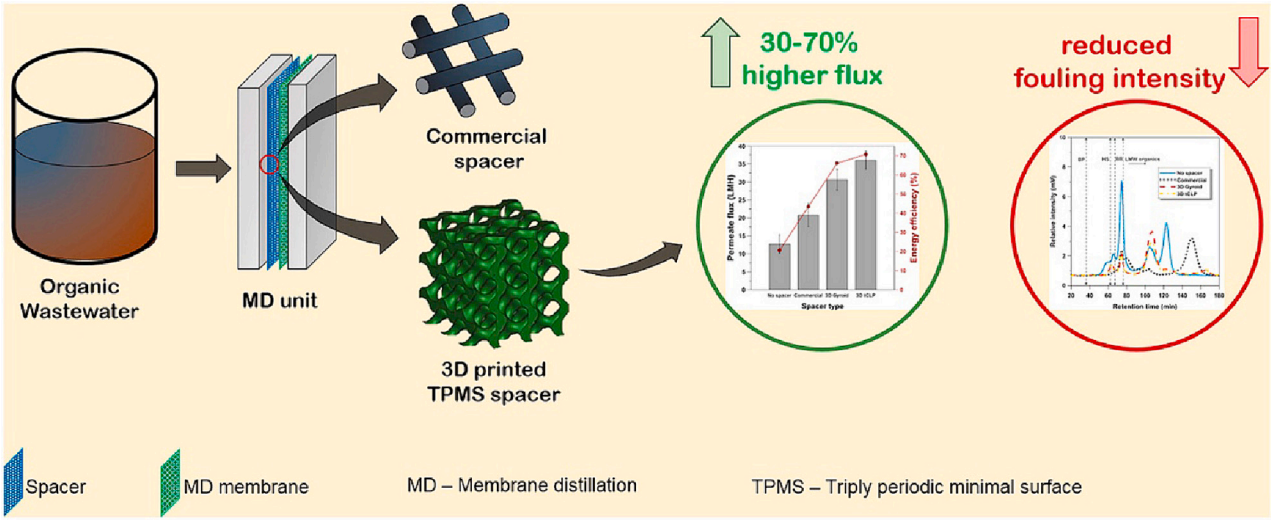

Fig. 14. 3D printed TPMS spacer and its effect on the MD performance in terms of permeate flux and fouling [236].

arrays was created using a 3D-printed molding phase separation method in which 3D-printed templates with micron-sized pillars of various shapes were used to generate air pockets when imprinted on a polymeric membrane. The results obtained revealed that the new MD module exhibited good anti-wetting performance with enhanced permeate flux and salt rejection.

4. Simulation for MD module design

In designing and optimizing MD modules, predicting the permeate flux and modeling the flow and thermal behaviors inside the module are important issues. This is because momentum, heat, and mass transfer simultaneously and concurrently happen inside an MD module. However, modeling the permeate flux and its predictions as well as studying thermal and flow behavior in the feed and permeate channels using the common modeling approaches would be complicated and need simplification assumptions. Moreover, these models have mostly been developed for a specific flow regime and module geometry. As a result, the accuracy of the results decreases, and they cannot be reliably used for optimizing MD modules [71,243]. Moreover, these common modeling approaches cannot provide local heat and mass transfer coefficients nor temperature and concentration distribution profiles in an MD module [61]. However, computational techniques, such as the computation fluid dynamics (CFD), can help to better understand the effect of module design and operating parameters on temperature and concentration polarizations and permeate flux inside an MD module. Moreover, CFD simulation can enable virtual module prototyping, as well as the estimation of local velocity, temperature, and concentration profiles for MD processes. All these are essential for understanding and overcoming bottlenecks in MD module design before expensive trials in fabricating physical prototypes [8,244].

4.1. CFD for hollow fiber modules

Tang et al. [245] reported the early results of applying CFD for the simulation of a hollow fiber module for VMD-based desalination. The authors studied a steady-state numerical simulation of the 2D model for a VMD module using FLUENT program. This work estimated and examined vapor volume rates at varied feed temperatures. Although the authors offered the premise and ideal for numerical modeling of HF modules with VMD configurations, the reported scenario overlooked the membrane wall thickness. Yu et al. investigated heat and mass transport in a DCMD module under laminar flow conditions [246]. The authors developed a 2D heat transfer model by linking latent heat from DCMD to the energy conservation equation. This could provide temperatures on the HF wall, temperature polarization, predicted thermal boundary layer build-up, local mass flux, local heat transfer coefficients, and thermal efficiency. According to the obtained results, temperature polarization increased along the fiber length. Local Nusselt numbers were higher at feed/permeate side openings. Moreover, heat transfer coefficients in the feed side were half the permeate side under the anticipated operating circumstances, demonstrating that shell-side hydrodynamics dominate the heat transfer in an HF DCMD system. Furthermore, the CFD-based simulation demonstrated that higher feed/permeate circulation velocities could increase transmembrane flow but reduce thermal efficiency owing to heat loss along the HF module.

As mentioned in the previous section, spacers can be used as turbulence promoters to enhance the heat transfer inside the MD modules. Yang et al. extensively investigated nine modified HF modules with different turbulence promoters to improve module performance for DCMD [247]. According to the obtained results, in comparison to the unmodified module, the heat-transfer coefficient in the feed side of modified modules showed substantially slower declining trends over the HF length. Using annular baffles and floating round spacers could increase the heat transfer coefficient by six times. Moreover, the temperature polarization coefficient and mass flux distribution curves of these spacer-modified modules consistently showed rising trends and improved optimally by 57 % and 74 %, respectively. It was proven using the local flow fields and temperature profiles from CFD simulations that the shell-side hydrodynamics and consequently heat transfer could be improved by careful selection of turbulence promoters. This was provided by promoting strong secondary flows and radial mixing. In another work, Yang et al. investigated the potential for micro-structured HF designs to improve the efficacy of DCMD [248]. The authors evaluated 10 distinct geometries of HF (wavy and gear-shaped surface topology, see Fig. 15(a)). According to the obtained results, the wavy fiber design could boost the heat transfer coefficients of the feed channel by up to 4.5 times, while a gear-shaped fiber design could increase the heat transfer coefficients of the permeate channel by ~5.5 times. Moreover, the gear-shaped fiber module outperformed the straight fiber design in terms of average temperature polarization coefficient and mass flux by 57 % and 66 %, respectively.

Want et al. designed novel feed distributors with three different shapes for a VMD module equipped with HF [249]. Results revealed that the pyramidal shape distributor (Fig. 15(b)) in the feed channel could raise the permeate flux by 6-12 %. Some other early studies also investigated the application of CFD for the simulation of different MD configurations. However, most of them were focused on simulating fluid hydrodynamics, temperature polarization, and transport phenomena in different HF modules [250–254]. Some recent studies, however, considered CFD along with experimental design techniques, such as response surface methodology (RSM) for optimization of HF modules for MD processes. For example, Qi et al. studied the remediation of mine water using a VMD module [255]. The authors examined the change in mass and thermal transmission during RO mine water treatment by VMD, using COMSOL Multiphysics and RSM to investigate the impacts of different parameters on the flux and heat transfer efficiency. According to the obtained results, vacuum pressure and membrane length showed the most and the least negative effects on the permeate flux, respectively. However, higher feed temperature could increase the convective heat transfer in the feed channel. In another work, Pang et al. developed a novel VMD module with a central perforated HF design [256]. According to the obtained results, the perforated HF design could decrease the mean vapor pressure more effectively than suction from the exterior. Moreover, double suction allowed for a more uniform distribution of pressure on the shell side, providing 50–70 % greater permeate flux under double suction than under single suction.

4.2. CFD for flat sheet modules

CFD simulations have also been applied for a better understanding of the transport phenomena inside the MD modules with flat sheet design [244]. Some other studies investigated the effect of spacers for imposing turbulence flow and reducing the temperature polarization on the feed channel. In one of the early studies, Cipollina et al. investigated the effect of nine different commercial and custom-made spacers designs on temperature polarization and pressure drop in the feed channel of a flat sheet MD module [257]. According to the obtained results, thinner spacers with filaments primarily parallel to the direction of fluid flow could perform better in terms of lower temperature polarization and pressure drop. Ghadiri et al. applied CFD to simulate pressure and temperature distributions as well as Reynolds number and diffusion flux in a DCMD module with counter-current flow arrangement containing a flat sheet, nanoporous membrane [258]. The authors observed good agreement between the simulation results and experimental data. Moreover, they concluded that for the investigated system, the Knudsen-Poiseuille flow model could simulate membrane water vapor diffusion. In another work, Al-Sharif et al. developed a tool based on an open-source OpenFOAM code in CFD for a better understanding of the effect of heat transfer parameters and hydrodynamics on MD module design [259]. The focus of this work was on how spacer geometrical aspects can affect pressure drop and temperature polarization. Based on

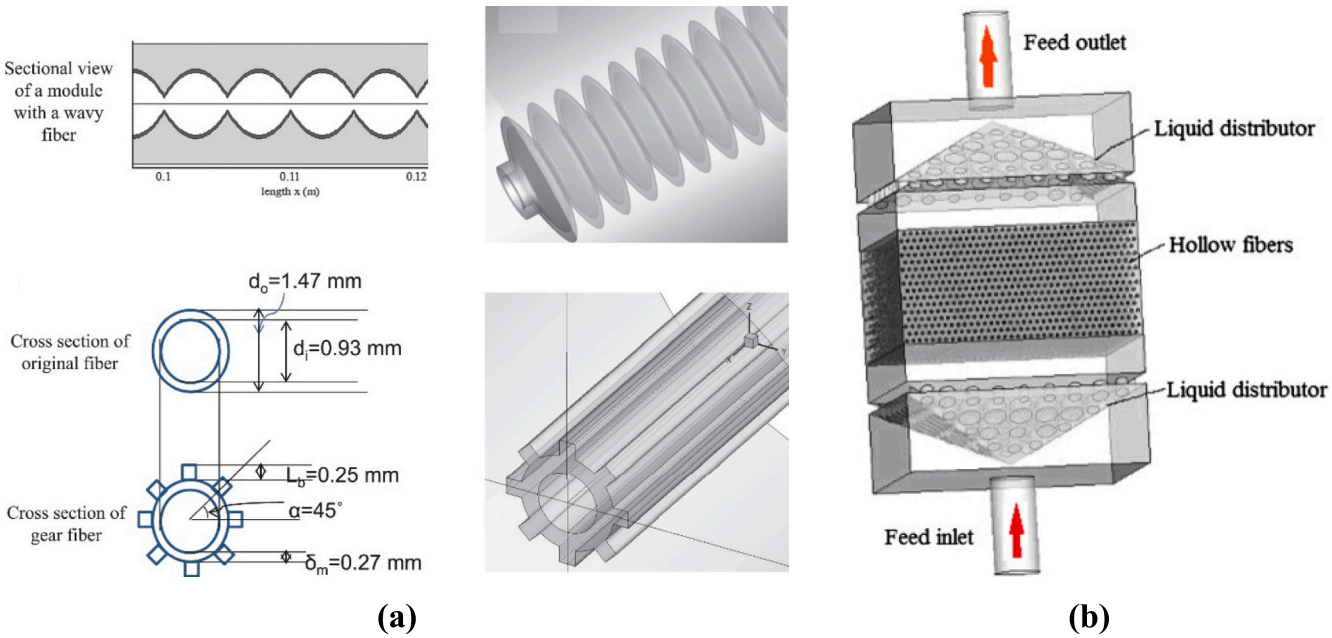

Fig. 15. (a) 3D geometric structures of modules with wavy fiber and gear-shaped fiber [220]. (b) A conceptual representation of the feed flow in a cross-flow HF module [221,222].

the provided discussion, it was observed that the 3-layer spacer with wall-adjacent filament layers aligned with the flow direction had the lowest pressure loss and symmetrical temperature profile, while the 2-layer flow-aligned square spacer had the worst pressure dips and uneven temperature and velocity profiles.

Further to spacers in the feed channel, the channel roughness can also be considered as an approach for designing better MD modules in terms of promoted mass transfer and minimized temperature polarization [260]. Chang et al. simulated DCMD modules with smooth and uneven surface channels, exhaustively [261]. According to the discussion in this work, although the heat transfer in the boundary layers near to the membrane surface is the limiting parameter for the permeate fluxes; nevertheless, it is disputed whether or not standard correlations derived for rigid heat exchangers can be applied to MD. According to the obtained results, the thermal entrance effect, which results in a very high permeate flux and heat transmission coefficient, was significant for the modules with rough channel surfaces. Another finding was that the averaged heat transmission coefficients of the entire module were quite far from what conventional correlations would predict. As a result, the authors concluded that it can be inappropriate to explicitly apply the conventional correlations of heat transfer coefficients to MD modules.

When it comes to the design and optimization of novel spacer-filled channels for MD modules, it is of the utmost significance to conduct an analysis of the flow fields as well as the temperature distributions. However, few studies provided any local information regarding the temperature distribution on the membrane surface. This can be due to the lack of reliable models and techniques and the limitation of experimental approaches to provide local data on the membrane surface. In this regard, Tamburini et al. developed a non-intrusive experimental technique that is based on the utilization of Thermochromic Liquid Crystals (TLCs) and Digital Image Analysis (IA) [262]. The proposed technique can provide comprehensive information about spacer-promoted feed channels in MD modules. According to the author's claim, this technique could ascertain the local distribution of convective heat transfer coefficients. Using this information, it would be possible to discuss the advantages and disadvantages of various spacer configurations and get excellent benchmark data for research using CFD.

In a comprehensive investigation, Katsandri conducted a simulation study to understand shear stress and velocity in a flat sheet DCMD module [263]. The author used ANSYS CFX to generate a three-dimensional CFD model to explore how hydrodynamic angles (45°, 90°, and 0°) affect shear stress and velocity profiles, with the assumption of a totally permeable membrane. Considering this assumption, heat, and mass transfer phenomena were analyzed using FORTRAN user-subroutines at the feed-permeate boundary intersection. According to the obtained results, flow alignment did not depend on Reynolds number (*Re*). Moreover, two main flow patterns were observed, including zig-zag bulk flow and filament-parallel flow, which were determined by hydrodynamic angle. According to the observations, among the investigated hydrodynamic angles, the greatest mixing which could provide higher shear stress was achieved at 45°, while the least favorable configuration was 0°. The author continued the study using the same developed model to investigate the temperature polarization and heat transfer in the considered DCMD module [264]. Same as in the previous part of the study, the hydrodynamic angle of 45^o was found the best option to reach the highest temperature on the membrane surface (i.e., the lowest temperature polarization). This was confirmed experimentally, where the system could generate the greatest permeate flux of ~100 kg/m^2h by using this hydrodynamic angle. However, the minimum value for the temperature polarization coefficient was achieved using the hydrodynamic angle of 0^o.

For MD-based desalination applications with feed salinity in the range of seawater (up to 35 g/L), temperature polarization is the main limiting issue which affects the permeate flux negatively [265–268]. However, treating hypersaline brines presents an additional obstacle in the form of concentration polarization, which both lowers the effectiveness of the MD system and causes mineral scaling [269]. In this regard, Luo et al. developed a 2D CFD model in order to explore coupled temperature and concentration polarization in treating highly saline brine using a flat sheet DCMD module, and the obtained results were confirmed by experimental tests [270]. According to the obtained results, substantial increases in solute concentration at the membrane surface, which were >1.6 times the feed value, were detected. This was even though the transmembrane vapor flow was rather low. The authors concluded that in the direction that was moving downstream, the temperatures, concentrations, and vapor flow all changed quite a bit, and they were not well characterized by the typical Nusselt and Sherwood relationships that were already used in other studies. In another study,

Amigo et al. explored the interaction between fouling and hydrodynamics by using a 3D CFD model [271]. The authors claimed that their model considers and compares the induction time of salts to the residence time on the membrane surface in order to identify locations on the membrane that are prone to fouling. The model was developed for three flat sheet module configurations, including one module with no spacers, two spacer-filled modules (woven-square and diamond spacers), and one unobstructed module. The simulation results revealed that the area near the beginning of the feed channel in the unobstructed module was the one that was most likely to become clogged with debris. In the modules that were filled with spacers, the fouling zones were equally dispersed over the feed channel in the form of tiny, isolated patches. The findings of the model indicated that diamond spacers are more effective in minimizing fouling because of the increased induction times that they provide. Choi et al. simulated baffled DCMD modules using CFD and investigated the effect of baffle type on mitigation of inorganic fouling [272]. The authors discussed that the baffled modules showed the ability to produce increased shear stress as well as oscillatory vortices and mixing (Fig. 16(a)). Moreover, the findings of the experiments demonstrated that fouling caused by scale development was prevented from occurring as effectively in the modules that had orifice baffles as opposed to the other modules.

4.3. CFD for other simulation approaches

Some other simulation studies also investigate other MD configurations and apply them for various purposes. For example, Yazgan-Birgi et al. [273] and Perfilov et al. [274] used CFD-simulations for the PGMD and SGMD modules, respectively. According to the results, in PGMD the permeate gap resistance dominates when the MD coefficient is high. In case of SGMD, the input flow temperature was significant, while the permeate flow temperature had minor influence on permeate flux. Shakin and Haque investigated the effect of spacer orientation on the momentum transfer in a DCMD module [275]. Based on the analysis of several spacer geometrical arrangements and orientations, the authors claimed that the configurations in which the spacer filaments are aligned in a direction that is counter to the membrane layers are the most optimal owing to the increased heat transfer rates. Janajreh et al. developed a CFD model for flat sheet DCMD module which is integrated with a superconductive layer and geometric undulation to study flux, energy efficiency, and temperature polarization coefficient [276]. Fig. 16 (b) shows the contours for temperature and velocity fields of baseline and undulating geometries with integration of superconductive layer. The authors discussed that combined undulated channels geometry could improve DCMD performance in terms of flux and energy efficiency more than superconductive feathering.

Choi et al. used CFD for exergy analysis of a DCMD module [278]. According to the obtained results, the exergy destruction was more important at higher feed temperatures and permeate fluxes. Moreover, although the greatest loss of exergy in the permeate occurred close to the feed intake, the effect became less significant as it moved closer to the feed exit. In addition, an investigation of the flow of exergy found that the efficiency loss on the permeate side equated to ~33 % to ~45 % of the total exergy that was destroyed. In another work, Choi et al. applied CFD in combination of design of experiments for developing and optimizing a flat sheet DCMD module [279]. In this work, the authors tried to optimize the performance ratio, permeate to feed ratio, and the permeate flux. According to the simulation results, the module length could significantly affect the permeate flux, while the channel height was more influence in terms of the two other investigated parameters. The authors concluded that the combination of CFD and design of experiments is a promising approach for optimizing DCMD modules.

In a recent study, Ansari et al. investigated the application of CFD to simulate a solar-assisted DCMD module with spacer-filled channels [280]. With a good agreement with experimental results, the authors discussed that considering a solar absorber membrane could improve the permeate flux and energy efficiency better than a solar absorber plate. The findings also shown that a module that had cylindrical spacer filaments that were detachable from the module could increase DCMD performance more than a module that contained rectangular and semicircular spacers that were connected. The authors used the same simulation technique to optimize a solar-assisted AGMD module [281]. The obtained results revealed that the application of the spacer-filled module led to an improvement in AGMD performance and produced a consistent water flow from the intake to the output. Moreover, the water flow got raised by 15 %, and the downstream performance variation of the new AGMD module was just 3 % across the board, whereas it was 21 % for the module that did not have any spacers.

In a recent study, Darman et al. simulated a wavy corrugated DCMD module. Fig. 16(c) shows the overview of the conducted simulation in this work [277]. The authors used a 3D model to look into DCMD module with both single and double sinusoidal corrugations. The performance of these module designs was then compared in term of polarizations coefficients as well as Nusselt and power numbers versus geometry parameters (i.e., spanwise frequency, streamwise, and amplitude of corrugation waves). The authors discussed that the new module design could disrupt the boundary layers, especially at higher flowrates. According to the obtained results, the permeate flux and temperature polarization coefficient could be improved by 32 and 25 %, and 45 and 36 %, for a single and double corrugated module, respectively ($Re = 1500$).

5. MD modules coupled with solar energy

As a non-isothermal separation technique, MD requires outside energy sources to warm the feed solution and to run the pumps. To enhance the competitiveness of MD in comparison to current technologies, it is imperative to focus research efforts on inexpensive energy sources or alternative heating techniques in process design. However, because the process is operated at atmospheric pressure, the contribution of the pumping energy to the overall energy consumption of the process remains low, and thermal energy is the main remains the dominant parameter. Due to this reason, it can be performed using only energy from renewable and potentially inexpensive (low-grade) energy sources such as solar thermal collectors and photovoltaics (PVs) [282,283]. This makes MD relatively attractive for water desalination because it can ensure a supply of potable water with minimal or zero greenhouse gas emissions [284].

5.1. MD modules coupled with solar energy

The integration of MD systems with solar energy could facilitate the development of improved standalone and portable water treatment systems for freshwater production in coastal and remote arid regions that could also provide valuable emergency water supplies in the aftermath of natural disasters such as earthquakes and tsunamis. If the objective is to use only solar energy to drive the MD process, it will be necessary to couple solar heat collectors with PV systems to supply energy for the pumps. Moreover, large-scale applications may require the integration of solar heat collectors with electrical energy sources to enable sustained process operation. Typical solar systems used in MD processes include flat plate collectors, solar concentrators, solar ponds, and evacuated tubes [285]. Flat plate solar collectors are the simplest of these systems, consisting of nothing more than thermally absorptive flat plates. However, several studies have investigated the use of evacuated tube solar collectors for the treatment of high saline brines using MD. For example, Kabeel et al. used an evaporative water cooler with an evacuated tube solar water heater in a pilot-scale DCMD system that produced 33.55 L/day with a pumping power and pressure drop of 0.0828 W and 158.9 N/m^2, respectively [286].

The first investigation on the potential of coupling solar energy with MD was reported by Fane et al. in 1987 [287] and a wide range of

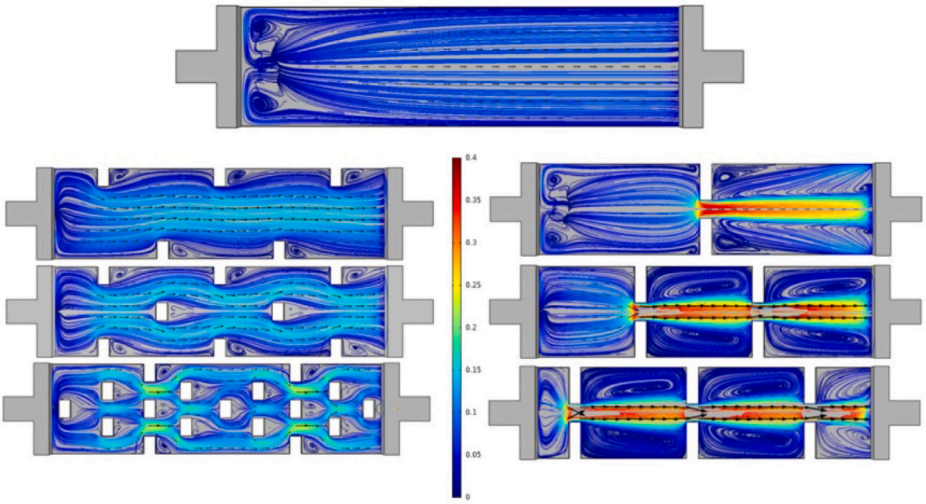

(a)

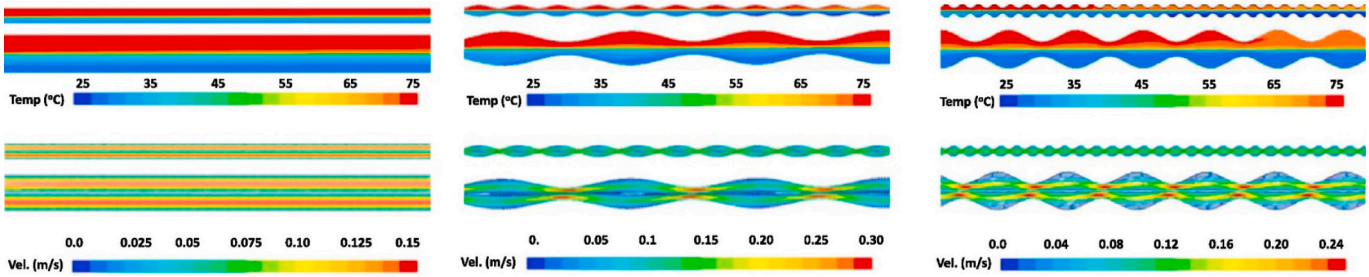

(b)

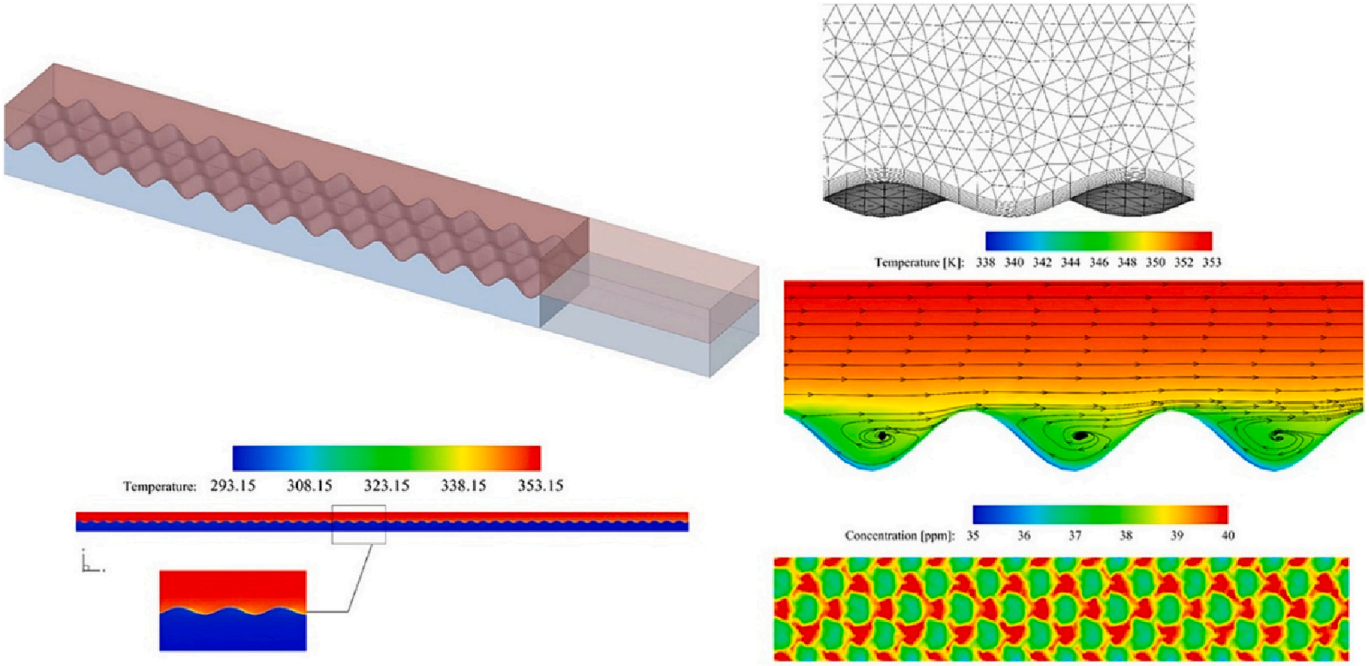

I

Fig. 16. Simulation results using CFD for flat sheet MD modules (a) CFD results of velocity magnitude (m/s) for fundamental module (top scheme), modules with plate baffles (left scheme), and modules with orifice baffles (write scheme) [272] (b) Contours for temperature and velocity fields of the baseline and two undulating geometries with superconductive thin layer integration ($Re = 100$) [276] (c) Overview of the corrugated DCMD module design by Darman et al. [277].

strategies have since been investigated to fulfill the thermal energy requirements of MD using solar energy. These strategies can be broadly classified into (*i*) heating of the feed solution externally by using solar collectors or the heat released by photovoltaic systems and using the heated feed to run an MD setup, (*ii*) integration of the membrane unit inside solar collectors or photovoltaic systems and (*iii*) photothermal conversion. These strategies have been shown schematically in Fig. 17.

The first strategy mentioned in the above paragraph is the most traditional arrangement used for heating the feed solution for MD applications. A lot of studies have been reported employing this strategy for water heating for MD. For instance, Guillén-Burrieza et al. conducted a test on a pilot-scale solar desalination system that included AGMD and a compound parabolic concentrator (CPC) that was used to heat the feed solution before entering the MD module [288]. The aforementioned system consisted of 252 CPC solar collectors, each with an individual area of 500 m^2, arranged in 84 parallel loops, each with 3 collectors connected in series. Additionally, the system included a flat sheet AGMD system with a membrane surface area measuring 2.8 m^2, which produced a high-purity distillate at a rate of 40.2 L/h. However, increasing the salt concentration in the feed stream reduced the distillate production rate by 14 % and caused the salt rejection to decline [289]. Chafidz et al. used a solar-driven V-MEMD module supplied by Memsys to create a hybrid system that can generate clean water from brackish water or seawater [290]. The proposed hybrid system uses PV panels and thermal collectors to power its electrical and thermal energy, respectively, producing high-quality water with a conductivity below 5 μS/cm and a reasonable permeate flux range (1.5–2.6 L/m^2 h). Wang et al. investigated the integration of an inclined VMD module with solar energy for seawater desalination application under real environmental circumstances in Wuhan, China [291]. This system reportedly produced 36 kg of fresh water per square meter of VMD module in a single day with a salt rejection rate of 99.67–99.987 %. The authors thus concluded that their proposed system is a promising tool for the desalination of water with a wide range of salinities. Kim et al. created a 24-stage system of this type using hollow fiber modules and found that the system's overall water production could reach 3.37 m^3/day, which is ~34 % higher than the value achieved using a system with a single heat recovery unit [292]. Moreover, the authors noted that the operating cost of MD using the solar heating system could be 28 %–36 % lower than that of the same system without solar heating.

A newly emerging variation of the "external heating" strategy is to use the excess heat removed from photovoltaic systems to heat the fed

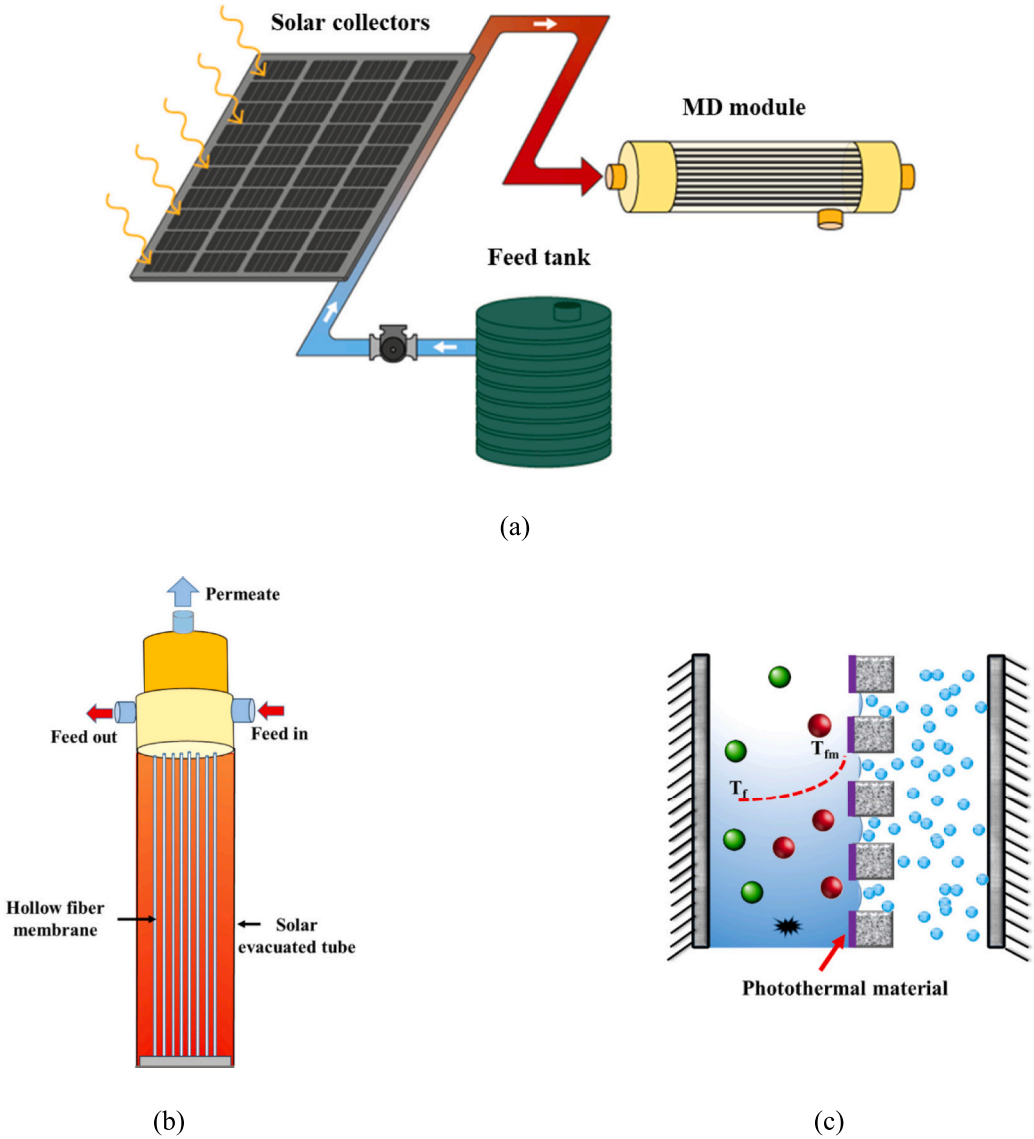

Fig. 17. Different heating strategies practiced in MD (a) traditional external heating, (b) integration of hollow fiber membranes within the evacuated tube and (c) membrane heating with photothermal materials.

solution. Elminshawy et al. studied the integration of concentrator photovoltaic module and membrane distillation as a novel cogeneration system designed to produce sustainable electricity and freshwater [293]. The results demonstrated that the system was not only capable of producing freshwater but also outperformed "non-cooled" system in terms of energy production efficiency. Thus, it was shown experimentally that the proposed cogeneration system was capable of converting up to ~83 % of the solar irradiance into useful gain and can improve power generation up to 26.90 % compared to the traditional system. The system was also capable of producing freshwater up to 19 m^3 per year and could contribute to the reduced CO_2 footprint associated with water and energy production. Some work has also been undertaken to optimize the performance of such systems and the initial results demonstrate that the maximum energy efficiency and power density of such systems are dramatically greater than those of conventional systems [294].

Solar thermal-powered MD setups mentioned in the above paragraphs consist of distinct solar thermal collector devices alongside modules for MD. Besides the additional hydraulic connections, the coupling usually requires components like a heat exchanger and a thermal storage tank for regulating the transfer of heat between the solar collectors and the membrane distillation units. To avoid this complexity and the associated impact of the investment in the solar field on the CAPEX of the total system, integrated solar-assisted MD systems are proposed where MD modules are incorporated into the design of the solar systems. For instance, Li et al. developed an integrated solar-assisted MD prototype system in which the MD modules are integrated directly into evacuated solar tubes [295]. Using this system, a 1.6 m^2 solar panel with an integrated 0.2 m^2 membrane could produce ~4 L of potable water and 4.5 kWh of excess heat energy per day. On a similar line, Bamasag proposed the integration of hollow fiber MD fibers with the evacuated solar collectors and operated the MD system in direct contact configuration [296]. The findings demonstrated that the direct application of radiation can boost efficiency and increase permeate flux by up to 17 % compared to the identical process conducted without radiation using identical operating conditions. When considering daily operations, a self-contained SP-MD unit with a membrane area of 0.035 m^2, which is heated directly, attained a permeate flux ranging from 2.2 to 6.5 $kg{\cdot}m^{-2}{\cdot}h^{-1}$, contingent on solar intensity. In another study, a floating MD module was proposed where a membrane was introduced inside a solar-eating bag used as a power source [297]. The findings suggest that employing floating solar-powered MD units is viable, as shown by their positive permeate flux and salt rejection rates. Moreover, the MD setup with upward evaporation exhibits superior permeate flux performance.

Although research on the integration of solar energy with MD modules is still at an early stage, other applications for such integrated modules are rapidly emerging. One innovative idea is to use solar-assisted VMD modules to regenerate a liquid desiccant stream in air conditioning systems [298]. Preliminary studies comparing a prototype system of this sort to a conventional thermal regeneration system showed that both systems are highly sensitive to air temperature, humidity ratio, and airflow velocity. However, the solar-assisted VMD module appears to be superior to traditional liquid desiccant regeneration systems in humid locations. Additionally, an energy analysis revealed that the amount of energy needed to regenerate 1 kg of desiccant was reduced by 10–37 % when using solar-assisted VMD, giving significant potential annual energy savings of 582.4 kWh. Another study showed that solar-assisted MD modules could be used for energy generation in addition to freshwater production or regeneration and wastewater treatment. Specifically, Li et al. integrated a hollow fiber MD module into the tubes of an evacuated solar thermal collector to create a productive and relatively inexpensive hybrid energy-water production system [299]. Their experiments indicated that a permeate flux of 4–10 L/m^2 h could be achieved with a high salt rejection rate with moderate feed temperatures of 50–70 °C. Moreover, a system with a solar absorbing area of 1.6 m^2 and 0.2 m^2 of membranes could provide 4.5 kWh of heat energy at 45 °C and 4 L/day of potable water per day. More recently, the same group developed a vertically integrated water treatment system based on the solar-assisted VMD module for use on balconies [300]. The authors claimed that they could enhance the performance of their previous solar-assisted VMD module by combining it with a compound parabolic collector for integration on a building's vertical facades. At operating temperatures of >60 °C under the most intense realistic insolation (which could provide >800 W/m^2 energy), their innovative VMD module could produce a >8 L/m^2 h fresh water. Moreover, because the module's performance when using saline feed solutions was almost identical to that for clean water, the authors claimed that this innovative system could be used for decentralized urban desalination.

Suárez et al. employed the integration of DCMD with a salt-gradient solar pond (SGSP) to generate freshwater from water with high salinity levels [301]. Despite the dissipation of heat energy in various components of the system, about 70 % of the heat produced by the SGSP was effectively utilized for the purpose of propelling thermal desalination [301].

Finally, in another innovative work, an underwater desalination system was developed by integrating an MD module with a solar-concentrating photovoltaic system to produce a so-called CPV-MD system (concentrating photovoltaic MD) [302]. This system can be made of non-metallic materials and is thus resistant to corrosion under harsh marine conditions. Fig. 18 shows the key components and operating principles of this system. It should be noted that because this integrated MD module is intended to work underwater, the angle of the incident light has important effects on its performance. However, an experimental study suggested that it performs well at various angles of illumination, giving a water yield efficiency of 28 % and a total freshwater yield of 67.8 g. Its development thus illustrates the great potential of integrating solar energy with MD systems and creates intriguing prospects to produce fresh water in marine environments.

5.2. Self-heating MD modules

Self-heating MD modules are a notable progress in the field of water treatment and desalination technologies. These advanced systems include heating mechanisms directly into the membrane module, hence improving the efficiency and energy consumption of the MD process. These modules efficiently minimize the thermal energy loss commonly experienced in traditional MD modules by producing heat near or on the membrane surface [303]. This design results in a homogeneous temperature distribution throughout the surface of the membrane, which is essential for maintaining a constant temperature difference across the membrane, a critical element to improve efficiency in the MD process. The implementation of the self-heating method not only enhances the total thermal efficiency but also enables better regulation and steadiness of the operating parameters [45]. Integrating this technology has the potential to reduce energy demands and operational expenses, therefore enhancing the accessibility and sustainability of MD. This is particularly beneficial in situations where there is a scarcity or high cost associated with external heat sources [304]. The concept of self-heating MD modules is presented in Fig. 19.

5.2.1. Photothermal MD modules

Photothermal conversion, which refers to the process of converting light energy into heat, can be considered as a self-heating strategy for MD module design. This is typically achieved using materials that can absorb light energy and convert it into thermal energy. Photothermal materials are chosen based on their ability to efficiently convert light, often in the near-infrared range, into heat [305]. Common photothermal materials include carbon-based nanomaterials such as graphene and carbon nanotubes, as well as plasmonic materials such as gold nanoparticles [306].

Photothermal heating in MD is an innovative technique that

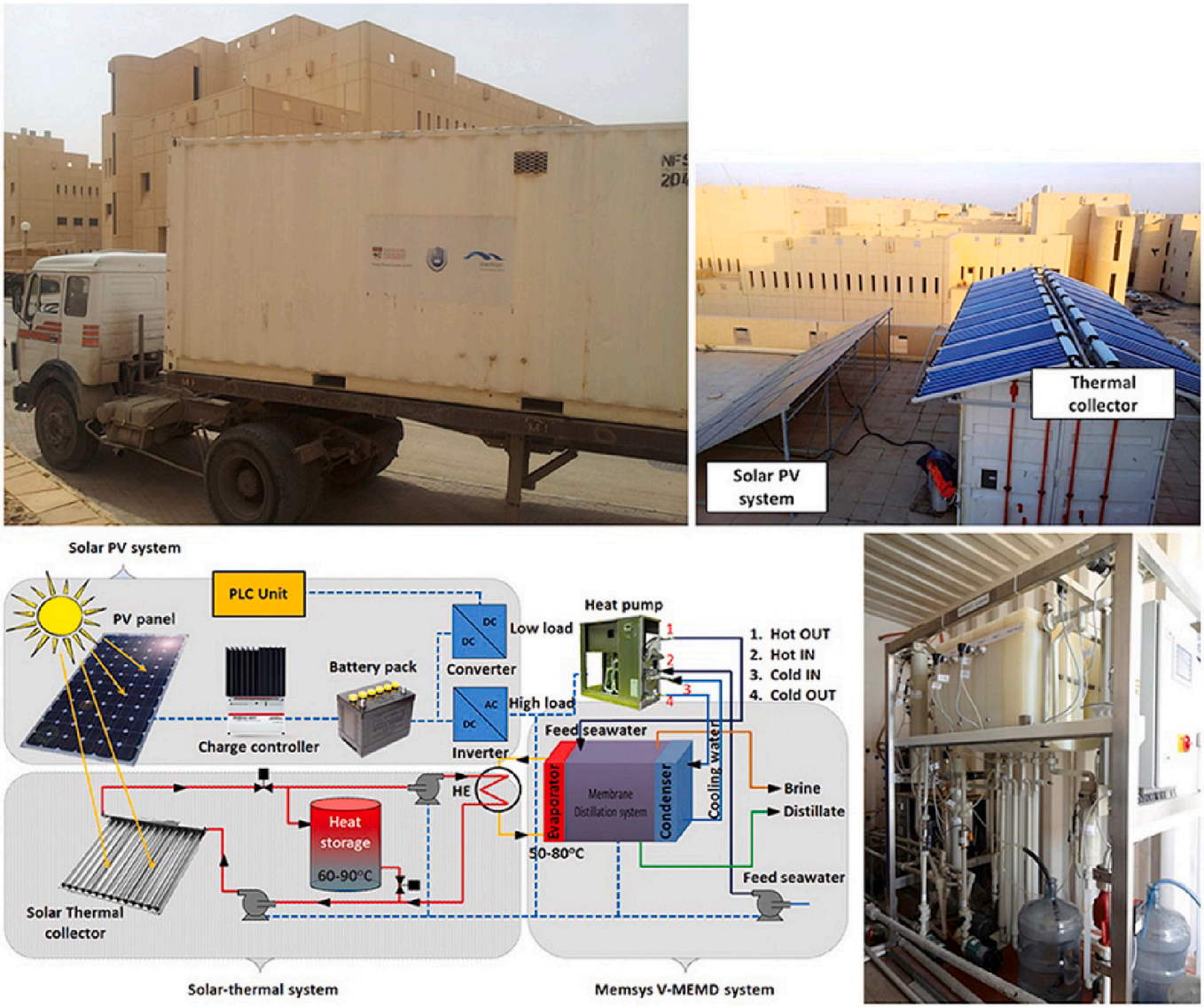

Fig. 18. Photos and schematic depiction of a portable solar-powered MD system suitable for use in remote and arid regions [290].

combines the principles of MD with the advantages of photothermal conversion to enhance the efficiency and effectiveness of the separation process. In the context of MD, photothermal heating involves incorporating photothermal materials into the membrane structure or within the feed solution [58]. When these materials are exposed to light, they generate heat, which raises the temperature of the feed solution. This localized heating at the membrane surface can significantly enhance the temperature difference between the hot feed solution and the cold permeate side, thus promoting the evaporation and subsequent condensation of water vapor more effectively [307]. Photothermal heating can reduce the energy required for heating the feed solution. This is particularly beneficial in cases where conventional heat sources might be expensive or inefficient. The localized heating provided by photothermal materials can create steep temperature gradients across the membrane, improving mass transfer rates and increasing the driving force for vapor transport. Photothermal heating also offers an excellent opportunity to combine it with renewable energy sources like solar energy, which aligns with sustainability goals and reduces the environmental impact of the desalination process [58]. Recently, the feasibility of combining photothermal and (photo)catalytic MD modules have been explored to create a very compact and efficient MD-based wastewater treatment system. This strategy has the potential to integrate several unit operations, resulting in a more sustainable and environmentally friendly MD process with the ability to reduce CO_2 emissions [308,309].

5.2.2. *Joule heated MD modules*

Joule heating, sometimes referred to as resistive heating or ohmic heating, is the phenomenon in which the flow of an electric current through a conductor can result in the generation of thermal energy [310]. Incorporating Joule heating into a MD module is a multifaceted approach that improves the efficiency of the distillation process. To do this, the membrane might be coated with a conductive layer or incorporate conductive wires or meshes, composed of materials such as copper or stainless steel, either within or beside the membrane [311]. When an electric current flows through these conductive components, they experience Joule heating, resulting in direct warming of the membrane surface. Alternatively, the membrane can be constructed using conductive materials, allowing for consistent heating when an electric current is sent across it [312]. Electrically heated spacers are also employed in certain designs to both support the structure and indirectly warm the membrane [313]. Recently, electrothermal hollow fiber modules were developed for Joule vacuum MD module, and it could achieve up to 70 % water recovery in a single pass [314]. In order

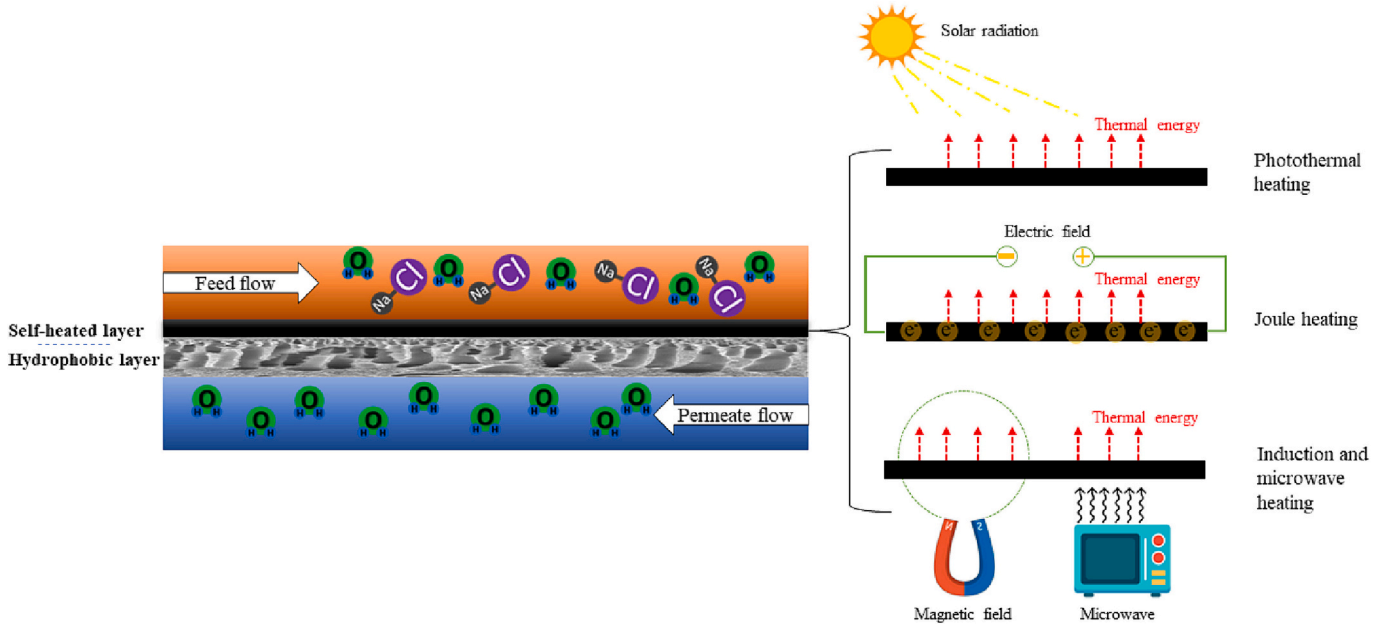

Fig. 19. Various concepts of self-heating MD modules.

to achieve the best performance and avoid excessive heat, a highly advanced control system is incorporated. Moreover, the origin of electrical energy for Joule heating might differ, including conventional grid electricity as well as sustainable sources like solar panels, which can impact the overall sustainability and cost-efficiency of the system. By incorporating Joule heating into MD modules, it becomes possible to consistently and efficiently maintain the required temperature gradient. This leads to enhanced performance, less scaling and fouling, and increased suitability in various situations, such as remote or off-grid places [315,316].

5.2.3. *Induction heated MD modules*

The incorporation of induction heating into an MD module entails utilizing a system in which membranes or module components, composed of or containing conductive materials, are heated through the use of electromagnetic induction. This is accomplished by including induction coils or conductive layers inside the module, which produce thermal energy in the conductive components of the membrane or module structure when an alternating current is applied to them [317]. Integrating ferromagnetic materials into the module can significantly improve the effectiveness of induction heating. These materials heat up quickly when exposed to an induced magnetic field. An important benefit of induction heating is its exact temperature control, which is essential for improving the performance of MD modules [318]. This control enables variations in the frequency and strength of the electromagnetic field to accurately regulate the temperature. This method is often more energy-efficient than traditional heating procedures, as it reduces heat loss and immediately focuses on the required components. The incorporation of induction heating in MD modules offers improved efficiency, enabling precise regulation of the temperature difference across the membrane. This results in higher flux rates and the potential reduction of fouling and scaling problems. Consequently, it becomes a highly appealing choice for a wide range of applications, particularly those that demand quick thermal adjustments [319,320].

5.2.4. *Microwaved assisted heating for MD module*

Microwave heating presents another novel method for heating in MD modules, capitalizing on the capacity of microwaves to produce heat within substances. This method entails using microwave radiation to either the solution being fed or directly to the membrane material, contingent upon the configuration of the module and the substances employed [321]. The primary benefit of microwave heating is its capacity to deliver fast and consistent heating, making it particularly advantageous for MD operations. Microwave heating differs from traditional heating technologies by uniformly warming materials throughout their volume, rather than only heating the surface inward. This can result in a more streamlined distillation process, since it reduces temperature polarization within the MD module. Moreover, the ability to accurately regulate heating rates and selectively focus on specific regions within the module renders microwave heating highly advantageous for MD applications that require precise temperature control [322]. This technique has also the ability to decrease the occurrence of scaling and fouling on the surfaces of membranes. The even heating prevents the formation of localized areas of high temperature, which are usually responsible for these problems [323].

5.2.5. *Thermal conduction heating for MD modules*

Recently introduced as an innovative approach, thermal conduction heating facilitates direct heat transfer to the membrane-water interface through the integration of thermally conducting layers [324]. These layers, which may take the form of meshes or shims, can be strategically positioned within the feed channel, on the permeate side, or on both sides of the membrane. Similar to membrane heating techniques, the utilization of conduction heating offers benefits such as mitigating temperature polarization, improving thermal efficiency, and present the prospect of eliminating external heat exchangers commonly employed in traditional MD heating systems [325].

6. Discussion and perspectives

6.1. *Research direction in module design for MD*

Module design is a key determinant of the performance and efficiency of MD systems. Therefore, the configuration of MD modules and their design should be guided by the application under consideration and the desired performance characteristics. A lot of interesting developments have been observed in developing new module designs for MD applications with a focus on the energy efficiency of the process. The most commercial interest in module design for MD has been on AGMD configuration where many new variants of the configuration have been

introduced. Though the main emphasis of the efforts on MD module designs in the past has been on flat sheet membranes, the focus is gradually shifting to hollow fiber membrane designs recently at the laboratory as well as commercial scale. The main innovations in new module designs for MD are targeting different hollow fiber shapes (curly, wavy, helical), outer surface designs, and new design variants of different configurations including submerged MD. New efforts have been reported also to develop AGMD using hollow fiber membrane modules. Integration of MD with solar energy has been identified as a promising method to fulfill the freshwater demand in several regions of the world where there is abundant sunshine and different module design strategies have been proposed to use solar energy for freshwater production. Despite all these efforts, there are numerous research directions where further research efforts must be devoted to broadening the commercial viability of the MD process:

- To enhance the energy efficiency of the MD process, new variants of different MD configurations and new module designs have been proposed. However, the new proposed strategies reduce the flux of the system which results in large membrane area requirements, huge footprints of the system, more electric energy consumption due to large pressure drops within the systems, and potentially higher cleaning costs. Thus, there is a critical need to develop energy-efficient module designs and strategies without compromising the flux of the system.
- Commercial scale developments on MD have dominantly been carried out by using plate and frame membrane modules which are less compact, require spacers, consume more electric energy, and are more susceptible to fouling. Therefore, more efforts should be focused on developing membrane modules using hollow fiber membranes and spiral wound configuration.
- One of the key advantages of MD is the possibility to use solar energy to fulfill its thermal energy requirements. Despite being free, the integration of solar energy with the process comes at a cost that strongly affects the economy of the process. Traditional integration strategies also require an external heat exchanger which, in addition to the cost, also increases the footprints of the system and associated electric energy cost due to the pressure drop within the heat exchangers. Therefore, economically viable, compact, and efficient solar-integrated MD systems and modules are required to improve the viability of the MD process. This requires developing advanced control systems and operational optimization for coupling MD with solar energy. In this regard, recently reported integrations of MD modules within solar collectors or photovoltaic systems are steps in the right direction. However, more research is needed to improve the design and commercial viability of these systems.
- Temperature polarization and temperature drop along the modules are identified as the major flux-limiting parameters in MD and therefore, for an economically viable process, new module designs should consider overcoming these process limitations. In this regard, module designs that promote better mixing within the flow channels as well as new feed heating strategies including membrane heating through the plasmonic effect, photothermal and electromagnetic heating can play an important role.
- Optimizing spacer and baffle design as well as flow patterns can enhance heat and mass transfer within MD modules, thereby improving performance and reducing temperature and concentration polarization. The use of advanced spacer designs in 3D-printed spacers or bio-inspired geometries can promote turbulence and minimize fouling. Thermally and electrically conductive spacers for MD modules also warrant further investigation, as do catalytic spacers because of their potential to increase the efficiency of wastewater treatment and freshwater production using MD.
- So far, the central focus of the effort on module design for MD has been the improvement of energy efficiency. However, one of the most important advantages of MD is its ability to extract freshwater from high-concentrated solutions which implies that scaling is expected to be more severe than the conventional processes. Thus, future module designs should also consider this aspect. Scaling-resistance modules could be attained by using suitable membrane materials, module designs that help in flushing the crystals from the systems and dimensioning the modules in such a way that temperature variations along the modules do not cause the precipitation of ions present in the feed at the membrane surface. The latter aspect requires the integration of knowledge of the solubility of ions and temperature polarization within the design package.
- A comprehensive strategy is necessary to tackle the reduction in permeate flux that happens during the scaling up of MD modules. An important contribution will come from the membrane materials designs which allow direct surface heating of the membrane to mitigate the temperature drop along the membrane which otherwise happened due to thermodynamic reasons. Membrane modules incorporated into the design of heat source may also overcome this issue. MD modules integrated within the photovoltaic panels to carry away the excessive heat and submerged membrane modules are two relevant examples in this regard. For the long-term operational stability of permeate flux, the proposed technique entails the development of advanced membrane materials that exhibit a high repulsion towards water and possess resistance against fouling and heat dissipation. Implementing advanced control systems for online and in-situ fouling monitoring can enhance the lifespan of the membrane in large-size modules by reducing flux decrease caused by fouling.
- With increasing applications of membranes in different fields, the volume of membrane modules to be disposed of at the end of their life will increase tremendously which may cause concerns regarding sustainability. MD modules should, therefore, address this issue right from the module design step. Thus, the module design must minimize the use of membranes as well as other housing materials and different glues used in the module manufacturing. Moreover, the module materials should be recyclable, and the assembly of the module should allow easy disintegration so that some parts may be reused or repurposed.
- A review of the published literature on MD module design indicates that the lab-scale research on the subject is not fully aligned with commercial trends. For instance, as mentioned above, most of the lab-scale investigations have been focused on DCMD and VMD applications, however, most of the commercial developments are taking place using AGMD due to its better energy efficiency. Thus, there is a need to align the lab scale efforts with the commercial interest.
- One important issue is the standardization of testing protocols for MD modules. In MD, the main performance parameters (flux and specific energy consumption) are a function of operative conditions as well as of the membrane and module characteristics. Thus, the same systems operating under different operative conditions may have different performances. Similarly, the performance of two different systems can match if they are operated under different conditions. In literature, different performance of the similar MD systems has been reported. This can be attributed to the fact that the performance of the MD system is a complex function of operating conditions, module design, and feed water characteristics. Thus, there is a dire need to standardize the testing protocols for MD for a fair comparison of different membranes, systems and module designs.
- Another important aspect to improve the viability of MD is to drive the process through a more stable source of energy, a problem especially when using renewable sources which are variable. In this regard, the incorporation of thermal energy storage systems, such as sensible heat storage, latent heat storage, or thermochemical storage, would be an innovative and attractive direction for the future development of MD modules. Such systems could help to maintain stable operating temperatures and continuous MD operation during periods of low or intermittent solar radiation and could thus

facilitate the use of MD technologies in countries with limited solar energy resources. Hybridizing different energy sources and integrating the process with geothermal heat offers an exciting opportunity to make the process stable.

- The module development for MD can also be facilitated by Artificial Intelligence (AI) techniques, which are increasingly developed for MD. The use of AI in scale-up simulation and modeling for MD involves a variety of applications: By utilizing large data sources from pilot systems, training on it, optimizing module configurations to achieve optimum efficiency, and recognizing possible scaling difficulties such as increased fouling or temperature polarization, it is able to forecast performance at greater scales. AI aids in the selection of appropriate materials for membranes and spacers, optimizing operational parameters such as temperature gradients and flow rates for large-scale systems, and performing cost-benefit assessments to evaluate the economic feasibility of scaling up. It can also optimize the incorporation of MD systems with sustainable energy sources, such as solar or geothermal power, to improve sustainability and efficiency in large-scale operations. The diverse utilization of AI in MD showcases its capacity to enhance the efficiency, cost-effectiveness, and technological feasibility of scaling up modules for different applications.
- Ultimately, by conducting thorough pilot-scale testing and implementing a progressive scale-up strategy, it becomes possible to identify and address any problems that arise at intermediate stages. This technique guarantees a smoother and more effective transition to full-scale implementation. The integration of technology innovation and strategic operational approaches is crucial for successfully addressing the problems related to scaling up MD modules.

Fig. 20 provides an overview diagram of this review. It includes several contents such as types, modeling and simulation, optimization, and challenges of MD membrane modules, so it can provide a clearer understanding of the overview of module design for MD processes.

6.2. *Future trends in module design for MD*

Prediction of the future of module design for MD necessitates the examination of several issues, such as technical progress, economic viability, environmental considerations, and special application needs. The selection of module type will further rely on the unique requirements of the application. For example, in the field of desalination and brine concentration, it is likely that larger-scale and more efficient spiral-wound modules may become the prevailing choice, while hollow fiber modules with modified designs to reach minimized polarization effects (e.g., wavy fiber shapes) can be more applicable for minerals and nutrients recovery from concentrated brines and effluents, respectively. Plate and frame modules with flat-sheet membranes may be favored in vacuum multi-effect systems for desalination and brine concentration, as well as in AGMD process for wastewater treatment or specialized applications where the importance of easy maintenance is paramount.

The utilization of advanced computational modeling and fluid dynamics in optimizing module designs is anticipated to have a significant impact, striving to achieve optimal efficiency while minimizing energy consumption.

The future trends will also be greatly influenced by the environmental effect and sustainability of the materials utilized in module design. Moreover, the mainstream adoption of a particular design will be significantly influenced by economic issues, including the expenses associated with the manufacture, operation, and maintenance of these modules. Furthermore, the ability of the technology to be scaled up to industrial levels and its capacity to adapt to different operational situations will be crucial factors.

In the future, there is also a possibility of introducing innovative module designs that integrate the most advantageous characteristics of current kinds or include new materials and technology. For example, the utilization of 3D-printed or nano-engineered modules might provide unparalleled manipulation of membrane characteristics and module structure. The emergence of 3D printing and other manufacturing techniques will enable the production of intricate module architectures

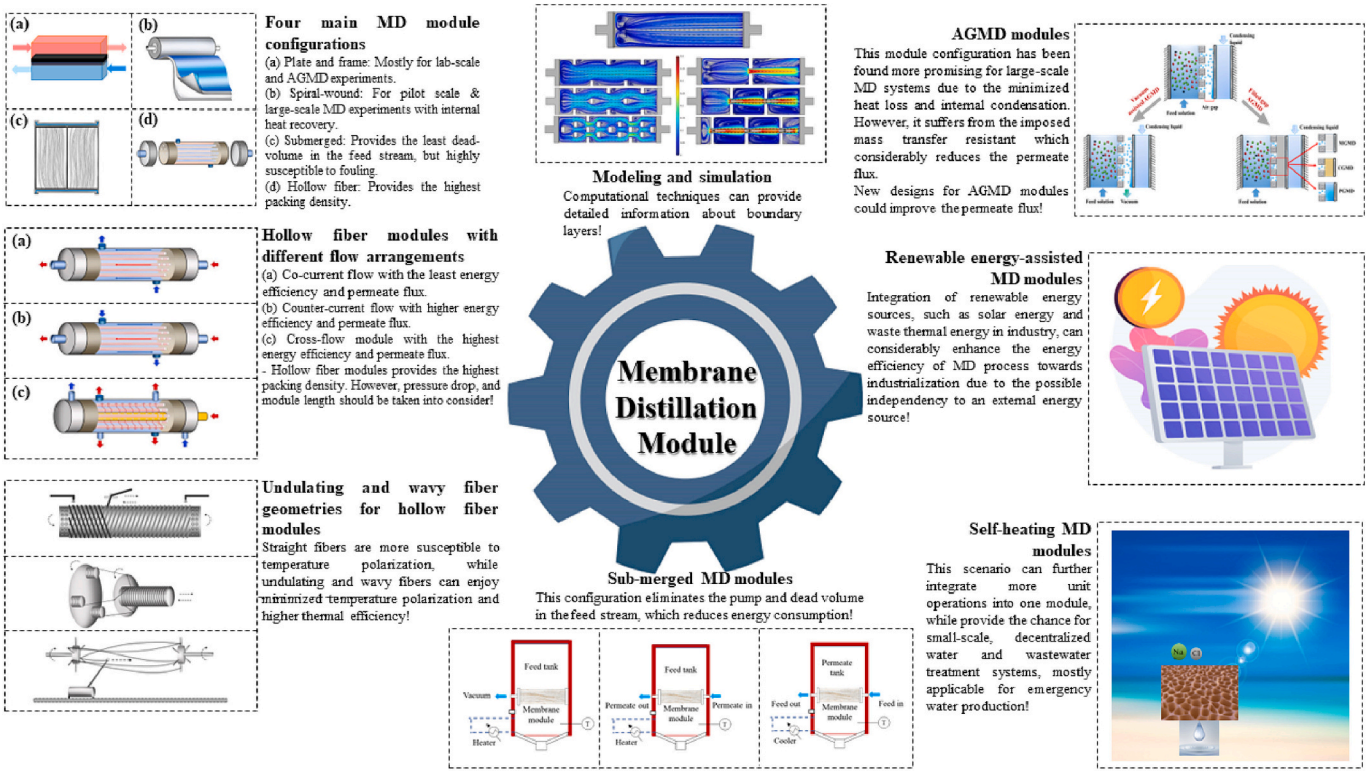

Fig. 20. Overview diagram of types, modeling, optimization, and challenges of MD module design.

tailored for specific applications.

Although it is difficult to predict with certainty which module type will dominate, it is likely that a combination of these factors will lead to the emergence of either an improved traditional design or a completely new module configuration for the MD technology.

CRediT authorship contribution statement

Aamer Ali: Writing – review & editing, Writing – original draft, Supervision, Methodology, Conceptualization. **Mohammad Mahdi Agha Shirazi:** Writing – review & editing, Writing – original draft, Methodology. **Lebea Nthunya:** Writing – review & editing, Writing – original draft. **Roberto Castro-Muñoz:** Writing – original draft, Writing – review & editing. **Norafiqah Ismail:** Writing – original draft. **Naser Tavajohi:** Methodology, Writing – original draft, Writing – review & editing. **Guillermo Zaragoza:** Writing – review & editing, Writing – original draft, Supervision, Methodology. **Cejna Anna Quist-Jensen:** Writing – original draft, Methodology, Funding acquisition, Conceptualization.

Declaration of competing interest

The authors declare that they have no known competing financial interests or personal relationships that could have appeared to influence the work reported in this paper.

Data availability

No data was used for the research described in the article.

Acknowledgment

This research is partly funded by The Ministry of Foreign Affairs of Denmark (MFA) through Danida Fellowship Centre (DFC) project no. 20-M01AAU ("Membrane crystallization for water and mineral recovery").

Appendix A. Supplementary data

Supplementary data to this article can be found online at https://doi.org/10.1016/j.desal.2024.117584.

References

[1] M. Khayet, Membranes and theoretical modeling of membrane distillation: a review, Adv. Colloid Interface Sci. 164 (2011) 56–88, https://doi.org/10.1016/j.cis.2010.09.005.
[2] L. Eykens, K. de Sitter, C. Dotremont, L. Pinoy, B. van der Bruggen, Membrane synthesis for membrane distillation: a review, Sep. Purif. Technol. 182 (2017) 36–51, https://doi.org/10.1016/j.seppur.2017.03.035.
[3] Y. Mi, H. Guo, J. Seo, Y. In, J. Ha, Numerical analysis of membrane distillation using hollow fiber membrane modules: a review, Desalin. Water Treat. 155 (2019) 23345, https://doi.org/10.5004/dwt.2019.23345.
[4] S.O. Olatunji, L.M. Camacho, Heat and mass transport in modeling membrane distillation configurations: a review, Front. Energy Res. 6 (2018) 1–18, https://doi.org/10.3389/fenrg.2018.00130.
[5] M.M.A. Shirazi, A. Kargari, A review on applications of membrane distillation (MD) process for wastewater treatment, J. Membr. Sci. Res. 1 (2015) 101–112.
[6] N. Ghaffour, S. Soukane, J. Lee, Y. Kim, A. Alpatova, Membrane distillation hybrids for water production and energy efficiency enhancement: a critical review, Appl. Energy 254 (2019) 113698, https://doi.org/10.1016/j.apenergy.2019.113698.
[7] M.M.A. Shirazi, C.A. Quist-Jensen, A. Ali, Membrane distillation, in: Experimental Methods for Membrane Applications in Desalination and Water Treatment, IWA Publishing, 2024, pp. 97–138, https://doi.org/10.2166/9781789062977_0097.
[8] M.M.A. Shirazi, A. Kargari, A.F. Ismail, T. Matsuura, Computational Fluid Dynamic (CFD) opportunities applied to the membrane distillation process: state-of-the-art and perspectives, Desalination 377 (2016) 73–90, https://doi.org/10.1016/j.desal.2015.09.010.
[9] A. Ali, C.A. Quist-Jensen, M.K. Jørgensen, A. Siekierka, M.L. Christensen, M. Bryjak, C. Hélix-Nielsen, E. Drioli, A review of membrane crystallization, forward osmosis and membrane capacitive deionization for liquid mining, Resour. Conserv. Recycl. 168 (2021), https://doi.org/10.1016/j.resconrec.2020.105273.
[10] P. Luis, D. van Aubel, B. van der Bruggen, Technical viability and exergy analysis of membrane crystallization: closing the loop of CO_2 sequestration, Int. J. Greenh. Gas Cont. 12 (2013) 450–459, https://doi.org/10.1016/j.ijggc.2012.11.027.
[11] E. Drioli, G. di Profio, E. Curcio, Progress in membrane crystallization, Curr. Opin. Chem. Eng. 1 (2012) 178–182, https://doi.org/10.1016/j.coche.2012.03.005.
[12] A.P. Straub, A. Deshmukh, M. Elimelech, A.P. Straub, Pressure-retarded osmosis for power generation from salinity gradients: is it viable? Energy Environ. Sci. 9 (2015) 31–48, https://doi.org/10.1039/C5EE02985F.
[13] A.P. Straub, M. Elimelech, Energy efficiency and performance limiting effects in thermo-osmotic energy conversion from low-grade heat, Environ. Sci. Technol. 51 (2017) 12925–12937, https://doi.org/10.1021/acs.est.7b02213.
[14] A.P. Straub, N.Y. Yip, S. Lin, J. Lee, M. Elimelech, Harvesting low-grade heat energy using thermo-osmotic vapour transport through nanoporous membranes, Nat. Energy 1 (2016) 16090, https://doi.org/10.1038/nenergy.2016.90.
[15] L. Eykens, K. De Sitter, C. Dotremont, L. Pinoy, B. Van der Bruggen, How to optimize the membrane properties for membrane distillation: a review, Ind. Eng. Chem. Res. 55 (2016) 9333–9343, https://doi.org/10.1021/acs.iecr.6b02226.
[16] E. Drioli, A. Ali, F. Macedonio, Membrane distillation: recent developments and perspectives, Desalination 356 (2015) 56–84, https://doi.org/10.1016/j.desal.2014.10.028.
[17] E. Curcio, E. Drioli, Membrane distillation and related operations—a review, Sep. Purif. Rev. 34 (2005) 35–86, https://doi.org/10.1081/SPM-200054951.
[18] A. Ruiz-Aguirre, J.A. Andrés-Mañas, G. Zaragoza, Evaluation of permeate quality in pilot scale membrane distillation systems, Membranes (Basel) 9 (2019) 69, https://doi.org/10.3390/membranes9060069.
[19] A. Alkhudhiri, N. Hilal, Membrane distillation—principles, applications, configurations, design, and implementation, in: Emerging Technologies for Sustainable Desalination Handbook, Elsevier Inc., 2018, pp. 55–106.
[20] W. Jantaporn, A. Ali, P. Aimar, Specific energy requirement of direct contact membrane distillation, Chem. Eng. Res. Des. 128 (2017) 15–26, https://doi.org/10.1016/j.cherd.2017.09.031.
[21] L. Martinez-Diez, M.I. Vazquez-Gonzalez, M. Martinez-Diez, L. Vazquez-Gonzalez, L. Martínez-Díez, M.I. Vázquez-González, Temperature and concentration polarization in membrane distillation of aqueous salt solutions, J. Membr. Sci. 156 (1999) 265–273.
[22] M.N. Chernyshov, G.W. Meindersma, A.B. de Haan, Comparison of spacers for temperature polarization reduction in air gap membrane distillation, Desalination 183 (2005) 363–374, https://doi.org/10.1016/j.desal.2005.04.029.
[23] M.N. Chernyshov, G.W. Meindersma, A.B. de Haan, Comparison of spacers for temperature polarization reduction in air gap membrane distillation, Desalination 183 (2005) 363–374, https://doi.org/10.1016/j.desal.2005.04.029.
[24] A. Ali, F. Macedonio, E. Drioli, S. Aljlil, O.A. Alharbi, Experimental and theoretical evaluation of temperature polarization phenomenon in direct contact membrane distillation, Chem. Eng. Res. Des. 91 (2013) 1966–1977, https://doi.org/10.1016/j.cherd.2013.06.030.
[25] Y.M. Manawi, M.A.M.M. Khraisheh, A. Kayvani, F. Benyahia, S. Adham, A predictive model for the assessment of the temperature polarization effect in direct contact membrane distillation desalination of high salinity feed, Desalination 341 (2014) 38–49, https://doi.org/10.1016/j.desal.2014.02.028.
[26] S. Lin, N.Y. Yip, M. Elimelech, Direct contact membrane distillation with heat recovery: thermodynamic insights from module scale modeling, J. Membr. Sci. 453 (2014) 498–515, https://doi.org/10.1016/j.memsci.2013.11.016.
[27] M. Khayet, C. Cojocaru, Air gap membrane distillation: desalination, modeling and optimization, Desalination 287 (2012) 138–145, https://doi.org/10.1016/j.desal.2011.09.017.
[28] V. Belessiotis, S. Kalogirou, E. Delyannis, Membrane distillation, in: Thermal Solar Desalination, Elsevier, 2016, pp. 191–251, https://doi.org/10.1016/B978-0-12-809656-7.00004-0.
[29] V.T. Shahu, S.B. Thombre, Air gap membrane distillation: a review, J. Renew. Sustain. Energy 11 (2019), https://doi.org/10.1063/1.5063766.
[30] S.S. Alsaadi, N. Ghaffour, J.-D. Li, S. Gray, L. Francis, H. Maab, G.L.L. Amy, Modeling of air-gap membrane distillation process: a theoretical and experimental study, J. Membr. Sci. 445 (2013) 53–65, https://doi.org/10.1016/j.memsci.2013.05.049.
[31] A. Chenggui, W. Kosar, Y. Zhang, X. Feng, Vacuum membrane distillation for desalination of water using hollow fiber membranes, J. Membr. Sci. 455 (2014) 131–142, https://doi.org/10.1016/j.memsci.2013.12.055.
[32] E. Drioli, A. Ali, S. Simone, F. MacEdonio, S.A. Al-Jlil, F.S. Al Shabonah, H.S. Al-Romaih, O. Al-Harbi, A. Figoli, A. Criscuoli, Novel PVDF hollow fiber membranes for vacuum and direct contact membrane distillation applications, Sep. Purif. Technol. 115 (2013) 27–38, https://doi.org/10.1016/j.seppur.2013.04.040.
[33] M. Alklaibi, N. Lior, Membrane-distillation desalination: status and potential, Desalination 171 (2005) 111–131, https://doi.org/10.1016/j.desal.2004.03.024.
[34] M. Rezaei, D.M. Warsinger, J.H. Lienhard V, M.C. Duke, T. Matsuura, W. M. Samhaber, Wetting phenomena in membrane distillation: mechanisms, reversal, and prevention, Water Res. 139 (2018) 329–352, https://doi.org/10.1016/j.watres.2018.03.058.
[35] C.-C.C.C. Ko, A. Ali, E. Drioli, K.-L.K.L. Tung, C.-H.C.H. Chen, Y.-R.Y.R. Chen, F. Macedonio, Performance of ceramic membrane in vacuum membrane distillation and in vacuum membrane crystallization, Desalination 440 (2018) 48–58, https://doi.org/10.1016/j.desal.2018.03.011.

[36] M. Khayet, C. Cojocaru, A. Baroudi, Modeling and optimization of sweeping gas membrane distillation, Desalination 287 (2012) 159–166, https://doi.org/10.1016/j.desal.2011.04.070.

[37] S. Zhao, P.H.M.M. Feron, Z. Xie, J. Zhang, M. Hoang, Condensation studies in membrane evaporation and sweeping gas membrane distillation, J. Membr. Sci. 462 (2014) 9–16, https://doi.org/10.1016/j.memsci.2014.03.028.

[38] M.M.A. Shirazi, A. Kargari, M. Tabatabaei, A.F. Ismail, T. Matsuura, Concentration of glycerol from dilute glycerol wastewater using sweeping gas membrane distillation, Chem. Eng. Process. Proc. Intens. 78 (2014) 58–66, https://doi.org/10.1016/j.cep.2014.02.002.

[39] R. Bagger-jørgensen, A.S. Meyer, M. Pinelo, C. Varming, G. Jonsson, Recovery of volatile fruit juice aroma compounds by membrane technology: sweeping gas versus vacuum membrane distillation, Innov. Food Sci. Emerg. Technol. 12 (2011) 388–397, https://doi.org/10.1016/j.ifset.2011.02.005.

[40] M.M.A. Shirazi, A. Kargari, M. Tabatabaei, Sweeping gas membrane distillation (SGMD) as an alternative for integration of bioethanol processing: study on a commercial membrane and operating parameters, Chem. Eng. Commun. (2014), https://doi.org/10.1080/00986445.2013.848805, 140917052218009.

[41] N. Thomas, M.O. Mavukkandy, S. Loutatidou, H.A. Arafat, Membrane distillation research & implementation: lessons from the past five decades, Sep. Purif. Technol. 189 (2017) 108–127, https://doi.org/10.1016/j.seppur.2017.07.069.

[42] E. Aytaç, M. Khayet, A deep dive into membrane distillation literature with data analysis, bibliometric methods, and machine learning, Desalination 553 (2023) 116482, https://doi.org/10.1016/j.desal.2023.116482.

[43] S. Shirazi, M.M.A. Kargari, A. Marzban, R. Naseri Rad, Application of membrane separation technology in downstream processing of *Bacillus thuringiensis* biopesticide: a review, J. Membr. Sci. Res. 2 (2016) 66–77.

[44] M.M.A. Shirazi, L.F. Dumée, Membrane distillation for sustainable wastewater treatment, J. Water Process Eng. 47 (2022) 102670, https://doi.org/10.1016/J.JWPE.2022.102670.

[45] F.E. Ahmed, B.S. Lalia, R. Hashaikeh, N. Hilal, Alternative heating techniques in membrane distillation: a review, Desalination 496 (2020) 114713, https://doi.org/10.1016/J.DESAL.2020.114713.

[46] A. Yadav, P.K. Labhasetwar, V.K. Shahi, Membrane distillation using low-grade energy for desalination: a review, J. Environ. Chem. Eng. 9 (2021) 105818, https://doi.org/10.1016/j.jece.2021.105818.

[47] B. Lin, M. Malmali, Energy and exergy analysis of multi-stage vacuum membrane distillation integrated with mechanical vapor compression, Sep. Purif. Technol. 306 (2023) 122568, https://doi.org/10.1016/j.seppur.2022.122568.

[48] W. Su, J. Li, Z. Lu, X. Jin, J. Zhang, Z. Liu, Z. Xiaosong, Performance analysis and optimization of a solar assisted heat pump-driven vacuum membrane distillation system for liquid desiccant regeneration, Energ. Conver. Manage. 301 (2024) 118047, https://doi.org/10.1016/j.enconman.2023.118047.

[49] M. Gryta, Calcium sulphate scaling in membrane distillation process, Chem. Pap. 63 (2009) 146–151, https://doi.org/10.2478/s11696-008-0095-y.

[50] L.D. Nghiem, T. Cath, A scaling mitigation approach during direct contact membrane distillation, Sep. Purif. Technol. 80 (2011) 315–322, https://doi.org/10.1016/j.seppur.2011.05.013.

[51] F. He, J. Gilron, H. Lee, L. Song, K.K. Sirkar, Potential for scaling by sparingly soluble salts in crossflow DCMD.pdf, J. Membr. Sci. 311 (2008) 68–80.

[52] K.S.S. Christie, T. Horseman, R. Wang, C. Su, T. Tong, S. Lin, Gypsum scaling in membrane distillation: impacts of temperature and vapor flux, Desalination 525 (2022), https://doi.org/10.1016/j.desal.2021.115499.

[53] D.M. Warsinger, J. Swaminathan, E. Guillen-Burrieza, H.A. Arafat, J. H. Lienhard V, Scaling and fouling in membrane distillation for desalination applications: a review, Desalination 356 (2015) 294–313, https://doi.org/10.1016/j.desal.2014.06.031.

[54] L. Eykens, K. De Sitter, C. Dotremont, L. Pinoy, B. Van der Bruggen, Membrane synthesis for membrane distillation: a review, Sep. Purif. Technol. 182 (2017) 36–51, https://doi.org/10.1016/j.seppur.2017.03.035.

[55] M. Qasim, I.U. Samad, N.A. Darwish, N. Hilal, Comprehensive review of membrane design and synthesis for membrane distillation, Desalination 518 (2021) 115168, https://doi.org/10.1016/j.desal.2021.115168.

[56] M. Pagliero, M. Khayet, C. García-Payo, L. García-Fernández, Hollow fibre polymeric membranes for desalination by membrane distillation technology: a review of different morphological structures and key strategic improvements, Desalination 516 (2021) 115235, https://doi.org/10.1016/j.desal.2021.115235.

[57] H. Sanaeepur, A. Ebadi Amooghin, M.M.A. Shirazi, M. Pishnamazi, S. Shirazian, Water desalination and ion removal using mixed matrix electrospun nanofibrous membranes: a critical review, Desalination 521 (2022) 115350, https://doi.org/10.1016/j.desal.2021.115350.

[58] N.S. Fuzil, N.H. Othman, N.H. Alias, F. Marpani, M.H.D. Othman, A.F. Ismail, W. J. Lau, K. Li, T.D. Kusworo, I. Ichinose, M.M.A. Shirazi, A review on photothermal material and its usage in the development of photothermal membrane for sustainable clean water production, Desalination 517 (2021) 115259, https://doi.org/10.1016/j.desal.2021.115259.

[59] D.M. Warsinger, J. Swaminathan, E. Guillen-Burrieza, H.A. Arafat, J. H. Lienhard V, Scaling and fouling in membrane distillation for desalination applications: a review, Desalination 356 (2015) 294–313, https://doi.org/10.1016/J.DESAL.2014.06.031.

[60] A. Abdel-Karim, S. Leaper, C. Skuse, G. Zaragoza, M. Gryta, P. Gorgojo, Membrane cleaning and pretreatments in membrane distillation — a review, Chem. Eng. J. 422 (2021) 129696, https://doi.org/10.1016/j.cej.2021.129696.

[61] I. Hitsov, T. Maere, K. De Sitter, C. Dotremont, I. Nopens, Modelling approaches in membrane distillation: a critical review, Sep. Purif. Technol. 142 (2015) 48–64, https://doi.org/10.1016/J.SEPPUR.2014.12.026.

[62] N. Ghaffour, S. Soukane, J.-G. Lee, Y. Kim, A. Alpatova, Membrane distillation hybrids for water production and energy efficiency enhancement: a critical review, Appl. Energy 254 (2019) 113698, https://doi.org/10.1016/j.apenergy.2019.113698.

[63] G. Naidu, L. Tijing, M.A.H. Johir, H. Shon, S. Vigneswaran, Hybrid membrane distillation: resource, nutrient and energy recovery, J. Memb. Sci. 599 (2020) 117832, https://doi.org/10.1016/j.memsci.2020.117832.

[64] J.A. Kharraz, N.K. Khanzada, M.U. Farid, J. Kim, S. Jeong, A.K. An, Membrane distillation bioreactor (MDBR) for wastewater treatment, water reuse, and resource recovery: a review, J. Water Process Eng. 47 (2022) 102687, https://doi.org/10.1016/j.jwpe.2022.102687.

[65] V.T. Shahu, S.B. Thombre, Air gap membrane distillation: a review, J. Renew. Sustain. Energy 11 (2019) 045901, https://doi.org/10.1063/1.5063766.

[66] M.A.E.-R. Abu-Zeid, Y. Zhang, H. Dong, L. Zhang, H.-L. Chen, L. Hou, A comprehensive review of vacuum membrane distillation technique, Desalination 356 (2015) 1–14, https://doi.org/10.1016/j.desal.2014.10.033.

[67] S. Kalla, S. Upadhyaya, K. Singh, Principles and advancements of air gap membrane distillation, Rev. Chem. Eng. 35 (2019) 817–859, https://doi.org/10.1515/revce-2017-0112.

[68] B.B. Ashoor, S. Mansour, A. Giwa, V. Dufour, S.W. Hasan, Principles and applications of direct contact membrane distillation (DCMD): a comprehensive review, Desalination 398 (2016) 222–246, https://doi.org/10.1016/j.desal.2016.07.043.

[69] I.A. Said, T. Chomiak, J. Floyd, Q. Li, Sweeping gas membrane distillation (SGMD) for wastewater treatment, concentration, and desalination: a comprehensive review, Chem. Eng. Process. Proc. Intens. 153 (2020) 107960, https://doi.org/10.1016/j.cep.2020.107960.

[70] H. Chamani, J. Woloszyn, T. Matsuura, D. Rana, C.Q. Lan, Pore wetting in membrane distillation: a comprehensive review, Prog. Mater. Sci. 122 (2021) 100843, https://doi.org/10.1016/J.PMATSCI.2021.100843.

[71] S.O. Olatunji, L.M. Camacho, Heat and mass transport in modeling membrane distillation configurations: a review, Front. Energy Res. 6 (2018), https://doi.org/10.3389/fenrg.2018.00130.

[72] X. Yang, R. Wang, A.G. Fane, C.Y. Tang, I.G. Wenten, Membrane module design and dynamic shear-induced techniques to enhance liquid separation by hollow fiber modules: a review, Desalin. Water Treat. 5327 (2013) 3604–3627.

[73] N.C. Mat, Y. Lou, G.G. Lipscomb, Hollow fiber membrane modules, Curr. Opin. Chem. Eng. 4 (2014) 18–24, https://doi.org/10.1016/j.coche.2014.01.002.

[74] J.H. Burban, R.O. Crowder, P.M. Rolchigo, J. Shanahan, Membrane module for fluid filtration, US Patent 7,875,176 B2, 2011.

[75] H. Julian, B. Lian, H. Li, X. Liu, Y. Wang, G. Leslie, V. Chen, Numerical study of $CaCO_3$ scaling in submerged vacuum membrane distillation and crystallization (VMDC), J. Membr. Sci. 559 (2018) 87–97, https://doi.org/10.1016/j.memsci.2018.04.050.

[76] Y. Choi, G. Naidu, S. Lee, S. Vigneswaran, Effect of inorganic and organic compounds on the performance of fractional-submerged membrane distillation-crystallizer, J. Membr. Sci. 582 (2019) 9–19, https://doi.org/10.1016/j.memsci.2019.03.089.

[77] T. Zou, G. Kang, M. Zhou, M. Li, Y. Cao, Submerged vacuum membrane distillation crystallization (S-VMDC) with turbulent intensification for the concentration of NaCl solution, Sep. Purif. Technol. 211 (2019) 151–161, https://doi.org/10.1016/j.seppur.2018.09.072.

[78] Module Design & Options and Fundamentals of System Design, 2013.

[79] J. Wu, V. Chen, Shell-side Mass Transfer Performance of Randomly Packed Hollow fiber Modules, 2000.

[80] J.M. Zheng, Z.K. Xu, J.M. Li, S.Y. Wang, Y.Y. Xu, Influence of random arrangement of hollow fiber membranes on shell side mass transfer performance: a novel model prediction, J. Membr. Sci. 236 (2004) 145–151, https://doi.org/10.1016/j.memsci.2004.02.016.

[81] M. Khayet, T. Matsuura, Membrane Distillation: Principles and Applications, Elsevier Amsterdam, Boston, Amsterdam, 2011.

[82] L. Martínez, J.M. Rodríguez-maroto, Effects of membrane and module design improvements on flux in direct contact membrane distillation, Desalination 205 (2007) 97–103, https://doi.org/10.1016/j.desal.2006.02.050.

[83] S.M. Alawad, A.E. Khalifa, Case studies in thermal engineering development of an efficient compact multistage membrane distillation module for water desalination, Case Stud. Ther. Eng. 25 (2021) 100979, https://doi.org/10.1016/j.csite.2021.100979.

[84] A. Ali, A. Criscuoli, F. Macedonio, E. Drioli, A comparative analysis of flat sheet and capillary membranes for membrane distillation applications, Desalination 456 (2019) 1–12, https://doi.org/10.1016/j.desal.2019.01.006.

[85] P. Wang, T.-S. Chung, Recent advances in membrane distillation processes: membrane development, configuration design and application exploring, J. Membr. Sci. 474 (2015) 39–56, https://doi.org/10.1016/j.memsci.2014.09.016.

[86] E. Guillén-Burrieza, D.C. Alarcón-Padilla, P. Palenzuela, G. Zaragoza, Techno-economic assessment of a pilot-scale plant for solar desalination based on existing plate and frame MD technology, Desalination 374 (2015) 70–80, https://doi.org/10.1016/j.desal.2015.07.014.

[87] J.A. Andrés-Mañas, A. Ruiz-Aguirre, F.G. Acién, G. Zaragoza, Performance increase of membrane distillation pilot scale modules operating in vacuum-enhanced air-gap configuration, Desalination 475 (2020) 114202, https://doi.org/10.1016/j.desal.2019.114202.

[88] Y. Xu, B.K. Zhu, Y.Y. Xu, Pilot test of vacuum membrane distillation for seawater desalination on a ship, Desalination 189 (2006) 165–169, https://doi.org/10.1016/j.desal.2005.06.024.

[89] Y. Shin, J. Choi, Y. Park, Y. Choi, S. Lee, Influence of operation conditions on the performance of pilot-scale vacuum membrane distillation (VMD), Desalin. Water Treat. 97 (2017) 1–7, https://doi.org/10.5004/dwt.2017.20664.
[90] KMX Technologies. https://kmxtechnologies.com/kmx-and-sumitomo-enter-mou-to-commercialize-kmxs-membrane-distillation-modules/, 2021.
[91] Tanal Water, https://www.tanalwater.com/e_productshow/?54-membrane-distillation-module-54.html, (n.d.).
[92] Memsift, https://www.memsift.com/products/, (n.d.).
[93] L. Song, Z. Ma, X. Liao, P.B. Kosaraju, J.R. Irish, K.K. Sirkar, Pilot plant studies of novel membranes and devices for direct contact membrane distillation-based desalination, J. Membr. Sci. 323 (2008) 257–270, https://doi.org/10.1016/j.memsci.2008.05.079.
[94] D. Winter, J. Koschikowski, M. Wieghaus, Desalination using membrane distillation: experimental studies on full scale spiral wound modules, J. Membr. Sci. 375 (2011) 104–112, https://doi.org/10.1016/j.memsci.2011.03.030.
[95] A. Hagedorn, G. Fieg, D. Winter, J. Koschikowski, T. Mann, Methodical design and operation of membrane distillation plants for desalination, Chem. Eng. Res. Des. 125 (2017) 265–281, https://doi.org/10.1016/j.cherd.2017.07.024.
[96] A. Ruiz-Aguirre, J.A. Andrés-Mañas, J.M. Fernández-Sevilla, G. Zaragoza, Modeling and optimization of a commercial permeate gap spiral wound membrane distillation module for seawater desalination, Desalination 419 (2017) 160–168, https://doi.org/10.1016/j.desal.2017.06.019.
[97] R. Schwantes, A. Cipollina, F. Gross, J. Koschikowski, D. Pfeifle, M. Rolletschek, V. Subiela, Membrane distillation: solar and waste heat driven demonstration plants for desalination, Desalination 323 (2013) 1–25, https://doi.org/10.1016/j.desal.2013.04.011.
[98] L. Eykens, I. Hitsov, K. de Sitter, C. Dotremont, L. Pinoy, B. van der Bruggen, Direct contact and air gap membrane distillation: differences and similarities between lab and pilot scale, Desalination 422 (2017) 91–100, https://doi.org/10.1016/j.desal.2017.08.018.
[99] H.C. Duong, A.R. Chivas, B. Nelemans, M. Duke, S. Gray, T.Y. Cath, L.D. Nghiem, Treatment of RO brine from CSG produced water by spiral-wound air gap membrane distillation — a pilot study, Desalination 366 (2015) 121–129, https://doi.org/10.1016/j.desal.2014.10.026.
[100] J. Minier-Matar, A. Hussain, A. Janson, F. Benyahia, S. Adham, Field evaluation of membrane distillation technologies for desalination of highly saline brines, Desalination 351 (2014) 101–108, https://doi.org/10.1016/j.desal.2014.07.027.
[101] G. Zaragoza, J.A. Andrés-Mañas, A. Ruiz-Aguirre, Commercial scale membrane distillation for solar desalination, NPJ Clean Water 1 (2018), https://doi.org/10.1038/s41545-018-0020-z.
[102] J. Günther, P. Schmitz, C. Albasi, C. Lafforgue, A numerical approach to study the impact of packing density on fluid flow distribution in hollow fiber module, J. Membr. Sci. 348 (2010) 277–286, https://doi.org/10.1016/j.memsci.2009.11.011.
[103] D. Li, R. Wang, T.-S. Chung, Fabrication of lab-scale hollow fiber membrane modules with high packing density, Sep. Purif. Technol. 40 (2004) 15–30, https://doi.org/10.1016/j.seppur.2003.12.019.
[104] D. Singh, L. Li, G. Obusckovic, J. Chau, K.K. Sirkar, Novel cylindrical cross-flow hollow fiber membrane module for direct contact membrane distillation-based desalination, J. Membr. Sci. 545 (2018) 312–322, https://doi.org/10.1016/j.memsci.2017.09.007.
[105] D. Singh, L. Li, G. Obusckovic, J. Chau, K.K. Sirkar, Novel cylindrical cross-flow hollow fiber membrane module for direct contact membrane distillation-based desalination, J. Membr. Sci. 545 (2018) 312–322, https://doi.org/10.1016/j.memsci.2017.09.007.
[106] A. Ali, C.A. Quist-Jensen, F. Macedonio, E. Drioli, Application of membrane crystallization for minerals' recovery from produced water, Membranes (Basel) 5 (2015), https://doi.org/10.3390/membranes5040772.
[107] C.A.C.A. Quist-Jensen, F. Macedonio, D. Horbez, E. Drioli, Reclamation of sodium sulfate from industrial wastewater by using membrane distillation and membrane crystallization, Desalination 401 (2017) 112–119, https://doi.org/10.1016/j.desal.2016.05.007.
[108] C.F. Wan, T. Yang, G.G. Lipscomb, D.J. Stookey, T.-S. Chung, Design and fabrication of hollow fiber membrane modules, in: Hollow Fiber Membranes, Elsevier, 2021, pp. 225–252, https://doi.org/10.1016/B978-0-12-821876-1.00007-X.
[109] G.B. Clark, Assembly of permeable hollow fibers and a tubesheet supportable at its face and opened by bores parallel thereto, 4,061,574 (1977).
[110] G.B. Clark, Hollow fiber permeator, 4,080,296 (1978).
[111] F. Coan, T.O. Jeanes, J.A. Jensvold, Boreside Feed Modules With Permeate Flow Channels, 2000.
[112] S. Giglia, B. Bikson, Hollow fiber membrane separation apparatus, 5,837,033 (1998).
[113] B. Li, K.K. Sirkar, Novel membrane and device for direct contact membrane distillation-based desalination process, Ind. Eng. Chem. Res. 43 (2004) 5300–5309, https://doi.org/10.1021/ie030871s.
[114] L. Song, Z. Ma, X. Liao, P.B. Kosaraju, J.R. Irish, K.K. Sirkar, Pilot plant studies of novel membranes and devices for direct contact membrane distillation-based desalination, J. Membr. Sci. 323 (2008) 257–270, https://doi.org/10.1016/j.memsci.2008.05.079.
[115] X. Yang, R. Wang, A.G. Fane, C.Y. Tang, I.G. Wenten, Membrane module design and dynamic shear-induced techniques to enhance liquid separation by hollow fiber modules: a review, Desalin. Water Treat. 51 (2013) 3604–3627, https://doi.org/10.1080/19443994.2012.751146.
[116] C.F. Wan, T. Yang, G.G. Lipscomb, D.J. Stookey, T.-S. Chung, Design and fabrication of hollow fiber membrane modules, J. Membr. Sci. 538 (2017) 96–107, https://doi.org/10.1016/j.memsci.2017.05.047.
[117] U. Baurmeister, Multilayer hollow fiber wound body, 4,940,192 (1990).
[118] J. Wu, V. Chen, Shell-side mass transfer performance of randomly packed hollow fiber modules, J. Membr. Sci. 172 (2000) 59–74, https://doi.org/10.1016/S0376-7388(00)00318-5.
[119] J.M. Zheng, Z.K. Xu, J.M. Li, S.Y. Wang, Y.Y. Xu, Influence of random arrangement of hollow fiber membranes on shell side mass transfer performance: a novel model prediction, J. Membr. Sci. 236 (2004) 145–151, https://doi.org/10.1016/j.memsci.2004.02.016.
[120] A.L. Kohl, Reverse osmosis fabric, 3,557,962 (1971).
[121] A. Ali, P. Aimar, E. Drioli, Effect of module design and flow patterns on performance of membrane distillation process, Chem. Eng. J. 277 (2015) 368–377, https://doi.org/10.1016/j.cej.2015.04.108.
[122] M.M. Teoh, S. Bonyadi, T.-S. Chung, Investigation of different hollow fiber module designs for flux enhancement in the membrane distillation process, J. Membr. Sci. 311 (2008) 371–379, https://doi.org/10.1016/j.memsci.2007.12.054.
[123] X. Yang, R. Wang, A.G. Fane, Novel designs for improving the performance of hollow fiber membrane distillation modules, J. Membr. Sci. 384 (2011) 52–62, https://doi.org/10.1016/j.memsci.2011.09.007.
[124] E.A. Mclain, Wound hollow fiber permeability apparatus and process of making the same, 3,442,008 (1969).
[125] H.I. Mahon, C.F. Oldershaw, Permeability separatory apparatus and processes of making and using the same, 3,455,460 (1969).
[126] M.J. Coplan, R.E. Sebring, Hollow filament separatory module, 4,210,536 (1980).
[127] M.J. Coplan, F. Bilewski, Permselective hollow fibers bundle, 4,631,128 (1986).
[128] N.I.M. Nawi, M.R. Bilad, N. Zolkhiflee, N.A.H. Nordin, W.J. Lau, T. Narkkun, K. Faungnawakij, N. Arahman, T.M.I. Mahlia, Development of a novel corrugated polyvinylidene difluoride membrane via improved imprinting technique for membrane distillation, Polymers (Basel) 11 (2019), https://doi.org/10.3390/polym11050865.
[129] Q. Wang, W. Lin, S. Chou, P. Dai, X. Huang, Pattern membrane for improving hydrodynamic properties and mitigating membrane fouling in water treatment: a review, Water Res. 119943 (2023), https://doi.org/10.1016/j.watres.2023.119943.
[130] L. García-Fernández, C. García-Payo, M. Khayet, Hollow fiber membranes with different external corrugated surfaces for desalination by membrane distillation, Appl. Surf. Sci. 416 (2017) 932–946, https://doi.org/10.1016/j.apsusc.2017.04.232.
[131] C.D. Ho, L. Chen, F.C. Tsai, G.H. Lin, J.W. Lim, Distillate flux enhancement of the concentric circular direct contact membrane distillation module with spiral wired flow channel, J. Taiwan Inst. Chem. Eng. 94 (2019) 70–80, https://doi.org/10.1016/j.jtice.2017.09.052.
[132] M. Gryta, The application of submerged modules for membrane distillation, Membranes (Basel) 10 (2020), https://doi.org/10.3390/membranes10020025.
[133] W. Bae, J. Kim, Permeate flux and rejection behavior in submerged direct contact membrane distillation process treating a low-strength synthetic wastewater, Appl. Sci. (Switzerland) 10 (2020), https://doi.org/10.3390/app10020677.
[134] W. Bae, J. Kim, Permeate flux and rejection behavior in submerged direct contact membrane distillation process treating a low-strength synthetic wastewater, Appl. Sci. (Switzerland) 10 (2020), https://doi.org/10.3390/app10020677.
[135] A. Bamasag, H. Daghooghi-Mobarakeh, T. Alqahtani, P. Phelan, Performance enhancement of a submerged vacuum membrane distillation (S-VMD) system using low-power ultrasound, J. Membr. Sci. 621 (2021), https://doi.org/10.1016/j.memsci.2020.119004.
[136] J. Phattaranawik, A.G. Fane, A.C.S. Pasquier, W. Bing, F.S. Wong, Experimental study and design of a submerged membrane distillation bioreactor, Chem. Eng. Technol. 32 (2009) 38–44, https://doi.org/10.1002/ceat.200800498.
[137] L. Francis, N. Ghaffour, A.S. Al-Saadi, G.L. Amy, Submerged membrane distillation for seawater desalination, Desalin. Water Treat. 55 (2015) 2741–2746, https://doi.org/10.1080/19443994.2014.946716.
[138] S. Meng, Y.C. Hsu, Y. Ye, V. Chen, Submerged membrane distillation for inland desalination applications, Desalination 361 (2015) 72–80, https://doi.org/10.1016/j.desal.2015.01.038.
[139] C.M. Guijt, G.W. Meindersma, T. Reith, A.B. de Haan, Air gap membrane distillation: 2. Model validation and hollow fibre module performance analysis, Sep. Purif. Technol. 43 (2005) 245–255, https://doi.org/10.1016/j.seppur.2004.09.016.
[140] H. Cho, Y.J. Choi, S. Lee, J. Koo, T. Huang, Comparison of hollow fiber membranes in direct contact and air gap membrane distillation (MD), Desalin. Water Treat. 57 (2016) 10012–10019, https://doi.org/10.1080/19443994.2015.1038113.
[141] D. Singh, K.K. Sirkar, Desalination by air gap membrane distillation using a two hollow-fiber-set membrane module, J. Membr. Sci. 421–422 (2012) 172–179, https://doi.org/10.1016/j.memsci.2012.07.007.
[142] H. Geng, H. Wu, P. Li, Q. He, Study on a new air-gap membrane distillation module for desalination, Desalination 334 (2014) 29–38, https://doi.org/10.1016/j.desal.2013.11.037.
[143] B.G. Im, L. Francis, R. Santosh, W.S. Kim, N. Ghaffour, Y.D. Kim, Comprehensive insights into performance of water gap and air gap membrane distillation modules using hollow fiber membranes, Desalination 525 (2022), https://doi.org/10.1016/j.desal.2021.115497.

[144] R. Aryapratama, H. Koo, S. Jeong, S. Lee, Performance evaluation of hollow fiber air gap membrane distillation module with multiple cooling channels, Desalination 385 (2016) 58–68, https://doi.org/10.1016/j.desal.2016.01.005.
[145] Z. Liu, Q. Gao, X. Lu, L. Zhao, S. Wu, Z. Ma, H. Zhang, Study on the performance of double-pipe air gap membrane distillation module, Desalination 396 (2016) 48–56, https://doi.org/10.1016/j.desal.2016.04.025.
[146] A. Alpatova, A.S. Alsaadi, M. Alharthi, J.G. Lee, N. Ghaffour, Co-axial hollow fiber module for air gap membrane distillation, J. Membr. Sci. 578 (2019) 172–182, https://doi.org/10.1016/j.memsci.2019.02.052.
[147] S. Bandini, C. Gostoli, G.C. Sarti, Separation efficiency in vacuum membrane distillation, J. Membr. Sci. 73 (1992) 217–229, https://doi.org/10.1016/0376-7388(92)80131-3.
[148] G.C. Sarti, C. Gostoli, S. Bandini, Extraction of organic components from aqueous streams by vacuum membrane distillation, J. Membr. Sci. 80 (1993) 21–33, https://doi.org/10.1016/0376-7388(93)85129-K.
[149] F.A. Banat, J. Simandl, Removal of benzene traces from contaminated water by vacuum membrane distillation, Chem. Eng. Sci. 51 (1996) 1257–1265, https://doi.org/10.1016/0009-2509(95)00365-7.
[150] B. Li, K.K. Sirkar, Novel membrane and device for vacuum membrane distillation-based desalination process, J. Membr. Sci. 257 (2005) 60–75, https://doi.org/10.1016/j.memsci.2004.08.040.
[151] D. Wirth, C. Cabassud, Water desalination using membrane distillation: comparison between inside/out and outside/in permeation, Desalination 147 (2002) 139–145, https://doi.org/10.1016/S0011-9164(02)00601-X.
[152] B. Wu, X. Tan, W. Teo, K. Li, Removal of benzene/toluene from water by vacuum membrane distillation in a PVDF hollow fiber membrane module, Sep. Sci. Technol. 40 (2005) 2679–2695, https://doi.org/10.1080/01496390500283456.
[153] J. Liu, Q. Wang, L. Han, B. Li, Simulation of heat and mass transfer with cross-flow hollow fiber vacuum membrane distillation: the influence of fiber arrangement, Chem. Eng. Res. Des. 119 (2017) 12–22, https://doi.org/10.1016/j.cherd.2017.01.013.
[154] A. Omar, Q. Li, A. Nashed, J. Guan, P. Dai, R.A. Taylor, Experimental and numerical investigation of a new hollow fiber-based multi-effect vacuum membrane distillation design, Desalination 501 (2021) 114908, https://doi.org/10.1016/j.desal.2020.114908.
[155] M.M.A. Shirazi, S. Bazgir, F. Meshkani, A dual-layer, nanofibrous styrene-acrylonitrile membrane with hydrophobic/hydrophilic composite structure for treating the hot dyeing effluent by direct contact membrane distillation, Chem. Eng. Res. Des. 164 (2020) 125–146, https://doi.org/10.1016/j.cherd.2020.09.030.
[156] M.C. García-Payo, C.A. Rivier, I.W. Marison, U. von Stockar, Separation of binary mixtures by thermostatic sweeping gas membrane distillation, J. Membr. Sci. 198 (2002) 197–210, https://doi.org/10.1016/S0376-7388(01)00649-4.
[157] M.M.A. Shirazi, A. Kargari, M. Tabatabaei, Evaluation of commercial PTFE membranes in desalination by direct contact membrane distillation, Chem. Eng. Process. Process Intensif. 76 (2014) 16–25, https://doi.org/10.1016/j.cep.2013.11.010.
[158] T.Y. Cath, A.E. Childress, M. Elimelech, Forward osmosis: principles, applications, and recent developments, J. Membr. Sci. 281 (2006) 70–87, https://doi.org/10.1016/j.memsci.2006.05.048.
[159] J. Schwinge, P.R. Neal, D.E. Wiley, D.F. Fletcher, A.G. Fane, Spiral wound modules and spacers, J. Membr. Sci. 242 (2004) 129–153, https://doi.org/10.1016/j.memsci.2003.09.031.
[160] W. Lin, Y. Zhang, D. Li, X. Wang, X. Huang, Roles and performance enhancement of feed spacer in spiral wound membrane modules for water treatment: a 20-year review on research evolvement, Water Res. 198 (2021) 117146, https://doi.org/10.1016/j.watres.2021.117146.
[161] W.L. Gore, R.W. Gore, United States Patent (19) Gore et al. Desalinaton device and process, n.d.
[162] A.-S. Jönsson, R. Wimmerstedt, A.-C. Harrysson, Membrane distillation — a theoretical study of evaporation through microporous membranes, Desalination 56 (1985) 237–249, https://doi.org/10.1016/0011-9164(85)85028-1.
[163] J. Koschikowski, M. Wieghaus, M. Rommel, Solar thermal-driven desalination plants based on membrane distillation, Desalination 156 (2003) 295–304, https://doi.org/10.1016/S0011-9164(03)00360-6.
[164] D. Winter, J. Koschikowski, F. Gross, D. Maucher, D. Düver, M. Jositz, T. Mann, A. Hagedorn, Comparative analysis of full-scale membrane distillation contactors — methods and modules, J. Membr. Sci. 524 (2017) 758–771, https://doi.org/10.1016/j.memsci.2016.11.080.
[165] A. Alkhudhiri, N. Darwish, N. Hilal, Membrane distillation: a comprehensive review, Desalination 287 (2012) 2–18, https://doi.org/10.1016/j.desal.2011.08.027.
[166] A. Alkhudhiri, N. Hilal, Membrane distillation—principles, applications, configurations, design, and implementation, in: Emerging Technologies for Sustainable Desalination Handbook, Elsevier, 2018, pp. 55–106, https://doi.org/10.1016/B978-0-12-815818-0.00003-5.
[167] A.S. Alsaadi, N. Ghaffour, J.-D. Li, S. Gray, L. Francis, H. Maab, G.L. Amy, Modeling of air-gap membrane distillation process: a theoretical and experimental study, J. Membr. Sci. 445 (2013) 53–65, https://doi.org/10.1016/j.memsci.2013.05.049.
[168] R. Tian, H. Gao, X.H. Yang, S.Y. Yan, S. Li, A new enhancement technique on air gap membrane distillation, Desalination 332 (2014) 52–59, https://doi.org/10.1016/j.desal.2013.10.016.
[169] H. Attia, S. Alexander, C.J. Wright, N. Hilal, Superhydrophobic electrospun membrane for heavy metals removal by air gap membrane distillation (AGMD), Desalination 420 (2017) 318–329, https://doi.org/10.1016/j.desal.2017.07.022.
[170] D.M. Warsinger, J. Swaminathan, L.L. Morales, J.H. Lienhard V, Comprehensive condensation flow regimes in air gap membrane distillation: visualization and energy efficiency, J. Membr. Sci. 555 (2018) 517–528, https://doi.org/10.1016/j.memsci.2018.03.053.
[171] L. Francis, N. Ghaffour, A.A. Alsaadi, G.L. Amy, Material gap membrane distillation: a new design for water vapor flux enhancement, J. Membr. Sci. 448 (2013) 240–247, https://doi.org/10.1016/j.memsci.2013.08.013.
[172] L. Francis, N. Ghaffour, A.A. Alsaadi, G.L. Amy, Material gap membrane distillation: a new design for water vapor flux enhancement, J. Membr. Sci. 448 (2013) 240–247, https://doi.org/10.1016/j.memsci.2013.08.013.
[173] J. Swaminathan, H.W. Chung, D.M. Warsinger, F.A. AlMarzooqi, H.A. Arafat, J. H. Lienhard V, Energy efficiency of permeate gap and novel conductive gap membrane distillation, J. Membr. Sci. 502 (2016) 171–178, https://doi.org/10.1016/j.memsci.2015.12.017.
[174] V.T. Shahu, S.B. Thombre, Air gap membrane distillation: a review, J. Renew. Sustain. Energy 11 (2019), https://doi.org/10.1063/1.5063766.
[175] R. Bahar, M.N.A. Hawlader, T.F. Ariff, Channeled coolant plate: a new method to enhance freshwater production from an air gap membrane distillation (AGMD) desalination unit, Desalination 359 (2015) 71–81, https://doi.org/10.1016/j.desal.2014.12.031.
[176] B.L. Pangarkar, S.K. Deshmukh, Theoretical and experimental analysis of multi-effect air gap membrane distillation process (ME-AGMD), J. Environ. Chem. Eng. 3 (2015) 2127–2135, https://doi.org/10.1016/j.jece.2015.07.017.
[177] A.E. Khalifa, S.M. Alawad, M.A. Antar, Parallel and series multistage air gap membrane distillation, Desalination 417 (2017) 69–76, https://doi.org/10.1016/j.desal.2017.05.003.
[178] A.S. Alsaadi, L. Francis, H. Maab, G.L. Amy, N. Ghaffour, Evaluation of air gap membrane distillation process running under sub-atmospheric conditions: experimental and simulation studies, J. Membr. Sci. 489 (2015) 73–80, https://doi.org/10.1016/j.memsci.2015.04.008.
[179] C.M. Guijt, G.W. Meindersma, T. Reith, A.B. de Haan, Air gap membrane distillation: 2. Model validation and hollow fibre module performance analysis, Sep. Purif. Technol. 43 (2005) 245–255, https://doi.org/10.1016/j.seppur.2004.09.016.
[180] J.A. Andrés-Mañas, I. Requena, A. Ruiz-Aguirre, G. Zaragoza, Performance modelling and optimization of three vacuum-enhanced membrane distillation modules for upscaled solar seawater desalination, Sep. Purif. Technol. 287 (2022) 120396, https://doi.org/10.1016/j.seppur.2021.120396.
[181] A. Narayan, R. Pitchumani, Analysis of an air-cooled air gap membrane distillation module, Desalination 475 (2020) 114179, https://doi.org/10.1016/j.desal.2019.114179.
[182] G. Zaragoza, A. Ruiz-Aguirre, E. Guillén-Burrieza, Efficiency in the use of solar thermal energy of small membrane desalination systems for decentralized water production, Appl. Energy 130 (2014) 491–499, https://doi.org/10.1016/j.apenergy.2014.02.024.
[183] E. Guillén-Burrieza, G. Zaragoza, S. Miralles-Cuevas, J. Blanco, Experimental evaluation of two pilot-scale membrane distillation modules used for solar desalination, J. Membr. Sci. 409–410 (2012) 264–275, https://doi.org/10.1016/j.memsci.2012.03.063.
[184] R. Tian, H. Gao, X.H. Yang, S.Y. Yan, S. Li, A new enhancement technique on air gap membrane distillation, Desalination 332 (2014) 52–59, https://doi.org/10.1016/j.desal.2013.10.016.
[185] M. Jabed Perves Bappy, R. Bahar, S. Ibrahim, T. Firdaus Ariff, Enhanced Freshwater Production Using Finned-plate Air Gap Membrane Distillation (AGMD), n.d.
[186] V.T. Shahu, S.B. Thombre, Experimental analysis of a novel helical air gap membrane distillation system, Water Sci. Technol. Water Supply 21 (2021) 1450–1463, https://doi.org/10.2166/WS.2021.002.
[187] Y. Pan, Y. Shi, H. Li, W. Wang, Experimental and numerical investigations on gas injection-enhanced air gap membrane distillation for water desalination, Ind. Eng. Chem. Res. 61 (2022) 1850–1862, https://doi.org/10.1021/acs.iecr.1c04527.
[188] D.E.M. Warsinger, J. Swaminathan, L.A. Maswadeh, J.H. Lienhard V, Superhydrophobic condenser surfaces for air gap membrane distillation, J. Membr. Sci. 492 (2015) 578–587, https://doi.org/10.1016/j.memsci.2015.05.067.
[189] D.M. Warsinger, J. Swaminathan, L.L. Morales, J.H. Lienhard V, Comprehensive condensation flow regimes in air gap membrane distillation: visualization and energy efficiency, J. Membr. Sci. 555 (2018) 517–528, https://doi.org/10.1016/j.memsci.2018.03.053.
[190] Y. Elhenawy, N.A.S. Elminshawy, M. Bassyouni, A. Alhathal Alanezi, E. Drioli, Experimental and theoretical investigation of a new air gap membrane distillation module with a corrugated feed channel, J. Membr. Sci. 594 (2020), https://doi.org/10.1016/j.memsci.2019.117461.
[191] M.A.E.R. Abu-Zeid, G. ElMasry, Experimental evaluation of two consecutive air-gap membrane distillation modules with heat recovery, Water Sci. Technol. Water Supply 20 (2020) 1678–1691, https://doi.org/10.2166/ws.2020.077.
[192] D.U. Lawal, A.E. Khalifa, Experimental investigation of an air gap membrane distillation unit with double-sided cooling channel, Desalin. Water Treat. 57 (2016) 11066–11080, https://doi.org/10.1080/19443994.2015.1042065.
[193] M. Jalayer, M. Karimi, S.M. Borghei, A.H. Hassani, Improving the performance of air gap membrane distillation process using a developed tubular condenser compared to a flat plate condenser, Desalin. Water Treat. 139 (2019) 39–52, https://doi.org/10.5004/dwt.2019.23359.
[194] M.A.E.R. Abu-Zeid, X. Lu, S. Zhang, Influence of module length on water desalination using air gap membrane distillation process: an experimental

comparative study, Arab. J. Sci. Eng. 46 (2021) 7989–8008, https://doi.org/10.1007/s13369-021-05628-1.
[195] L. Gao, J. Zhang, S. Gray, J. de Li, Influence of PGMD module design on the water productivity and energy efficiency in desalination, Desalination 452 (2019) 29–39, https://doi.org/10.1016/j.desal.2018.10.005.
[196] C.-D. Ho, H. Chang, C. Chang, C. Huang, Theoretical and experimental studies of flux enhancement with roughened surface in direct contact membrane distillation desalination, J. Membr. Sci. 433 (2013) 160–166, https://doi.org/10.1016/j.memsci.2012.12.044.
[197] H. Guo, H.M. Ali, A. Hassanzadeh, Simulation study of flat-sheet air gap membrane distillation modules coupled with an evaporative crystallizer for zero liquid discharge water desalination, Appl. Therm. Eng. 108 (2016) 486–501, https://doi.org/10.1016/j.applthermaleng.2016.07.131.
[198] R. Schwantes, J. Seger, L. Bauer, D. Winter, T. Hogen, J. Koschikowski, S.-U. Geißen, Characterization and assessment of a novel plate and frame MD module for single pass wastewater concentration–FEED gap air gap membrane distillation, Membranes (Basel) 9 (2019) 118, https://doi.org/10.3390/membranes9090118.
[199] Y. Kim, S. Li, L. Francis, Z. Li, R.V. Linares, A.S. Alsaadi, M. Abu-Ghdaib, H.S. Son, G. Amy, N. Ghaffour, Osmotically and thermally isolated forward osmosis-membrane distillation (FO-MD) integrated module, Environ. Sci. Technol. 53 (2019) 3488–3498, https://doi.org/10.1021/acs.est.8b05587.
[200] F. Khaled, B. Chaouachi, K. Hidouri, Study of vacuum membrane distillation coupled with solar energy, in: International Conference on Green Energy and Conversion Systems 2017, GECS, 2017, pp. 1–5, https://doi.org/10.1109/GECS.2017.8066220.
[201] Z.P. Zhao, L. Xu, X. Shang, K. Chen, Water regeneration from human urine by vacuum membrane distillation and analysis of membrane fouling characteristics, Sep. Purif. Technol. 118 (2013) 369–376, https://doi.org/10.1016/j.seppur.2013.07.021.
[202] K. Zhao, W. Heinzl, M. Wenzel, S. Büttner, F. Bollen, G. Lange, S. Heinzl, N. Sarda, Experimental study of the memsys vacuum-multi-effect-membrane-distillation (V-MEMD) module, Desalination 323 (2013) 150–160, https://doi.org/10.1016/j.desal.2012.12.003.
[203] J.A. Andrés-Mañas, A. Ruiz-Aguirre, F.G. Acién, G. Zaragoza, Assessment of a pilot system for seawater desalination based on vacuum multi-effect membrane distillation with enhanced heat recovery, Desalination 443 (2018) 110–121, https://doi.org/10.1016/j.desal.2018.05.025.
[204] A. Najib, J. Orfi, H. Alansary, E. Ali, Z. Abdulwahed, S. Alzahrani, A. Chafidz, An experimental investigation of a solar-driven desalination system based on multi-effect membrane distillation, Desalin. Water Treat. 198 (2020) 1–18, https://doi.org/10.5004/dwt.2020.26099.
[205] C.-K. Lee, C. Park, Y.C. Woo, J.-S. Choi, J.-O. Kim, A pilot study of spiral-wound air gap membrane distillation process and its energy efficiency analysis, Chemosphere 239 (2020) 124696, https://doi.org/10.1016/j.chemosphere.2019.124696.
[206] A. Ruiz-Aguirre, D.C. Alarcón-Padilla, G. Zaragoza, Productivity analysis of two spiral-wound membrane distillation prototypes coupled with solar energy, Desalin. Water Treat. 55 (2015) 2777–2785, https://doi.org/10.1080/19443994.2014.946711.
[207] A. Ruiz-Aguirre, J.A. Andrés-Mañas, J.M. Fernández-Sevilla, G. Zaragoza, Experimental characterization and optimization of multi-channel spiral wound air gap membrane distillation modules for seawater desalination, Sep. Purif. Technol. 205 (2018) 212–222, https://doi.org/10.1016/j.seppur.2018.05.044.
[208] C.K. Lee, C. Park, Y.C. Woo, J.S. Choi, J.O. Kim, A pilot study of spiral-wound air gap membrane distillation process and its energy efficiency analysis, Chemosphere 239 (2020), https://doi.org/10.1016/j.chemosphere.2019.124696.
[209] J.A. Andrés-Mañas, I. Requena, G. Zaragoza, Characterization of the use of vacuum enhancement in commercial pilot-scale air gap membrane distillation modules with different designs, Desalination 528 (2022), https://doi.org/10.1016/j.desal.2021.115490.
[210] H.C. Duong, A.R. Chivas, B. Nelemans, M. Duke, S. Gray, T.Y. Cath, L.D. Nghiem, Treatment of RO brine from CSG produced water by spiral-wound air gap membrane distillation — a pilot study, Desalination 366 (2015) 121–129, https://doi.org/10.1016/j.desal.2014.10.026.
[211] D. Winter, J. Koschikowski, F. Gross, D. Maucher, D. Düver, M. Jositz, T. Mann, A. Hagedorn, Comparative analysis of full-scale membrane distillation contactors — methods and modules, J. Membr. Sci. 524 (2017) 758–771, https://doi.org/10.1016/j.memsci.2016.11.080.
[212] D. Winter, J. Koschikowski, M. Wieghaus, Desalination using membrane distillation: experimental studies on full scale spiral wound modules, J. Membr. Sci. 375 (2011) 104–112, https://doi.org/10.1016/j.memsci.2011.03.030.
[213] A.E. Jansen, J.W. Assink, J.H. Hanemaaijer, J. van Medevoort, E. van Sonsbeek, Development and pilot testing of full-scale membrane distillation modules for deployment of waste heat, Desalination 323 (2013) 55–65, https://doi.org/10.1016/j.desal.2012.11.030.
[214] A. Hagedorn, G. Fieg, D. Winter, J. Koschikowski, T. Mann, Methodical design and operation of membrane distillation plants for desalination, Chem. Eng. Res. Des. 125 (2017) 265–281, https://doi.org/10.1016/j.cherd.2017.07.024.
[215] L. Eykens, I. Hitsov, K. de Sitter, C. Dotremont, L. Pinoy, B. van der Bruggen, Direct contact and air gap membrane distillation: differences and similarities between lab and pilot scale, Desalination 422 (2017) 91–100, https://doi.org/10.1016/j.desal.2017.08.018.
[216] A. Najib, J. Orfi, E. Ali, J. Saleh, Thermodynamics analysis of a direct contact membrane distillation with/without heat recovery based on experimental data, Desalination 466 (2019) 52–67, https://doi.org/10.1016/j.desal.2019.05.009.
[217] D. Winter, J. Koschikowski, F. Gross, D. Maucher, D. Düver, M. Jositz, T. Mann, A. Hagedorn, Comparative analysis of full-scale membrane distillation contactors — methods and modules, J. Membr. Sci. 524 (2017) 758–771, https://doi.org/10.1016/j.memsci.2016.11.080.
[218] A. Ruiz-Aguirre, J.A. Andrés-Mañas, J.M. Fernández-Sevilla, G. Zaragoza, Experimental characterization and optimization of multi-channel spiral wound air gap membrane distillation modules for seawater desalination, Sep. Purif. Technol. 205 (2018) 212–222, https://doi.org/10.1016/j.seppur.2018.05.044.
[219] A. Ali, J.-H. Tsai, K.-L. Tung, E. Drioli, F. Macedonio, Designing and optimization of continuous direct contact membrane distillation process, Desalination 426 (2018) 97–107, https://doi.org/10.1016/j.desal.2017.10.041.
[220] J.H. Tsai, C. Quist-Jensen, A. Ali, Multipass hollow fiber membrane modules for membrane distillation, Desalination 548 (2023), https://doi.org/10.1016/j.desal.2022.116239.
[221] A. Yadav, C.P. Singh, R.V. Patel, A. Kumar, P.K. Labhasetwar, Investigations on the effect of spacer in direct contact and air gap membrane distillation using computational fluid dynamics, Colloids Surf. A Physicochem. Eng. Asp. 654 (2022) 130111, https://doi.org/10.1016/j.colsurfa.2022.130111.
[222] A. Anvari, A. Azimi Yancheshme, K.M. Kekre, A. Ronen, State-of-the-art methods for overcoming temperature polarization in membrane distillation process: a review, J. Membr. Sci. 616 (2020) 118413, https://doi.org/10.1016/j.memsci.2020.118413.
[223] J. Cai, H. Yin, F. Guo, Transport analysis of material gap membrane distillation desalination processes, Desalination 481 (2020) 114361, https://doi.org/10.1016/j.desal.2020.114361.
[224] Y.Z. Tan, H.E. Anga, J.W. Chewa, Metallic spacers to enhance membrane distillation, J. Membr. Sci. 572 (2019) 171–183, https://doi.org/10.1016/j.memsci.2018.10.073.
[225] B. Gu, C.S. Adjiman, X.Y. Xu, The effect of feed spacer geometry on membrane performance and concentration polarisation based on 3D CFD simulations, J. Membr. Sci. 527 (2017) 78–91, https://doi.org/10.1016/j.memsci.2016.12.058.
[226] M. Shakaib, S.M.F. Hasani, E.M. Haque, I. Ahmed, R.M. Yunus, A CFD study of heat transfer through spacer channels of membrane distillation modules, Desalin. Water Treat. 51 (2013) 3662–3674, https://doi.org/10.1080/19443994.2013.789234.
[227] M. La Cerva, A. Cipollina, M. Ciofalo, M. Albeirutty, N. Turkmen, S. Bouguecha, G. Micale, CFD investigation of spacer-filled channels for membrane distillation, Membranes (Basel) 9 (2019) 1–13, https://doi.org/10.3390/membranes9080091.
[228] K. El, K. Isam, J. Raed, Numerical simulation and evaluation of spacer — filled direct contact membrane distillation module, Appl Water Sci 10 (2020) 1–17, https://doi.org/10.1007/s13201-020-01261-9.
[229] A.H. Haidari, S.G.J. Heijman, W.G.J. van der Meer, Optimal design of spacers in reverse osmosis, Sep. Purif. Technol. 192 (2018) 441–456, https://doi.org/10.1016/j.seppur.2017.10.042.
[230] Y.C. Kim, M. Elimelech, Adverse impact of feed channel spacers on the performance of pressure retarded osmosis, Environ. Sci. Technol. 46 (2012) 4673–4681, https://doi.org/10.1021/es3002597.
[231] S.M. Ali, A. Qamar, S. Kerdi, S. Phuntsho, J.S. Vrouwenvelder, N. Ghaffour, H. K. Shon, Energy efficient 3D printed column type feed spacer for membrane filtration, Water Res. 164 (2019) 114961, https://doi.org/10.1016/j.watres.2019.114961.
[232] S.M. Ali, A. Qamar, S. Phuntsho, N. Ghaffour, J.S. Vrouwenvelder, H.K. Shon, Conceptual design of a dynamic turbospacer for efficient low pressure membrane filtration, Desalination 496 (2020) 114712, https://doi.org/10.1016/j.desal.2020.114712.
[233] C. Ho, L. Chen, J. Lim, P. Lin, P. Lu, Distillate flux enhancement of direct contact membrane distillation modules with inserting cross-diagonal carbon-fiber spacers, Membranes (Basel) 11 (2021) 1–21, https://doi.org/10.3390/membranes11120973.
[234] A. Alpatova, A. Qamar, M. Alhaddad, S. Kerdi, H. Soo, N. Amin, N. Ghaffour, In situ conductive spacers for early pore wetting detection in membrane distillation, Sep. Purif. Technol. 294 (2022) 121162, https://doi.org/10.1016/j.seppur.2022.121162.
[235] P. Taylor, Y. Yun, J. Wang, R. Ma, A.G. Fane, Y. Yun, J. Wang, R. Ma, A. Gordon, Effects of channel spacers on direct contact membrane distillation, Desalin. Water Treat. 34 (2013) 63–69, https://doi.org/10.5004/dwt.2011.2870.
[236] E.H.C. Castillo, N. Thomas, O. Al-Ketan, R. Rowshan, R.K. Abu Al-Rub, L. D. Nghiem, S. Vigneswaran, H.A. Arafat, G. Naidu, 3D printed spacers for organic fouling mitigation in membrane distillation, J. Membr. Sci. 581 (2019) 331–343, https://doi.org/10.1016/j.memsci.2019.03.040.
[237] Q. Li, B. Lian, W. Zhong, A. Omar, A. Razmjou, P. Dai, J. Guan, G. Leslie, R. A. Taylor, Improving the performance of vacuum membrane distillation using a 3D-printed helical baffle and a superhydrophobic nanocomposite membrane, Sep. Purif. Technol. 248 (2020) 117072, https://doi.org/10.1016/j.seppur.2020.117072.
[238] N. Thomas, J. Swaminathan, G. Zaragoza, R.K. Abu Al-Rub, J.H. Lienhard V, H. A. Arafat, Comparative assessment of the effects of 3D printed feed spacers on process performance in MD systems, Desalination 503 (2021) 114940, https://doi.org/10.1016/j.desal.2021.114940.
[239] S. Jeong, B. Gu, S. Choi, S. Ahn, J. Lee, J. Lee, S. Jeong, Engineered multi-scale roughness of carbon nanofiller-embedded 3D printed spacers for membrane distillation, Water Res. 231 (2023) 119649, https://doi.org/10.1016/j.watres.2023.119649.

[240] N. Thomas, M. Kumar, G. Palmisano, R.K.A. Al-Rub, R.Y. Alnuaimi, E. Alhseinat, R. Rowshan, H.A. Arafat, Antiscaling 3D printed feed spacers via facile nanoparticle coating for membrane distillation, Water Res. 189 (2021) 116649, https://doi.org/10.1016/j.watres.2020.116649.
[241] O. Heinz, M. Aghajani, A.R. Greenberg, Y. Ding, Surface-patterning of polymeric membranes: fabrication and performance, Curr. Opin. Chem. Eng. 20 (2018) 1–12, https://doi.org/10.1016/j.coche.2018.01.008.
[242] S. Sinha Ray, H. Dommati, J.-C. Wang, H.K. Lee, Y.-I. Park, H. Park, I.-C. Kim, S.-S. Chen, Y.-N. Kwon, Facile approach for designing a novel micropatterned antiwetting membrane by utilizing 3D printed molds for improved desalination performance, J. Membr. Sci. 637 (2021) 119641, https://doi.org/10.1016/j.memsci.2021.119641.
[243] P.M. Hylle, J.T. Falden, J.L. Rauff, P. Rasmussen, M. Moltzen-Juul, M.L. Trudslev, C.A. Quist-Jensen, A. Ali, Determination of heat and mass transport correlations for hollow membrane distillation modules, Energies (Basel) 16 (2023) 3447, https://doi.org/10.3390/en16083447.
[244] L. Chen, B. Wu, Research progress in computational fluid dynamics simulations of membrane distillation processes: a review, Membranes (Basel) 11 (2021) 513, https://doi.org/10.3390/membranes11070513.
[245] N. Tang, H. Zhang, W. Wang, Computational fluid dynamics numerical simulation of vacuum membrane distillation for aqueous NaCl solution, Desalination 274 (2011) 120–129, https://doi.org/10.1016/j.desal.2011.01.078.
[246] H. Yu, X. Yang, R. Wang, A.G. Fane, Numerical simulation of heat and mass transfer in direct membrane distillation in a hollow fiber module with laminar flow, J. Membr. Sci. 384 (2011) 107–116, https://doi.org/10.1016/j.memsci.2011.09.011.
[247] X. Yang, H. Yu, R. Wang, A.G. Fane, Analysis of the effect of turbulence promoters in hollow fiber membrane distillation modules by computational fluid dynamic (CFD) simulations, J. Membr. Sci. 415–416 (2012) 758–769, https://doi.org/10.1016/j.memsci.2012.05.067.
[248] X. Yang, H. Yu, R. Wang, A.G. Fane, Optimization of microstructured hollow fiber design for membrane distillation applications using CFD modeling, J. Membr. Sci. 421–422 (2012) 258–270, https://doi.org/10.1016/j.memsci.2012.07.022.
[249] L. Wang, H. Wang, B. Li, Y. Wang, S. Wang, Novel design of liquid distributors for VMD performance improvement based on cross-flow membrane module, Desalination 336 (2014) 80–86, https://doi.org/10.1016/j.desal.2014.01.004.
[250] Y. Zhang, Y. Peng, S. Ji, S. Wang, Numerical simulation of 3D hollow-fiber vacuum membrane distillation by computational fluid dynamics, Chem. Eng. Sci. 152 (2016) 172–185, https://doi.org/10.1016/j.ces.2016.05.040.
[251] H. Chang, J.-A. Hsu, C.-L. Chang, C.-D. Ho, CFD simulation of direct contact membrane distillation modules with rough surface channels, Energy Procedia 75 (2015) 3083–3090, https://doi.org/10.1016/j.egypro.2015.07.634.
[252] J. Liu, Q. Wang, L. Han, B. Li, Simulation of heat and mass transfer with cross-flow hollow fiber vacuum membrane distillation: the influence of fiber arrangement, Chem. Eng. Res. Des. 119 (2017) 12–22, https://doi.org/10.1016/j.cherd.2017.01.013.
[253] Y. Zhang, Y. Peng, S. Ji, J. Qi, S. Wang, Numerical modeling and economic evaluation of two multi-effect vacuum membrane distillation (ME-VMD) processes, Desalination 419 (2017) 39–48, https://doi.org/10.1016/j.desal.2017.05.032.
[254] F. Kavousi, E. Syron, M. Semmens, E. Casey, Hydrodynamics and gas transfer performance of confined hollow fibre membrane modules with the aid of computational fluid dynamics, J. Membr. Sci. 513 (2016) 117–128, https://doi.org/10.1016/j.memsci.2016.04.038.
[255] J. Qi, J. Lv, Z. Li, W. Bian, J. Li, S. Liu, A numerical simulation of membrane distillation treatment of mine drainage by computational fluid dynamics, Water (Basel) 12 (2020) 3403, https://doi.org/10.3390/w12123403.
[256] Z. Pang, C. Hou, S. Xie, N.H. Wong, J. Sunarso, Y. Peng, Optimization of hollow fiber membrane module for vacuum membrane distillation (VMD) via experimental study, Desalination 542 (2022) 116068, https://doi.org/10.1016/j.desal.2022.116068.
[257] A. Cipollina, G. Micale, L. Rizzuti, Membrane distillation heat transfer enhancement by CFD analysis of internal module geometry, Desalin. Water Treat. 25 (2011) 195–209, https://doi.org/10.5004/dwt.2011.1455.
[258] M. Ghadiri, S. Fakhri, S. Shirazian, Modeling of water transport through nanopores of membranes in direct-contact membrane distillation process, Polym. Eng. Sci. 54 (2014) 660–666, https://doi.org/10.1002/pen.23601.
[259] S. Al-Sharif, M. Albeirutty, A. Cipollina, G. Micale, Modelling flow and heat transfer in spacer-filled membrane distillation channels using open source CFD code, Desalination 311 (2013) 103–112, https://doi.org/10.1016/j.desal.2012.11.005.
[260] C.-D. Ho, H. Chang, C.-L. Chang, C.-H. Huang, Theoretical and experimental studies of flux enhancement with roughened surface in direct contact membrane distillation desalination, J. Membr. Sci. 433 (2013) 160–166, https://doi.org/10.1016/j.memsci.2012.12.044.
[261] H. Chang, J.-A. Hsu, C.-L. Chang, C.-D. Ho, CFD simulation of direct contact membrane distillation modules with rough surface channels, Energy Procedia 75 (2015) 3083–3090, https://doi.org/10.1016/j.egypro.2015.07.634.
[262] A. Tamburini, P. Pitò, A. Cipollina, G. Micale, M. Ciofalo, A thermochromic liquid crystals image analysis technique to investigate temperature polarization in spacer-filled channels for membrane distillation, J. Membr. Sci. 447 (2013) 260–273, https://doi.org/10.1016/j.memsci.2013.06.043.
[263] A. Katsandri, A theoretical analysis of a spacer filled flat plate membrane distillation modules using CFD: part I: velocity and shear stress analysis, Desalination 408 (2017) 145–165, https://doi.org/10.1016/j.desal.2015.09.001.
[264] A. Katsandri, A theoretical analysis of a spacer filled flat plate membrane distillation modules using CFD: part II: temperature polarisation analysis, Desalination 408 (2017) 166–180, https://doi.org/10.1016/j.desal.2015.11.021.
[265] M. Shokrollahi, M. Rezakazemi, M. Younas, Producing water from saline streams using membrane distillation: modeling and optimization using CFD and design expert, Int. J. Energy Res. 44 (2020) 8841–8853, https://doi.org/10.1002/er.5578.
[266] D.J. Park, E. Norouzi, C. Park, Experimentally-validated computational simulation of direct contact membrane distillation performance, Int. J. Heat Mass Transf. 129 (2019) 1031–1042, https://doi.org/10.1016/j.ijheatmasstransfer.2018.10.035.
[267] Y. Taamneh, K. Bataineh, Improving the performance of direct contact membrane distillation utilizing spacer-filled channel, Desalination 408 (2017) 25–35, https://doi.org/10.1016/j.desal.2017.01.004.
[268] M. La Cerva, A. Cipollina, M. Ciofalo, M. Albeirutty, N. Turkmen, S. Bouguecha, G. Micale, CFD investigation of spacer-filled channels for membrane distillation, Membranes (Basel) 9 (2019) 91, https://doi.org/10.3390/membranes9080091.
[269] Z. Kuang, R. Long, Z. Liu, W. Liu, Analysis of temperature and concentration polarizations for performance improvement in direct contact membrane distillation, Int. J. Heat Mass Transf. 145 (2019) 118724, https://doi.org/10.1016/j.ijheatmasstransfer.2019.118724.
[270] J. Lou, J. Vanneste, S.C. DeCaluwe, T.Y. Cath, N. Tilton, Computational fluid dynamics simulations of polarization phenomena in direct contact membrane distillation, J. Membr. Sci. 591 (2019) 117150, https://doi.org/10.1016/j.memsci.2019.05.074.
[271] J. Amigo, R. Urtubia, F. Suárez, Exploring the interactions between hydrodynamics and fouling in membrane distillation systems — a multiscale approach using CFD, Desalination 444 (2018) 63–74, https://doi.org/10.1016/j.desal.2018.07.009.
[272] J. Choi, Y. Choi, J. Ju, Y. Park, S. Lee, Inorganic fouling mitigation using the baffle system in direct contact membrane distillation (DCMD), Desalination 496 (2020) 114714, https://doi.org/10.1016/j.desal.2020.114714.
[273] P. Yazgan-Birgi, M.I. Hassan Ali, J. Swaminathan, J.H. Lienhard, H.A. Arafat, Computational fluid dynamics modeling for performance assessment of permeate gap membrane distillation, J. Membr. Sci. 568 (2018) 55–66, https://doi.org/10.1016/j.memsci.2018.09.061.
[274] V. Perfilov, V. Fila, J. Sanchez Marcano, A general predictive model for sweeping gas membrane distillation, Desalination 443 (2018) 285–306, https://doi.org/10.1016/j.desal.2018.06.007.
[275] M. Shakaib, M.E. Haque, Numerical simulations for fluid dynamics and temperature patterns in membrane distillation channels, Heat Mass Transf. 55 (2019) 3509–3522, https://doi.org/10.1007/s00231-019-02678-y.
[276] I. Janajreh, M.N. Hussain, R. Hashaikeh, R. Ahmed, Thermal efficiency enhancement of the direct contact membrane distillation: conductive layer integration and geometrical undulation, Appl. Energy 227 (2018) 7–17, https://doi.org/10.1016/j.apenergy.2017.10.048.
[277] M. Darman, N. Niknafs, A. Jalali, Effect of wavy corrugations on the performance enhancement of direct contact membrane distillation modules: a numerical study, Chem. Eng. Process. Proc. Intens. 109421 (2023), https://doi.org/10.1016/j.cep.2023.109421.
[278] J. Choi, Y. Choi, J. Lee, Y. Kim, S. Lee, Exergy analysis of a direct contact membrane distillation (DCMD) system based on computational fluid dynamics (CFD), Membranes (Basel) 11 (2021) 525, https://doi.org/10.3390/membranes11070525.
[279] J. Choi, H. Cho, Y. Choi, S. Lee, Combination of computational fluid dynamics and design of experiments to optimize modules for direct contact membrane distillation, Desalination 524 (2022) 115460, https://doi.org/10.1016/j.desal.2021.115460.
[280] A. Ansari, F.M. Galogahi, G. Millar, F. Helfer, D.V. Thiel, S. Soukane, N. Ghaffour, Computational fluid dynamics simulations of solar-assisted, spacer-filled direct contact membrane distillation: seeking performance improvement, Desalination 545 (2023) 116181, https://doi.org/10.1016/j.desal.2022.116181.
[281] A. Ansari, F.M. Galogahi, G. Millar, F. Helfer, D.V. Thiel, S. Soukane, N. Ghaffour, Computational fluid dynamics modelling of air-gap membrane distillation: spacer-filled and solar-assisted modules, Desalination 546 (2023) 116207, https://doi.org/10.1016/j.desal.2022.116207.
[282] A. Kargari, M.M.A. Shirazi, Water desalination: solar-assisted membrane distillation, in: Encyclopedia of Energy Engineering and Technology, Second edition, CRC Press, 2014, pp. 2095–2109, https://doi.org/10.1081/E-EEE2-120051388.
[283] M.R. Rahimpour, N.M. Kazerooni, M. Parhoudeh, Water treatment by renewable energy-driven membrane distillation, in: Current Trends and Future Developments on (Bio-) Membranes, Elsevier, 2019, pp. 179–211, https://doi.org/10.1016/B978-0-12-813545-7.00008-8.
[284] V. Okati, A.J. Moghadam, M. Farzaneh-Gord, M. Moein-Jahromi, Thermo-economical and environmental analyses of a Direct Contact Membrane Distillation (DCMD) performance, J. Clean. Prod. 340 (2022) 130613, https://doi.org/10.1016/j.jclepro.2022.130613.
[285] S.M. Shalaby, A.E. Kabeel, H.F. Abosheiasha, M.K. Elfakharany, A. Shama, R. D. Vidic, Membrane distillation driven by solar energy: a review, J. Clean. Prod. 366 (2022) 132949, https://doi.org/10.1016/j.jclepro.2022.132949.
[286] A.E. Kabeel, M. Abdelgaied, E.M.S. El-said, Study of a solar-driven membrane distillation system: evaporative cooling effect on performance enhancement, Renew. Energy 106 (2017) 192–200, https://doi.org/10.1016/j.renene.2017.01.030.

[287] A.G. Fane, R.W. Schofield, C.J.D. Fell, The efficient use of energy in membrane distillation, Desalination 64 (1987) 231–243, https://doi.org/10.1016/0011-9164(87)90099-3.
[288] E. Guillén-burrieza, J. Blanco, G. Zaragoza, D. Alarcón, P. Palenzuela, M. Ibarra, W. Gernjak, Experimental analysis of an air gap membrane distillation solar desalination pilot system, J. Membr. Sci. 379 (2011) 386–396, https://doi.org/10.1016/j.memsci.2011.06.009.
[289] E. Guillén-Burrieza, J. Blanco, G. Zaragoza, D. Alarcón, P. Palenzuela, M. Ibarra, W. Gernjak, Experimental analysis of an air gap membrane distillation solar desalination pilot system, J. Membr. Sci. 379 (2011) 386–396, https://doi.org/10.1016/j.memsci.2011.06.009.
[290] A. Chafidz, E.D. Kerme, I. Wazeer, Y. Khalid, A. Ajbar, S.M. Al-Zahrani, Design and fabrication of a portable and hybrid solar-powered membrane distillation system, J. Clean. Prod. 133 (2016) 631–647, https://doi.org/10.1016/j.jclepro.2016.05.127.
[291] F. Wang, S. Wang, J. Li, D. Xia, J. Liu, Seawater desalination with solar-energy-integrated vacuum membrane distillation system, J. Water Reuse Desalin. 7 (2017) 16–24, https://doi.org/10.2166/wrd.2016.207.
[292] Y.-D. Kim, K. Thu, S.-H. Choi, Solar-assisted multi-stage vacuum membrane distillation system with heat recovery unit, Desalination 367 (2015) 161–171, https://doi.org/10.1016/j.desal.2015.04.003.
[293] N.A.S. Elminshawy, M.A. Gadalla, M. Bassyouni, K. El-Nahhas, A. Elminshawy, Y. Elhenawy, A novel concentrated photovoltaic-driven membrane distillation hybrid system for the simultaneous production of electricity and potable water, Renew. Energy 162 (2020) 802–817, https://doi.org/10.1016/j.renene.2020.08.041.
[294] Q. Zhao, H. Zhang, Z. Hu, S. Hou, A solar driven hybrid photovoltaic module/direct contact membrane distillation system for electricity generation and water desalination, Energ. Conver. Manage. 221 (2020), https://doi.org/10.1016/j.enconman.2020.113146.
[295] Q. Li, L. Beier, J. Tan, C. Brown, B. Lian, W. Zhong, Y. Wang, C. Ji, P. Dai, T. Li, P. Le, H. Tyagi, X. Liu, G. Leslie, R.A. Taylor, An integrated, solar-driven membrane distillation system for water purification and energy generation, Appl. Energy 237 (2019) 534–548, https://doi.org/10.1016/j.apenergy.2018.12.069.
[296] A. Bamasag, T. Alqahtani, S. Sinha, N. Ghaffour, P. Phelan, Experimental investigation of a solar-heated direct contact membrane distillation system using evacuated tube collectors, Desalination 487 (2020), https://doi.org/10.1016/j.desal.2020.114497.
[297] Q. Miao, Y. Zhang, S. Cong, F. Guo, Experimental investigation on floating solar-driven membrane distillation desalination modules, Membranes (Basel) 11 (2021), https://doi.org/10.3390/membranes11050304.
[298] J. Zhou, X. Zhang, B. Sun, W. Su, Performance analysis of solar vacuum membrane distillation regeneration, Appl. Therm. Eng. 144 (2018) 571–582, https://doi.org/10.1016/j.applthermaleng.2018.08.052.
[299] Q. Li, L.-J. Beier, J. Tan, C. Brown, B. Lian, W. Zhong, Y. Wang, C. Ji, P. Dai, T. Li, P. Le Clech, H. Tyagi, X. Liu, G. Leslie, R.A. Taylor, An integrated, solar-driven membrane distillation system for water purification and energy generation, Appl. Energy 237 (2019) 534–548, https://doi.org/10.1016/j.apenergy.2018.12.069.
[300] Q. Li, A.J. Charlton, A. Omar, B. Dang, P. Le-Clech, J. Scott, R.A. Taylor, A novel concentrated solar membrane-distillation for water purification in a building integrated design, Desalination 535 (2022) 115828, https://doi.org/10.1016/j.desal.2022.115828.
[301] F. Suárez, J.A. Ruskowitz, S.W. Tyler, A.E. Childress, Renewable water: direct contact membrane distillation coupled with solar ponds, Appl. Energy 158 (2015) 532–539, https://doi.org/10.1016/j.apenergy.2015.08.110.
[302] S. Liang, H. Zheng, Z. Zhao, X. Ma, K.C. Ng, Investigation on an underwater solar concentrating photovoltaic-membrane distillation (CPV-MD) integrated system, Desalination 546 (2023) 116193, https://doi.org/10.1016/j.desal.2022.116193.
[303] S. Soukane, H.S. Son, M. Mustakeem, M. Obaid, A. Alpatova, A. Qamar, Y. Jin, N. Ghaffour, Materials for energy conversion in membrane distillation localized heating: review, analysis and future perspectives of a paradigm shift, Renew. Sustain. Energy Rev. 167 (2022) 112702, https://doi.org/10.1016/j.rser.2022.112702.
[304] E. Gontarek-Castro, R. Castro-Muñoz, How to make membrane distillation greener: a review of environmentally friendly and sustainable aspects, Green Chem. 26 (2024) 164–185, https://doi.org/10.1039/D3GC03377E.
[305] F. Zhao, Y. Guo, X. Zhou, W. Shi, G. Yu, Materials for solar-powered water evaporation, Nat. Rev. Mater. 5 (2020) 388–401, https://doi.org/10.1038/s41578-020-0182-4.
[306] F.E. Ahmed, B.S. Lalia, R. Hashaikeh, N. Hilal, Alternative heating techniques in membrane distillation: a review, Desalination 496 (2020), https://doi.org/10.1016/j.desal.2020.114713.
[307] F. Alessandro, F. Macedonio, E. Drioli, Plasmonic phenomena in membrane distillation, Membranes (Basel) 13 (2023) 254, https://doi.org/10.3390/membranes13030254.
[308] M.U. Farid, J.A. Kharraz, J. Sun, M. Boey, M.A. Riaz, P.W. Wong, M. Jia, X. Zhang, B.J. Deka, N.K. Khanzada, J. Guo, A.K. An, Advancements in nanoenabled membrane distillation for a sustainable water-energy-environment nexus, Adv. Mater. (2023), https://doi.org/10.1002/adma.202307950.
[309] L. Han, J. Mao, A.-Q. Xie, Y. Liang, L. Zhu, S. Chen, Synergistic enhanced solar-driven water purification and CO_2 reduction via photothermal catalytic membrane distillation, Sep. Purif. Technol. 309 (2023) 123003, https://doi.org/10.1016/j.seppur.2022.123003.
[310] N. Kaur, A.K. Singh, Ohmic heating: concept and applications—a review, Crit. Rev. Food Sci. Nutr. 56 (2016) 2338–2351, https://doi.org/10.1080/10408398.2013.835303.
[311] X. Liao, Y.J. Lim, M. Khayet, Y. Liao, L. Yao, Y. Zhao, A.G. Razaqpur, Applications of electrically conductive membranes in water treatment via membrane distillation: joule heating, membrane fouling/scaling/wetting mitigation and monitoring, Water Res. 244 (2023) 120511, https://doi.org/10.1016/j.watres.2023.120511.
[312] J. Huang, Y. He, Z. Shen, Joule heating membrane distillation enhancement with multi-level thermal concentration and heat recovery, Energ. Conver. Manage. 238 (2021) 114111, https://doi.org/10.1016/j.enconman.2021.114111.
[313] Y.Z. Tan, S.P. Chandrakant, J.S.T. Ang, H. Wang, J.W. Chew, Localized induction heating of metallic spacers for energy-efficient membrane distillation, J. Membr. Sci. 606 (2020) 118150, https://doi.org/10.1016/j.memsci.2020.118150.
[314] K. Li, H. Liu, Y. Zhang, D. Hou, Y. Zhang, J. Wang, Electrothermal hollow fiber membrane for convenient heat management in Joule vacuum membrane distillation, Chem. Eng. J. 443 (2022) 136521, https://doi.org/10.1016/j.cej.2022.136521.
[315] K. Li, Y. Zhang, Z. Wang, L. Liu, H. Liu, J. Wang, Electrothermally driven membrane distillation for low-energy consumption and wetting mitigation, Environ. Sci. Technol. 53 (2019) 13506–13513, https://doi.org/10.1021/acs.est.9b04861.
[316] F.E. Ahmed, B.S. Lalia, R. Hashaikeh, N. Hilal, Intermittent direct joule heating of membrane surface for seawater desalination by air gap membrane distillation, J. Membr. Sci. 648 (2022) 120390, https://doi.org/10.1016/j.memsci.2022.120390.
[317] A. Anvari, K.M. Kekre, A. Azimi Yancheshme, Y. Yao, A. Ronen, Membrane distillation of high salinity water by induction heated thermally conducting membranes, J. Membr. Sci. 589 (2019) 117253, https://doi.org/10.1016/j.memsci.2019.117253.
[318] W. Qing, Z. Hu, Q. Ma, W. Zhang, Conductive Fe_3O_4/PANI@PTFE membrane for high thermal efficiency in interfacial induction heating membrane distillation, Nano Energy 89 (2021) 106339, https://doi.org/10.1016/j.nanoen.2021.106339.
[319] M. Pan, Y.Z. Tan, J.W. Chew, Superior membrane distillation by induction heating of 3D rGO/Nafion/Ni foam for water treatment, J. Membr. Sci. 616 (2020) 118609, https://doi.org/10.1016/j.memsci.2020.118609.
[320] A. Anvari, K.M. Kekre, A. Ronen, Scaling mitigation in radio-frequency induction heated membrane distillation, J. Membr. Sci. 600 (2020) 117859, https://doi.org/10.1016/j.memsci.2020.117859.
[321] Z. Ji, J. Wang, D. Hou, Z. Yin, Z. Luan, Effect of microwave irradiation on vacuum membrane distillation, J. Membr. Sci. 429 (2013) 473–479, https://doi.org/10.1016/j.memsci.2012.11.041.
[322] S. Roy, M.S. Humoud, W. Intrchom, S. Mitra, Microwave-induced desalination via direct contact membrane distillation, ACS Sustain. Chem. Eng. 6 (2018) 626–632, https://doi.org/10.1021/acssuschemeng.7b02950.
[323] M.S. Humoud, W. Intrchom, S. Roy, S. Mitra, Reduction of scaling in microwave induced membrane distillation on a carbon nanotube immobilized membrane, Environ. Sci. (Camb.) 5 (2019) 1012–1021, https://doi.org/10.1039/C9EW00153K.
[324] J. Wang, Y. Liu, U. Rao, M. Dudley, N.D. Ebrahimi, J. Lou, F. Han, E.M.V. Hoek, N. Tilton, T.Y. Cath, C.S. Turchi, M.B. Heeley, Y.S. Ju, D. Jassby, Conducting thermal energy to the membrane/water interface for the enhanced desalination of hypersaline brines using membrane distillation, J. Membr. Sci. 626 (2021), https://doi.org/10.1016/j.memsci.2021.119188.
[325] F. Han, S. Liu, K. Wang, X. Zhang, Enhanced performance of membrane distillation using surface heating process, Membranes (Basel) 11 (2021), https://doi.org/10.3390/membranes11110866.